1968

Kinetics and mechanisms of some rapid substitution and oxidation-reduction reactions of iron (III), europium (II), and chromium (II) ions

David Wesley Carlyle
Iowa State University

CARLYLE, David Wesley, 1938-
KINETICS AND MECHANISMS OF SOME RAPID SUBSTITUTION AND OXIDATION-REDUCTION REACTIONS OF IRON(III), EUROPIUM(II), AND CHROMIUM(II) IONS.

Iowa State University, Ph.D., 1968
Chemistry, inorganic

KINETICS AND MECHANISMS OF SOME RAPID SUBSTITUTION AND OXIDATION-REDUCTION REACTIONS OF IRON(III), EUROPIUM(II), AND CHROMIUM(II) IONS

by

David Wesley Carlyle

A Dissertation Submitted to the
Graduate Faculty in Partial Fulfillment of
The Requirements for the Degree of
DOCTOR OF PHILOSOPHY

Major Subject: Inorganic Chemistry

Approved:

Signature was redacted for privacy.

In Charge of Major Work

Signature was redacted for privacy.

Head of Major Department

Signature was redacted for privacy.

Dean of Graduate College

Iowa State University
Ames, Iowa

1968

TABLE OF CONTENTS

LIST OF TABLES

LIST OF FIGURES

INTRODUCTION

The rates of electron transfer reactions between metal ions in solution have been widely studied (1-21) recently in efforts to understand the details of the mechanisms. Most oxidation-reduction reactions between metal ions in solution are believed to occur by one of two mechanisms: inner sphere or outer sphere.

A mechanism is referred to as an inner sphere electron transfer when the transfer of one or more electrons from one metal ion to another occurs by way of a bridging ligand that occupies the inner coordination sphere of each metal ion during the transfer.

Chloride ion is shown as an example of a bridging ligand in the following diagram. The diagram refers to the reaction

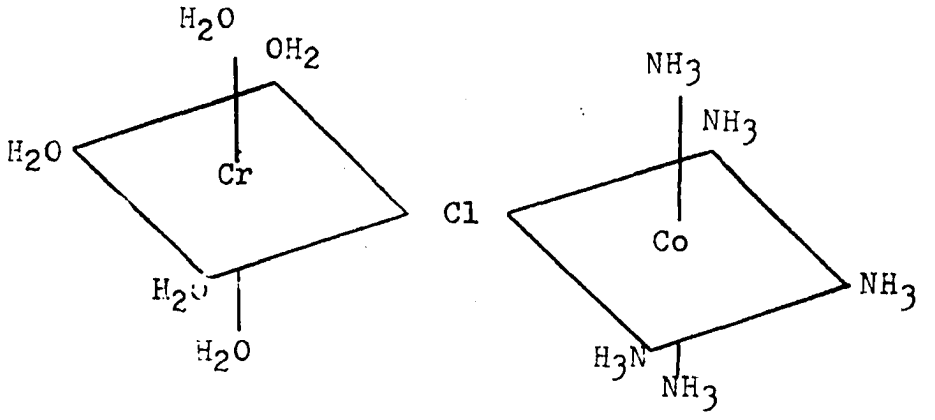

between $Cr(H_2O)_6^{2+}$ and $Co(NH_3)_5Cl^{2+}$, shown to be chloride-bridged by Taube and Myers (20).

After completion of the electron transfer and dissociation of the activated complex, the bridging ligand will

remain bound to the least labile of the product metal ions, for a time governed by the solvation rate characteristic of the particular complex ion. The classic proof of an inner sphere mechanism is the demonstration of transfer of the bridging ligand from one metal to the other. This proof is possible only when the relative labilities of the reactants are opposite those of the products, and when a method is available for identifying the more inert product before solvation occurs.

An example of this proof is provided by the work of Taube and Myers (20), involving the reaction between Cr^{2+} and $Co(NH_3)_5Cl^{2+}$. The Cr(II) reactant is labile and the Co(III) reactant is inert. The products were demonstrated to be inert $CrCl^{2+}$ and labile Co^{2+}. The chloride ion in the chromium(III) product was transferred directly from the Co (III) reactant; radioactive Cl^- in the reactant solution was not incorporated into the $CrCl^{2+}$ product (20). Radiotracer experiments are not necessary to show that ligands in reaction products were transferred directly from the reactants; determination of the form of the rate law is sufficient to show how many ligand ions or molecules (except solvent) are in the activated complex. The ion or molecule transfer criterion has been used to show that a great many reactions occur by an inner sphere mechanism (for example, see reference 2).

Failure to demonstrate group transfer does not, however, eliminate the possibility of an inner sphere mechanism. An inner sphere reaction will not result in ligand transfer unless the relative labilities of the product ions are opposite those of the reactant ions. Even though ligand transfer may occur, it cannot be demonstrated unless both the reactant and the product containing the bridging group can be identified and unless replacement of the bridging ligand by substitution on both the reactant and the product is negligible during the oxidation-reduction reaction. Thus, inner sphere mechanisms can rarely be demonstrated by the ligand transfer method when both reactants or both products are labile.

Indirect evidence often invoked (1,2) for inner sphere mechanisms is the variation in rate noted upon changing the ligands that are claimed to be bridging. The rates of inner sphere reactions are more dependent on the identity of the bridging ligands than outer sphere reactions are on the identity of nonbridging ligands; particularly, the rates noted for N_3^- bridged reactions are normally considerably greater (1) than the rates for NCS^- bridged reactions that are otherwise identical. Other indirect evidence that has been used to establish mechanisms has been obtained from variations in entropies of activation (2,22,23,24), volumes of activation (25), isotope effects on reaction rates (26,27) and nonbridging ligand effects (9,28).

A mechanism is referred to as outer sphere when the transfer of one or more electrons from one metal ion to another occurs without occupation of the inner coordination sphere of both ions by a common ligand. Outer sphere mechanisms necessarily occur in reactions involving inert metal complexes that do not contain ligands capable of acting as electron transfer bridges. For example, reactions of $Ru(NH_3)_6^{2+}$ (21) could not occur by an inner sphere mechanism. Outer sphere mechanisms can also occur in reactions not involving their clear requirement. Indirect evidence often invoked (1,2) for outer sphere mechanisms is the small dependence of the rate on the identity of ligands bound to the reactants, particularly the ligands N_3^- and NCS^-, as well as the effects mentioned in connection with inner sphere mechanisms.

Theoretical prediction of rate constants for electron transfer reactions in solution is difficult; a rigorous treatment would require consideration of solvent and ligand reorganizations, electrostatic factors, electronic interactions between the reacting species, electron transfer properties of ligands, and free energy changes. Marcus (1, 29) has developed a simplified theory, for application to outer sphere reactions, in which the electron transfer rates are related to the free energy of reaction. More recently, attempts have also been made to apply the Marcus relation

(1,17) to inner sphere reactions as well. Application of this theory will be made later in this paper.

The rate of electron transfer between europium(II) and iron(III) has not been previously measured. In view of recent attempts (1-21) to understand the details of the mechanisms of electron transfer reactions of metal complexes, data on new systems are especially useful.

Europium(II) reactions have not been widely studied although measurements have been made on the Eu(II)-Eu(III) exchange reaction (18), on the reduction of several cobalt-(III) complexes (14), and on the reduction of V^{3+} and Cr^{3+} (10). An earlier attempt (30) to study the rate of the rapid Eu^{2+}-Fe^{3+} reaction was not successful.

The extent to which reactions of Eu^{2+} should parallel those of the first-row transition metal ions is not clear, especially since the electron to be transferred is an f and not a d electron.

Chromium(II) reactions have been studied intensively (1, 3); in particular, studies of Cr^{2+} reductions of iron(III) and its complexes have been reported (13,16).

The studies to be described here are a series of measurements of the rate of reduction of Fe(III) by Eu(II) and Cr(II); the measurements were done in perchlorate media, and also in the presence of the complexing anions F^-, Cl^-, Br^-, N_3^-, NCO^-, and NCS^-.

Some information is available for other iron(III) reductions, notably by V^{2+} (6) and Fe^{2+} (19), as well as by the previously mentioned Cr^{2+}. A feature of major interest in this work is a comparison of the reactivity patterns exhibited by various reducing agents toward Fe(III) complexes, with the patterns of the same reducing agents toward other complexes.

The rates of substitution of the complexing anions on iron(III) was needed for treatment of the kinetic data obtained here for the oxidation-reduction reactions. These rates were generally available from the literature, but they were measured in this study for the anions N_3^- and Br^-. Although these anions had received some attention previously (31-37), more extensive measurements in this study provided more accurate rate and equilibrium parameters.

EXPERIMENTAL SECTION

Reagents

Hydrated iron(III) perchlorate was prepared from solutions of the chloride in perchloric acid, by heating to remove HCl. After the solution failed to produce a visible precipitate in a test with silver ion, two successive crystallizations were done. Iron(III) perchlorate solutions were analyzed by reduction with tin(II), destruction of excess tin(II) with mercury(II), (or by reduction with amalgamated zinc) and titration of iron(II) with cerium(IV), to the disappearance of the orange ferroin indicator. The cerium(IV) was standardized by titration of weighed samples of dried primary standard arsenic(III) oxide to the ferroin endpoint. Iron(III) perchlorate solutions were also analyzed spectrophotometrically in 0.3-0.6M perchloric acid using the peak of aquoiron(III) at 2400Å with a molar absorptivity of 4230 M^{-1} cm^{-1}. The perchloric acid content of the iron(III) solutions was determined by passing samples through columns of Dowex 50W-X8 cation exchange resin in the hydrogen ion form and titrating the washings with sodium hydroxide. The hydrogen ion concentration was calculated from the base in excess of that required for the three moles of hydrogen ion displaced per mole of iron(III).

Europium(III) perchlorate solutions were prepared by dissolving europium(III) oxide in perchloric acid, followed by

electrolytic reduction to europium(II) at a mercury cathode. The concentration of chloride in freshly prepared and in stored europium(II) solutions was at or below the limit of visual detection ($\leq 6 \times 10^{-5}$ M) in a test with silver ion. Europium(II) solutions were stored and handled in an atmosphere of cylinder nitrogen from which traces of oxygen had been scrubbed by bubbling through chromium(II) solutions. Europium(II) solutions were kept in pyrex bottles with self-sealing rubber caps, under a positive pressure. Europium(II) solutions were analyzed by oxidation with a small excess of pentaamminechlorocobalt(III); the cobalt(II) produced was analyzed spectrophotometrically in a solution 1.3M in thiocyanate and 50 volume percent acetone. The absorbance of the solution was measured at 6230Å, a wavelength of maximum absorption; the molar absorptivity is 1842 $M^{-1}cm^{-1}$.

Chromium(II) perchlorate solutions were prepared by dissolving high-purity chromium metal in perchloric acid or by reduction of chromium(III) in perchloric acid with zinc amalgam. The preparation of chromium(III) perchlorate by reduction of chromium(VI) has been described (38). Chromium (II) analyses were done in the same way as europium(II) analyses.

Reagent grade hydrofluoric, hydrochloric, perchloric, and hydrobromic acids were used without further purification. These acids were analyzed by titration with sodium hydroxide

to a phenolphthalein endpoint.

Sodium thiocyanate, sodium azide, lithium chloride, and lithium perchlorate were each prepared by dissolution of the salt in water, followed by filtration and two successive recrystallizations. Lithium and sodium perchlorates were also made by reaction of the reagent grade carbonates with perchloric acid, followed by two crystallizations. Each of these salts except sodium azide was analyzed by replacing the metal ions with protons from acid form Dowex 50-W cation exchange resin and titrating with sodium hydroxide. Sodium azide was used directly in some experiments but was converted to HN_3 in experiments at low acidity, to avoid undertainty in $[H^+]$. Hydrazoic acid solutions were prepared from the sodium salt by ion exchange (32). Azide solutions were analyzed by oxidation with cerium(IV) and titration of excess cerium(IV) with iron(II). Hydrazoic acid solutions were also analyzed by direct titration with sodium hydroxide, to check completeness of ion exchange. A sodium flame test was used as a more severe completeness check; no sodium was detected by either method in hydrazoic acid solutions.

A stock solution of lithium thiocyanate was prepared from sodium thiocyanate by ion exchange. A flame test revealed some sodium ions remaining after the exchange procedure. The lithium thiocyanate solution was analyzed in the same way as sodium thiocyanate solutions.

Reagent grade potassium cyanate was dried at 65°, stored in a desiccator, and measured by weighing. Solutions of NCO^- or HNCO could not be stored or accurately analyzed due to the hydrolysis of HNCO to form CO_2 and NH_4^+ (39). A sodium cyanate solution was made by adding silver cyanate crystals to an analyzed solution of sodium chloride at ca. 0°. Silver chloride and excess silver cyanate were removed by filtration; the number of moles of sodium cyanate in the solution was taken as the number of moles of sodium chloride present initially. The silver cyanate crystals were made by adding recrystallized reagent grade silver nitrate to a solution made from recrystallized reagent grade urea, and heating to 70-90°. Sodium cyanate was also prepared by titration of a weighed sample of the potassium salt with sodium perchlorate at ca. 0°, until additional perchlorate failed to precipitate potassium perchlorate. Potassium perchlorate was removed by filtration.

Sodium hydroxide solutions used for acid analyses were made from reagent grade pellets and standardized with dried potassium hydrogen phthalate.

The water used in most experiments was redistilled from alkaline permanganate in a tin-lined Barnstead still. Laboratory distilled water was used for a few kinetic studies; this change in source of water did not change the measured rate constants.

Equipment

Most of the kinetic measurements were made by a stopped-flow technique. The stopped-flow apparatus was based on the design of Dulz and Sutin (17). A diagram of the apparatus is given in Figure 1. Mixing was accomplished by causing a motor-driven block (with slip clutch) to push the plungers of two reactant syringes, forcing reagents through an eight-jet Teflon mixing chamber into a 2 or 3-mm ID quartz observation tube, and finally into a stopping syringe. As a measure of mixing effectiveness, reaction between .01M p-nitrophenol and .01M sodium hydroxide (40) was complete in the time required for the solution to reach the observation point (3-5 msec). The most efficient mixing was obtained when the two solutions had approximately equal densities, a condition satisfactorily obtained by preventing large ionic strength disparities in the two solutions.

The changing transmittance of the solution in the observation tube was observed spectrophotometrically. A Beckman Model DU monochromator was used. A tungsten lamp operated by three 6-V storage batteries wired in parallel with a conventional battery charger was used initially; later a quartz iodide lamp (General Electric 1959) operated by a Sorensen (QRC 40-8A) power supply and a deuterium lamp operated by a Beckman Model 2965 hydrogen lamp power supply were used. The light intensity was monitored by an EMI 6256 B photomultiplier

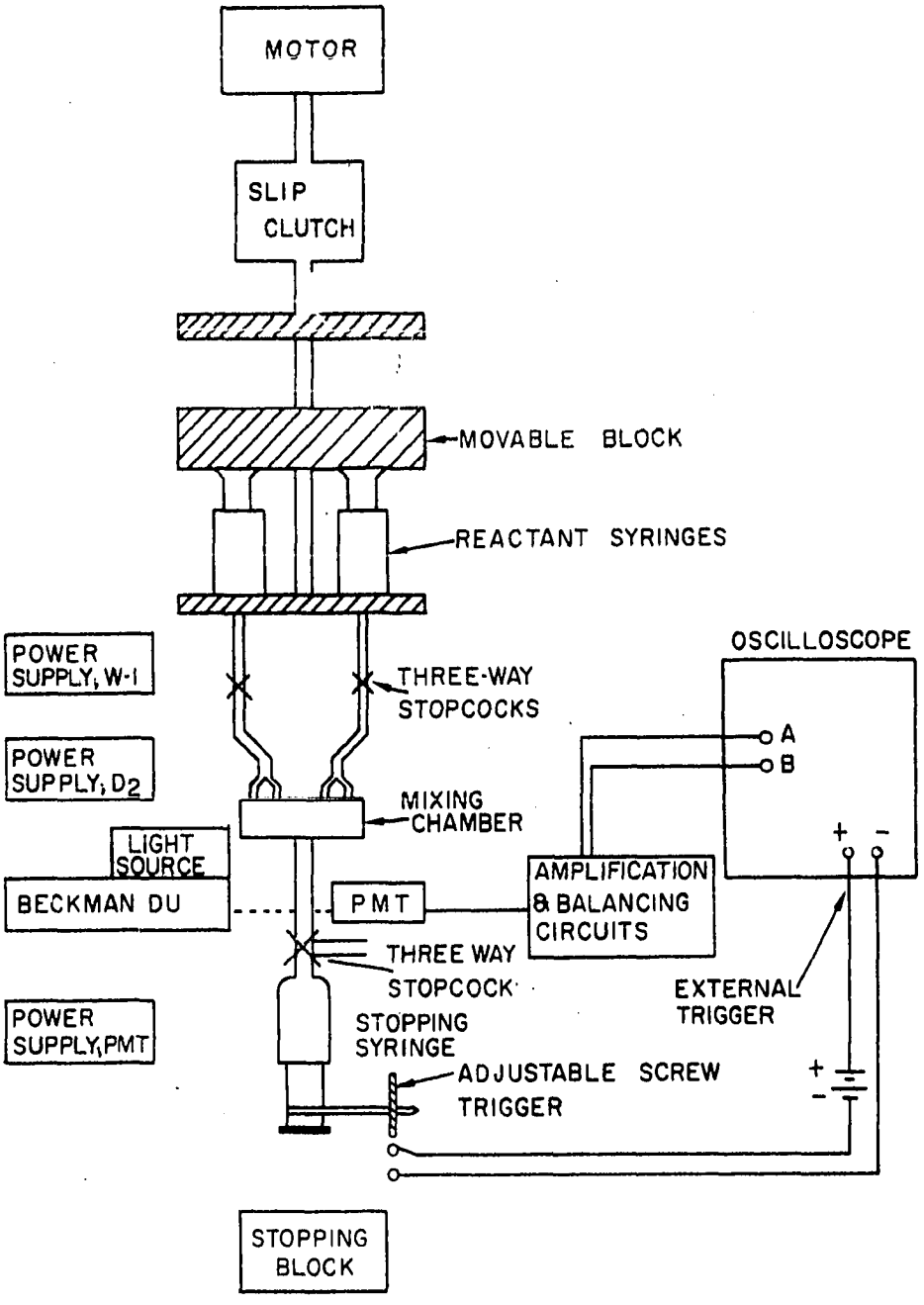

Figure 1. Stopped-flow apparatus

tube (PMT), biased by a continuously variable 0-1000 V, 0-20 ma, regulated power supply (Kepco No. ABC 1000M). The monochromator slit was opened to 2.0 mm; the resulting high light level permitted the bias voltage to be kept low, thus minimizing noise.

The signal from the photomultiplier provided the A input of a Tektronix 535A or Tektronix 564 oscilloscope, via an amplifying and smoothing circuit (41). A constant balancing potential was connected to the B input of the oscilloscope, and the difference (A-B) was amplified. The balancing potential permitted amplification of changes as small as 6 mv to the full vertical scale of the oscilloscope. A triggering circuit initiated a single oscilloscope trace sweep at the instant mixed solution filled the stopping syringe, and a second sweep could be provided manually. The oscilloscope traces were recorded with a Polaroid camera. The time scale of the oscilloscope was checked with a time mark generator, Tektronix Model 181. The vertical displacement of the trace represents the transmittance change. Provided the absorbance change is limited to less than ca. 0.1, absorbance and transmittance are proportional, and the trace may be treated as a concentration-time curve.

Temperature control in the stopped-flow apparatus was maintained by a constant temperature water bath, with water circulating through a system of jackets. The reactant

syringes and the mixing chamber were jacketed, and the reactant flasks were immersed in the bath. Reactions occurring at temperatures 10° or more removed from room temperature were not assumed to occur at the temperature of the water bath; the temperature of solution leaving the observation tube was measured by thermometer or thermistor.

Stopped-Flow Experiments

A typical stopped-flow experiment with an air-oxidizable reagent was done in the following way. Each of the two reactant solutions was prepared complete but for the air-sensitive reagent, and positioned in the water bath. Each reactant flask contained a glass tube with a male ground glass taper for attachment to the corresponding female taper pointing downward from the 3-way stopcock (see Figure 1). Each reactant flask contained a second glass tube for introduction of deoxygenated N_2. The top of each flask was covered with Parafilm and N_2 was bubbled vigorously for 20-30 minutes. After the bubbling period, the air sensitive reagent was added to the appropriate reactant flask from a syringe with a long needle. The reactant solutions were drawn into the stopped-flow reactant syringes by causing the motor to pull the movable block (see Figure 1) backward. Air initially in the pathways from reactant flasks to reactant syringes was prevented from entering the syringes by drawing air only to the

syringe tips, changing the 3-way stopcocks and forcing the air through the mixing chamber, again changing the stopcocks, drawing in more air, and continuing in a cyclic process until the air was removed. The reactant syringes were partially filled and emptied three times before data were recorded. The monochromator was set to provide light of the desired wavelength, the photomultiplier voltage and oscilloscope sensitivity were adjusted to give a deflection change suitable for photographing, an appropriate trigger adjustment was made (see Figure 1) and the stopped-flow sequence (described above) was carried out. Four or five duplicate photographs were made for each set of solutions. Immediately after the last photograph, the air sensitive reagent was sampled (using a syringe with a long Teflon needle) for analysis for Cr^{2+} or Eu^{2+}.

A Cary Model 14 recording spectrophotometer with a thermostated cell compartment was used for equilibrium absorbance measurements, recording of spectra, spectrophotometric analyses, and some kinetics experiments.

Substitution Kinetics Experiments

All experiments were done at 1.0M ionic strength, maintained with $LiClO_4$ unless otherwise noted. Experiments were done measuring the rate at which ligands (X) coordinate to $Fe(H_2O)_6^{3+}$, or leave $Fe(H_2O)_5X^{2+}$, where X was N_3, Cl, Br, NCS, or NCO. The most complete study was done with the ligand

$X = N_3$. The stopped-flow apparatus was used to make two basic observations (in experiments to be called formation, or dilution); in formation experiments the separate reagents Fe^{3+} and HN_3 were mixed and the subsequent absorbance increase (at or near 4600Å) due to the formation of FeN_3^{2+} was observed (31). Dilution experiments were done by mixing an equilibrium solution of FeN_3^{2+}, Fe^{3+}, and HN_3 with $HClO_4$ solution; the subsequent absorbance decrease at 4600Å was observed. Since the initial concentration of FeN_3^{2+} was above its equilibrium value in dilution experiments, these experiments resulted in observable absorbance changes at concentrations of Fe(III) and HN_3 considerably below the limit in formation experiments.

Formation experiments involving two different types of concentration choices were done. One set of concentrations was chosen so that the small equilibrium concentration of FeN_3^{2+} appreciably affected the concentrations of neither Fe^{3+} nor HN_3. As will be shown later, these experiments provided only aquation rate data, despite the fact that net complexation was occurring. The other set of concentrations was chosen so that the equilibrium concentration of FeN_3^{2+} was large relative to the total limiting reagent concentration (e.g., either Fe^{3+} or HN_3 was present in large excess). Low hydrogen ion concentrations were chosen for these experiments, again to facilitate complexation. These experiments provided both aquation and complexation rate data.

Dilution experiments involving the corresponding concentration choices provided rate data that had the same significance as data from formation experiments, despite the different direction of net reaction in the two instances.

Values of the ordinate were read from the photographed oscilloscope trace in arbitrary units proportional to the output voltage V of the photomultiplier follower, and proportional to transmittance change, to absorbance change, and to concentration change (see above). First-order rate constants were calculated from slopes of conventional plots of log V_t-V_∞ vs. time, or from plots (based on the method of Guggenheim (42)) of log $V_t-V_{t+\tau}$ vs. time.

Limited stopped-flow measurements were made for substitution reactions involving the ligands Cl, Br and SCN. The techniques and concentration choices employed for these ligands were chosen from those described above for the studies on azidoiron(III) ion.

Some conventional spectrophotometric kinetic measurements were made for substitution reactions involving the ligand NCO^-. These experiments were not in principle different from the stopped-flow substitution experiments. Both formation and dilution experiments were done (using NaNCO from each of the preparations described above) and concentrations were chosen so that much of the HNCO would be complexed at equilibrium, in order to obtain both complexation and aquation rate data.

The instability of HNCO in water required special techniques; the NaNCO was prepared just before use and was added to acid-containing solutions only a few seconds before each experiment was to begin (acid catalyzes the decomposition of HNCO (39)). The absorbance-time traces recorded for the reactions did not appear first-order; in all experiments a slow absorbance decrease occurred after the rapid initial change was complete. The slow decrease was attributed to decomposition of HNCO. After each absorbance-time trace was corrected for the slow decrease, assumed to be uniform and occurring from the start of the experiment, satisfactory first order plots were obtained.

Aquoion Oxidation-Reduction Experiments

The reduction of Fe(III) by Eu(II) and by Cr(II) was studied in the absence of anions other than perchlorate. All rate measurements on these rapid reactions were accomplished by the stopped-flow technique. A fresh dilution of the reactants was used for successive kinetic experiments in order to vary the reactant concentrations. Since these concentrations ranged as low as 5×10^{-5} M, it was deemed necessary to sample each reductant solution (generally in triplicate) directly in the stopped-flow reactant flask at the conclusion of the rate measurements. In some Eu^{2+} reductions sampling was also done at the start of the measurements, but the decrease in $[Eu^{2+}]$

was so slight that this double analysis was eventually abandoned.

Reactions were initiated by mixing the solution containing iron(III) with the solution containing europium(II) or chromium(II). The europium(II) reductions were studies at wavelengths where absorption was due mainly to Eu^{2+} (4000-3200Å) as well as at wavelengths where both reactants absorbed (2700-2400Å). The chromium reductions were studied at wavelengths where absorption was primarily due to iron(III) (2600-2400Å). Molar absorptivities of reactants (those of the products are negligible in these experiments) are as follows at the wavelength of interest: Fe^{3+}, λ = 4000-2400Å (ϵ = 0-4230); Eu^{2+}, λ = 4000-2400Å (ϵ = 75-1600), with maxima at 3200 (ϵ = 640) and about 2500Å (ϵ = 1700).

Anion Catalysis of Oxidation-Reduction Reactions

Iron(III) species were reduced by europium(II) and by chromium(II) species in the presence of the following ions or their acids: F^-, Cl^-, Br^-, N_3^-, NCS^-, and NCO^-. The catalytic effects of these ions were observed in two types of experiments. In one type of experiment the ions X^- were contained in the Fe(III) reactant prior to mixing; second order reactions Eqs 1, 2 were observable in these experiments. In the other type of catalysis the ions X^- were contained in the Cr(II) or Eu(II) reactant prior to mixing; third order

reactions Eqs 3,4 were observable in these experiments.

$$FeX^{2+} + Eu^{2+} = Fe^{2+} + Eu^{3+} + X^- \quad (1)$$

$$FeX^{2+} + Cr^{2+} = Fe^{2+} + CrX^{2+} \quad (2)$$

$$Fe^{3+} + X^- + Eu^{2+} = Fe^{2+} + Eu^{3+} + X^- \quad (3)$$

$$Fe^{3+} + X^- + Cr^{2+} = Fe^{2+} + CrX^{2+} \quad (4)$$

The third order reactions were not observed for the basic ions F^-, N_3^-, or NCO^-. Treatment of reactions Eq 1,2 as second order processes implies the assumption that reduction of Fe^{3+} as well as substitution equilibria are slow relative to reduction of FeX^{2+}. These assumptions are held to be valid in the experiments reported here, except for the Eu^{2+} reduction of $FeBr^{2+}$; evidence supporting these contentions will be presented later.

Two reductions of the inner-sphere FeX^{2+} complexes were too fast for direct measurement by the stopped-flow technique described above. These reactions were the Eu^{2+} reduction of FeF^{2+} and the Cr^{2+} reduction of $FeBr^{2+}$. A competition method was used to obtain k_F for the reaction of Eu^{2+} and FeF^{2+}. A solution containing both the complexes FeF^{2+} and FeN_3^{2+} was prepared, and it was reacted with Eu^{2+}. Azidoiron(III) was chosen because (a) its rate of reaction with Eu^{2+}, compared to the Eu^{2+}-FeF^{2+} rate, was suitable for partial reduction of each complex and (b) FeN_3^{2+} absorbs intensely

(λ_{max} = 4600Å, ε = 4400 M-1cm-1). The experiment was designed to measure the residual FeN_3^{2+} immediately after complete oxidation of Eu^{2+}, compared to its starting concentration.

Product Analysis

The 2+ charged chromium products of the Cr^{2+} reductions of FeF^{2+} and $FeBr^{2+}$ were separated from iron species and from $Cr(H_2O)_6^{3+}$ by a cation exchange technique. A chromium(II) solution was mixed with an excess of FeX^{2+} using the stopped-flow mixing chamber (slow addition of Cr^{2+} to a stirred iron (III) solution did not provide adequate mixing). The material collected after mixing was treated with H_2O_2 to oxidize Fe^{2+}, diluted to an ionic strength of less than 0.3, and passed through a 15-25 cm column of Dowex 50W-X8 cation exchange resin in the hydrogen ion form. The 2+ ions were eluted from the resin with 1 M $HClO_4$; the visible spectrum was recorded and total Cr was determined by the alkaline chromate method (43). The separation technique was checked by separating known quantities of independently prepared CrX^{2+} from iron (III) solutions; recovery generally exceeded 96%, independent of the presence of Cr^{3+}, Fe^{2+}, and Fe^{3+}.

The ion exchange separation was also used to evaluate $Q^i_{Br} = [FeBr^{2+}]/[Fe^{3+}][Br^-]$. An excess of Cr^{2+} was mixed with a solution of $FeBr^{2+}$; the concentration of $CrBr^{2+}$ in the

resulting solution was used to calculate Q^1_{Br}, after making appropriate corrections as discussed in a later section.

The absorbances of equilibrium mixtures of Fe^{3+}, HN_3, and FeN_3^{2+} were measured to determine $Q_{N_3} = [FeN_3^{2+}][H^+]/[Fe^{3+}][HN_3]$. The absorbances were measured at 4600Å, the wavelength of maximum absorbance for FeN_3^{2+}; other species did not absorb at 4600Å. These measurements were done under conditions of excess HN_3 (0.01-0.1F, with 10^{-4} M Fe(III) in 0.05 M acid) and under conditions of excess Fe^{3+} (0.01-0.07F, with 10^{-4} F HN_3 in 0.05 and 0.1 M H^+). The experiments in excess HN_3 were similar to those reported earlier (32). Similar measurements were made for the Fe^{3+}, Br^-, $FeBr^{2+}$ system, at 4050Å.

The absorbances of equilibrium mixtures of Fe^{3+}, FeF^{2+}, FeN_3^{2+}, HF, and HN_3 were measured at 4600Å, where FeN_3^{2+} was the only absorbing species. The value of $Q_F = [FeF^{2+}][H^+]/[Fe^{3+}][HF]$ was calculated from these measurements by a method described in the results section.

Approximate values of the equilibrium constants for formation of $FeNCS^{2+}$ and FeN_3^{2+} at various temperatures were determined from values known at one temperature, assuming the molar absorptivity of the complex is independent of temperature.

RESULTS

Azidoiron(III) Substitution and Equilibrium Properties

Rate law

The net equation describing the equilibrium among the species Fe^{3+}, HN_3, and FeN_3^{2+} in acidic aqueous solution is

$$Fe(H_2O)_6^{3+} + HN_3 = (H_2O)_5FeN_3^{2+} + H^+ + H_2O. \qquad (5)$$

A study of the rate of the reverse of Eq 5 (aquation) at 25° has been reported by Seewald and Sutin (31). Using available equilibrium data (32,33), Seewald and Sutin computed rate constants for the forward (complexation) reaction. The present work extended the earlier studies on FeN_3^{2+} and provided the following results: (1) a direct measure of the rate of complexation, (2) a study of the temperature dependence of the aquation rate constants, (3) a study of the rate of approach to equilibrium from both sides, and (4) a kinetic check on the equilibrium quotient for reaction 5.

The hydrogen ion concentration was large relative to the amount of chemical change in every experiment designed to measure the rate of approach to equilibrium by reaction 5. As a working hypothesis, the rate law in Eq 6 was assumed,

$$d[FeN_3^{2+}]/dt = k_f'[Fe^{3+}][HN_3] - k_{aq}'[FeN_3^{2+}] \qquad (6)$$

in terms of the species predominant at the acidities under consideration (e.g. .01-.98 M H^+).

The rate constants in Eq 6 are pseudo-constants dependent upon $[H^+]$, both because of the form of the net reaction

(Eq 5) and because the aquation mechanism consists of parallel paths with different numbers of protons in the activated complexes (31). If Eq 6 is valid at a particular acidity, then an expression for the observed rate can be derived in the following manner.

$$[Fe^{3+}] = [Fe^{3+}]_{eq} + \left\{ [FeN_3^{2+}]_{eq} - [FeN_3^{2+}] \right\}$$

$$[HN_3] = [HN_3]_{eq} + \left\{ [FeN_3^{2+}]_{eq} - [FeN_3^{2+}] \right\}$$

$$[FeN_3^{2+}] = - \left\{ [FeN_3^{2+}]_{eq} - [FeN_3^{2+}] \right\} + [FeN_3^{2+}]_{eq}$$

$$\frac{d\left\{[FeN_3^{2+}]_{eq}-[FeN_3^{2+}]\right\}}{dt} = k_f'[Fe^{3+}]_{eq}[HN_3]_{eq} + k_f' \left\{ [FeN_3^{2+}]_{eq} + [HN_3]_{eq} \right\} \left\{ [FeN_3^{2+}]_{eq} - [FeN_3^{2+}] \right\} + k_f' \left\{ [FeN_3^{2+}]_{eq} - [FeN_3^{2+}] \right\}^2 + k_{aq}' \left\{ [FeN_3^{2+}]_{eq} - [FeN_3^{2+}] \right\} - k_{aq}' [FeN_3^{2+}]_{eq} .$$

But, from the equilibrium condition, $k_f'[Fe^{3+}]_{eq}[HN_3]_{eq} = k_{aq}'[FeN_3^{2+}]_{eq}$, and under some concentration conditions, including all those employed here, $k_f' \left\{ [FeN_3^{2+}]_{eq} - [FeN_3^{2+}] \right\}^2$ is negligible; thus, the expression simplifies to Eq 7 .

$$\frac{d \ln \left\{ [FeN_3^{2+}]_{eq} - [FeN_3^{2+}] \right\}}{dt} = k_f' \left\{ [Fe^{3+}]_{eq} + [HN_3]_{eq} \right\} + k_{aq}' \qquad (7)$$

The working hypothesis, by way of Eq 7 , thus permits the following deductions, each amenable to experimental checking: (1) the rate of approach to equilibrium will follow pseudo-

first-order kinetics, (2) the pseudo-first-order rate constant for approach to equilibrium will be $k_f' \{[Fe^{3+}]_{eq} + [HN_3]_{eq}\} + k_{aq}'$, (3) in experiments (either formation or dilution) where the sum $[Fe^{3+}]_{eq} + [HN_3]_{eq}$ is very small (which are also experiments in which neither reactant is complexed significantly at equilibrium), the observed rate constant for approach to equilibrium will be k_{aq}', and (4) in experiments with high $[HN_3]_{eq}$ or $[Fe^{3+}]_{eq}$, where an appreciable fraction of the limiting reagent is complexed, each term in the pseudo-first-order rate constant indicated in Eq 7 will contribute appreciably to the observed rate constant, permitting evaluation of both k_{aq}' and k_f'.

Point (1) above was verified in a series of rate measurements in solutions containing 0.44M H^+; the rate of approach to equilibrium did indeed follow first order kinetics. The observed rate constant was the same in formation as in dilution experiments. The results of the experiments are presented in Table 1; typical stopped-flow transmittance-time curves from experiments leading to the seventh and ninth entries in Table 1 are shown in Figure 2. The curves shown in Figure 2 are the basis for the first-order Guggenheim (42) plots shown in Figure 3. All the first order rate constants measured in this study were evaluated from the slope of Guggenheim plots, as in Figure 3, or from the slope of plots of $D-D_\infty$ vs time (where D represents deflection, or absorbance,

Figure 2. Typical stopped-flow transmittance-time plots for approach to equilibrium by azidoiron(III) solutions. The upper plot is from one of the formation experiments leading to the seventh entry in Table 1. The lower plot is from one of the dilution experiments leading to the ninth entry. The time scale in both plots is 50 msec per major division

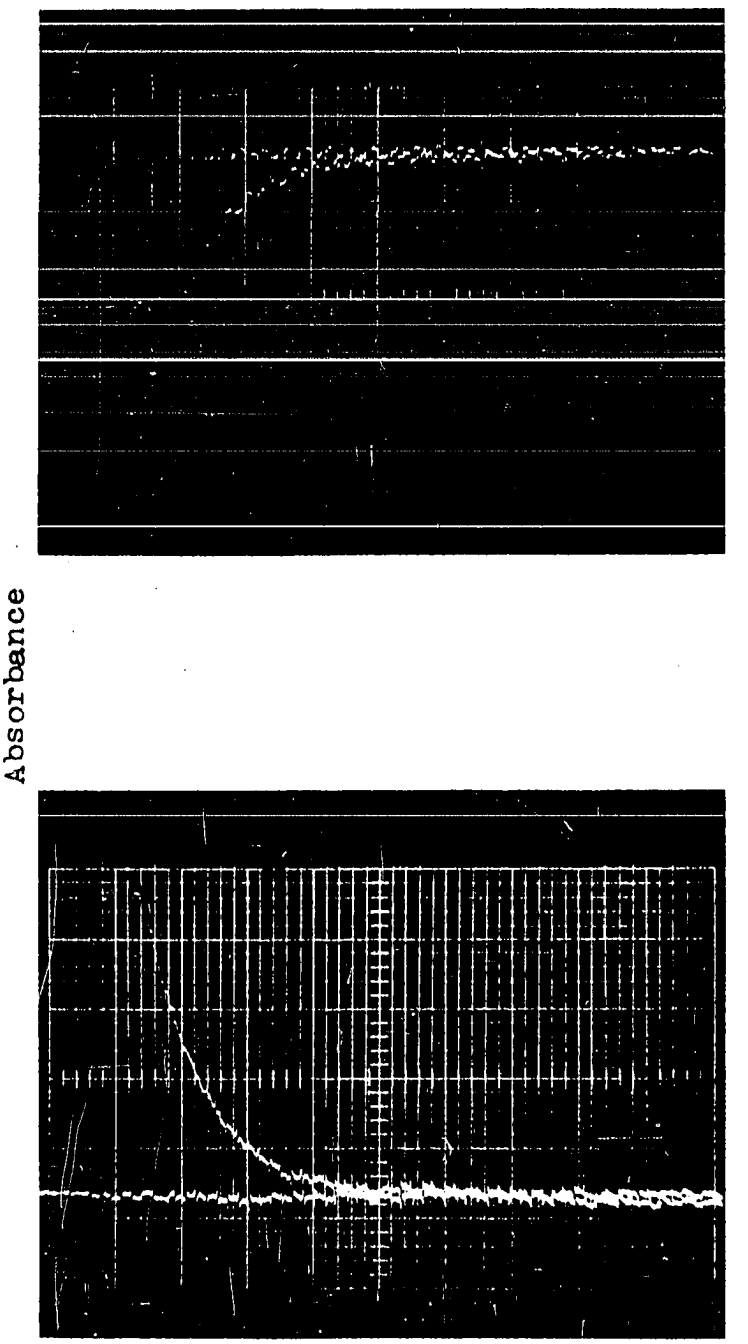
Absorbance
Time

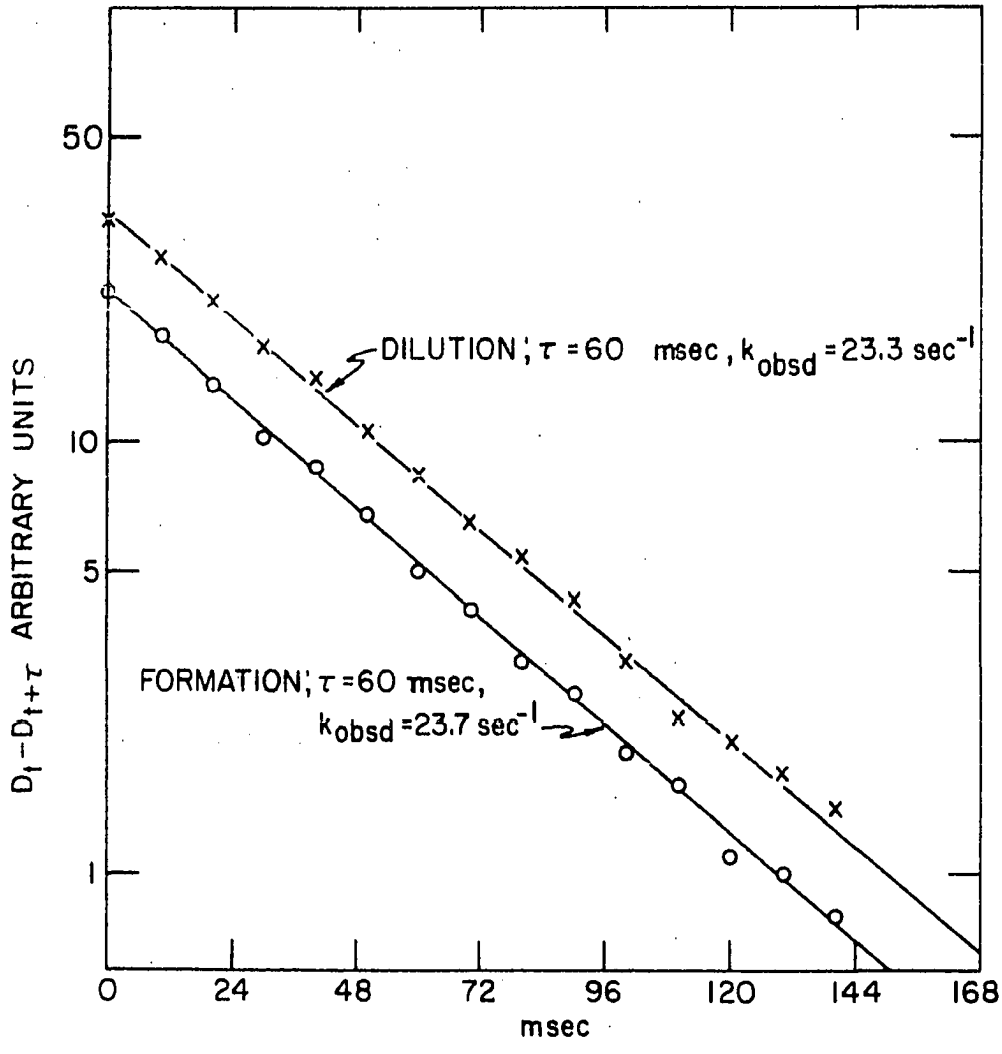

Figure 3. First-order Guggenheim plots, for approach to equilibrium by azidoiron(III) solutions, obtained from Figure 2

in arbitrary units).

Table 1. Aquation rate of azidoiron(III) at 0.44M H^+, 25.0°, 1.00M ionic strength

Expt. No.	$10^3[Fe^{3+}]$ M	$10^3[HN_3]$ M	Type[a]	k_{obsd} sec^{-1}	$k'_{aq}(cor)$[a] sec^{-1}
1	0.10	4.00	Dilution	22.0	21.9
2	0.30	0.30	Dilution	24.1	23.9
3	0.90	3.00	Formation	22.5	22.4
4	2.00	1.50	Formation	23.2	23.1[b]
5	2.00	8.00	Formation	22.3	22.0
6	2.00	15.0	Formation	23.8	23.4
7	3.38	3.00	Formation	23.3	23.1
8	3.38	3.00	Formation	22.9	22.8[b]
9	3.38	3.00	Dilution	23.7	23.6[c]
10	4.00	0.10	Dilution	24.4	24.3
11	4.00	1.80	Formation	23.5	23.3
12	6.00	6.00	Formation	23.3	23.0
13	8.00	0.75	Formation	22.9	22.7
14	10.0	3.00	Formation	23.6	23.2
15	10.0	3.00	Formation	22.9	22.6[b]
16	10.0	15.0	Formation	24.4	23.8[d]
17	10.0	15.0	Formation	23.8	23.2[e]

[a]See text; λ = 4600Å unless noted otherwise.

[b]Sodium perchlorate rather than lithium perchlorate was used to maintain ionic strength.

[c]λ = 4200Å.

[d]λ = 3950Å.

[e]λ = 6000Å.

The initial concentration ranges described in Table 1 are 1.00×10^{-4}-1.00×10^{-2}M Fe(III), a 100-fold variation, and 1.00×10^{-4}-1.50×10^{-2}M HN_3, a 150-fold variation. The constancy of the observed rate constant over this entire range of reactant concentrations confirmed point (4) above (e.g. the

observed rate constant was not expected to be sensitive to the sum $[Fe^{3+}]_{eq} + [HN_3]_{eq}$ when that sum was small). These results also confirmed the earlier report (31) that the observed rate constant was first order and independent of $[Fe^{3+}]$ and $[HN_3]$ over an extended range of concentrations.

Even though the contribution to k_{obsd} from the k_f' term in Eq 7 is small, it can be estimated from the measured k_{aq}' value and from previously reported (32,33) measurements of Q_{N_3},

$$Q_{N_3} = \frac{[FeN_3^{2+}][H^+]}{[Fe^{3+}][HN_3]} .$$

The expression $k_f' = Q_{N_3}k_{aq}'/[H^+]$ follows from the form of Eq 6 and of the quotient Q_{N_3}. Values of the expression $k_f' \{[Fe^{3+}]_{eq} + [HN_3]_{eq}\}$ were calculated for each experiment; though these values were small they were subtracted from k_{obsd} to give the values labeled k_{aq}'(cor) in Table 1 (and in Table 2). The correction was only 3% of k_{obsd} at the highest value of $[FeN_3^{2+}]_{eq} + [HN_3]_{eq}$ studied (0.026M) at 0.44M H^+ and was within the experimental error, although the correction was more important when applied to experiments at lower $[H^+]$.

Hydrogen ion and temperature variations

The acid dependence of the rate constant k_{aq}' was reported by Seewald and Sutin (31) to be of the form given by Eq 8 with $k_{2aq} = 19.0 \pm 1.4$ sec^{-1} and $k_{1aq} = 7.0 \pm 1.4$M^{-1}sec^{-1} at

$$k_{aq}' = k_{2aq} + k_{1aq}[H^+] \qquad (8)$$

25.0° and I = 1.00M ($NaClO_4$). Experiments done in connection with this work, covering the range 0.01-0.98M H^+ led to the same acid dependence, with $k_{2aq} = 20.0 \pm 0.9$ sec^{-1} and $k_{1aq} = 5.1 \pm 1.3 M^{-1}sec^{-1}$ at 25.0° and I = 1.00M ($LiClO_4$); see Figure 4 and Tables 2 and 3. Systematic differences exist between the results of this work and those of the previous work (31), but the differences are within the variation one might expect between Na^+ and Li^+ media (9). The uncertainties associated with the individual parameters suggest, however, that the results of the two studies are not greatly different.

Rate measurements as a function of $[H^+]$ were also made at 15.8 and 34.2° in order to obtain the temperature dependences of k_{2aq} and k_{1aq}; the results are described in Figure 4 and Tables 2 and 3. The corrected aquation rate constants (the value H^o = 2.03 kcal/mole for Eq 5 (32), together with observed k'_{aq} values, was used in the calculation of k'_f at 15.8 and 34.2°) were fitted to Eq 8, assuming the absolute rate theory expression 9, with $\kappa = 1$, holds for each rate

$$k = \kappa (RT/Nh)\exp(\Delta S^*/R - \Delta H^*/RT) \qquad (9)$$

constant. This fit of $[H^+]$ and temperature dependence was carried out simultaneously using a non-linear least-squares computer program (44). Each rate constant was weighted according to the square of its reciprocal because the per

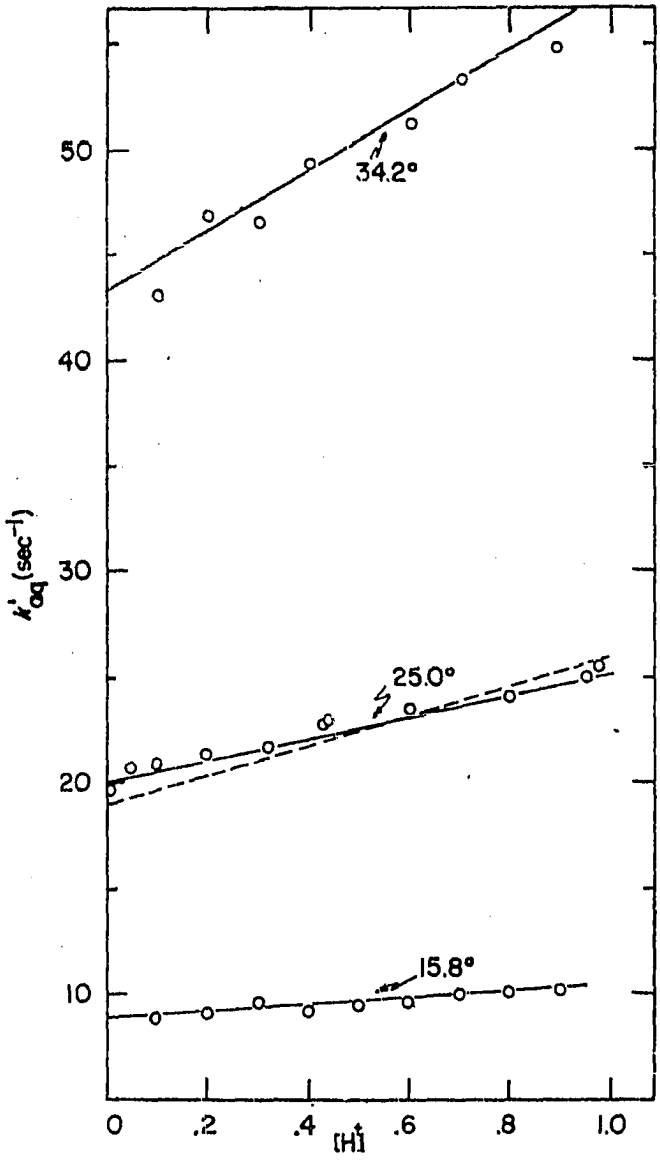

Figure 4. Temperature and $[H^+]$ dependence of k'. The points represent measured information. The solid lines are the computer-calculated best fit to the points. The dashed line represents the data of Seewald and Sutin (31)

cent uncertainty in a given measurement was roughly constant. Of the 252 individual rate constants, 25 had values $\{k_{obsd(cor)} - k_{calc}\}/k_{obsd(cor)}$ greater than 0.1; these were not included in a second computation, and are not reflected in Tables 2 and 3. The activation parameters, with standard deviations calculated by the program are listed in Table 3.

Competing equilibria

The competing equilibria described by Eq 10 and 11 change the molarities of H^+ and Fe^{3+} from their formal values.

$$Fe^{3+} + H_2O = FeOH^{2+} + H^+ \qquad (10)$$

$$2Fe^{3+} + 2H_2O = Fe(OH)_2Fe^{4+} + 2H^+ \qquad (11)$$

These equilibria are important in calculating $[Fe^{3+}]$ and $[H^+]$ in both kinetic and equilibrium studies at high iron(III) concentrations. The equilibrium quotients for reactions 10 and 11 are: $Q_a = 1.65\times10^{-3}M$, $Q_d = (1.9\pm0.6)\times10^{-3}M$ (45) at 25.0° and unit ionic strength. Agreement among the several kinetic measurements and between kinetic and equilibrium measurements led to selection of the value $Q_d = 2.4\times10^{-3}M$; this is within the reported (45) range of values for Q_d.

Formation rate constants

As described earlier and as implied by Eq 7 , it was possible to do experiments (both of the formation and of the dilution type) in which the sum $[Fe^{3+}]_{eq} + [HN_3]_{eq}$ was made large and to measure rate constants that contained an appreciable k_f' contribution. Equation 7 suggests that a plot of

Table 2. Aquation rate of azidoiron(III) as a function of hydrogen ion concentration and temperature

Expt. No.	Temp. °C	$[H^+]$ M	$10^3[Fe^{3+}]$ M	$10^3[HN_3]$ M	k_{obsd} sec^{-1}	$k'_{aq}(cor)$[a] sec^{-1}
1	15.8	0.10	1.00	4.00	9.46	9.26
2	15.8	0.10	2.00	2.00	8.73	8.57
3	15.8	0.20	5.00	2.00	9.08	8.94
4	15.8	0.20	3.00	3.00	9.22	9.08
5	15.8	0.30	1.00	9.00	9.70	9.56
6	15.8	0.40	2.00	4.50	9.23	9.16
7	15.8	0.50	10.0	3.00	9.60	9.49
8	15.8	0.60	6.00	3.00	10.04	9.98
9	15.8	0.60	2.00	9.00	9.29	9.21
10	15.8	0.70	3.00	6.00	10.1	10.0
11	15.8	0.80	10.0	4.00	10.0	9.92
12	15.8	0.80	6.00	10.0	10.3	10.2
13	15.8	0.90	9.00	8.00	10.4	10.3
14	15.8	0.90	10.0	7.0	10.3	10.2
15	25.0	0.01	0.375	2.40	22.1	19.3
16	25.0	0.01	2.40	0.750	22.3	19.2
17	25.0	0.01	0.800	0.375	21.5	20.3
18	25.0	0.05	1.00	3.00	21.7	20.9
19	25.0	0.05	3.00	1.00	21.2	20.4
20	25.0	0.05	0.900	5.00	21.9	20.7
21	25.0	0.10	2.00	4.00	21.3	20.7
22	25.0	0.10	4.00	2.00	22.1	21.5
23	25.0	0.10	1.00	8.00	21.6	20.7
24	25.0	0.20	1.50	10.0	22.1	21.5
25	25.0	0.20	10.0	1.50	21.8	21.2
26	25.0	0.20	5.00	3.00	21.8	21.4
27	25.0	0.32	1.00	9.40	22.6	22.2
28	25.0	0.32	9.40	1.00	21.7	21.4
29	25.0	0.32	3.00	3.00	21.6	21.4
30	25.0	0.43	0.100	4.00	22.0	21.9
31	25.0	0.43	4.00	0.100	23.3	23.2
32	25.0	0.43	0.300	0.300	24.1	23.9
	25.0	0.44				23.0[b]
33	25.0	0.60	2.00	15.00	23.6	23.3

[a]See text.

[b]Data at 0.44M H^+, 25.0° are shown in Table 1.

Table 2. (Continued)

Expt. No.	Temp. °C	$[H^+]$ M	$10^3[Fe^{3+}]$ M	$10^3[HN_3]$ M	k_{obsd} sec^{-1}	$k'_{aq}(cor)^a$ sec^{-1}
34	25.0	0.60	8.00	4.00	23.9	23.7
35	25.0	0.60	4.00	8.00	23.8	23.6
36	25.00	0.80	10.0	6.00	23.6	23.4
37	25.0	0.80	6.00	10.0	25.2	25.0
38	25.0	0.80	5.00	8.00	23.9	23.7
39	25.0	0.954	6.00	10.0	25.2	25.0
40	25.0	0.974	4.00	2.00	25.6	25.5
41	25.0	0.980	2.00	8.00	25.2	25.1
42	34.2	0.10	2.00	2.00	44.2	43.2
43	34.2	0.10	1.00	4.00	44.1	42.9
44	34.2	0.20	3.00	6.00	48.1	46.9
45	34.2	0.30	1.00	9.00	47.5	46.6
46	34.2	0.40	10.0	4.50	50.4	49.4
47	34.2	0.60	9.00	6.00	51.9	51.2
48	34.2	0.70	3.00	6.00	53.7	53.3
49	34.2	0.888	17.0	10.0	55.8	54.8

Table 3. Temperature dependences of the rate constants for aquation of FeN_3^{2+}

Rate constant	Value of rate constant 15.8°	25.0°	34.2°	$\Delta S^{\ddagger}$ eu	$\Delta H^{\ddagger}$ kcal/mole
$k_{2aq}(sec^{-1})$	8.76	20.0	43.3	-3.2 ± 0.6	14.7 ± 0.2
$k_{1aq}(M^{-1}sec^{-1})$	1.7	5.1	14	11 ± 5	19.6 ± 1.4

k_{obsd} vs $\{[Fe^{3+}]_{eq} + [HN_3]_{eq}\}$ should be linear at a particular acid concentration, (e.g. constant $[H^+]$ was assumed in deriving Eq 7) with slope k_f'. The experiments done in solutions of high Fe(III) concentration had varying values of $[H^+]$, because of Eq 10 and 11; the nominal value of $[H^+]$ was 0.05M, but the exact value ranged from 0.051 - 0.058M. Because of the variation in $[H^+]$, the approximate Eq 12 was derived to suggest an alternate graphical method for getting k_f' from the data. Equation 12 is only approximately valid

$$k_{obsd} = k_{2f} [Fe^{3+}]_{eq} + [HN_3]_{eq} /[H^+] + k_{2aq} \qquad (12)$$

because it neglects the acid dependent aquation term and the opposing acid independent formation term. However the neglected k_{1aq} term carries only 1.3% of the aquation reaction at .05M H^+ as shown by results given earlier for k_{aq}'. The principle of microscopic reversibility requires that the opposing formation rate term (the one neglected) likewise carries only 1.3% of the formation reaction.

Figure 5 is the plot suggested by Eq 12. Points plotted in Figure 5 were obtained both from formation and from dilution measurements; each type of measurement included experiments with excess iron(III) and experiments with excess hydrazoic acid. The numerical results of these experiments are given in Table 4.

The points plotted in Figure 5 seem to yield two values for $k_f'[H^+]$ (e.g., slope): 13.5 $\pm$ 0.5 sec^{-1} obtained from

Table 4. Results of experiments measuring the rate of approach to equilibrium by Eq 5 in the presence of a large excess of Fe^{3+} or HN_3

Expt No.	$[H^+]$ M	$10^3 C_{Fe}$ M	$10^3 C_{HN_3}$ M	Type of[a] expt	k_{obsd} sec^{-1}	$\frac{([Fe^{3+}]+[HN_3])}{[H^+]}$[b]
1	0.0500	0.600	11.8	Dilution	24.3	0.236
2	0.0500	0.400	24.8	Dilution	27.6	0.496
3	0.0500	0.260	38.8	Dilution	30.0	0.776
4	0.0500	0.150	66.0	Dilution	39.2	1.320
5	0.0500	0.140	78.7	Dilution	40.3	1.574
6	0.0500	0.120	95.0	Dilution	49.2	1.900
7	0.0500	0.600	10.56	Formation	22.8	0.211
8	0.0500	0.400	25.6	Formation	24.8	0.512
9	0.0500	0.260	38.0	Formation	28.1	0.760
10	0.0500	0.080	48.7	Formation	29.9	0.974
11	0.0500	0.150	67.2	Formation	36.6	1.244
12	0.0500	0.140	81.3	Formation	35.2	1.626
13	0.050	0.120	96.8	Formation	40.1	1.936
14	0.0510	13.0	0.542	Dilution	22.8	0.235
15	0.0529	28.0	0.300	Dilution	25.6	0.475
16	0.0553	45.0	0.220	Dilution	26.9	0.718
17	0.0578	60.0	0.187	Dilution	30.9	0.903
18	0.0512	18.0	0.460	Formation	22.7	0.329
19	0.0526	32.0	0.290	Formation	26.3	0.560
20	0.0549	51.0	0.210	Formation	29.8	0.840
21	0.0558	70.0	0.170	Formation	32.2	1.151

[a]See text.

[b]The quantity $([Fe^{3+}]+[HN_3])/[H^+]$ is plotted in Figure 5.

dilution experiments with excess HN_3, or 10.1 $\pm$ 0.2 sec^{-1} obtained from the other three series of experiments. All the series of experiments gave an intercept (20 sec^{-1}) agreeing with the value of k'_{aq} at 0.05M H^+, obtained in measurements without large excesses of HN_3 of Fe^{3+}. The two values of

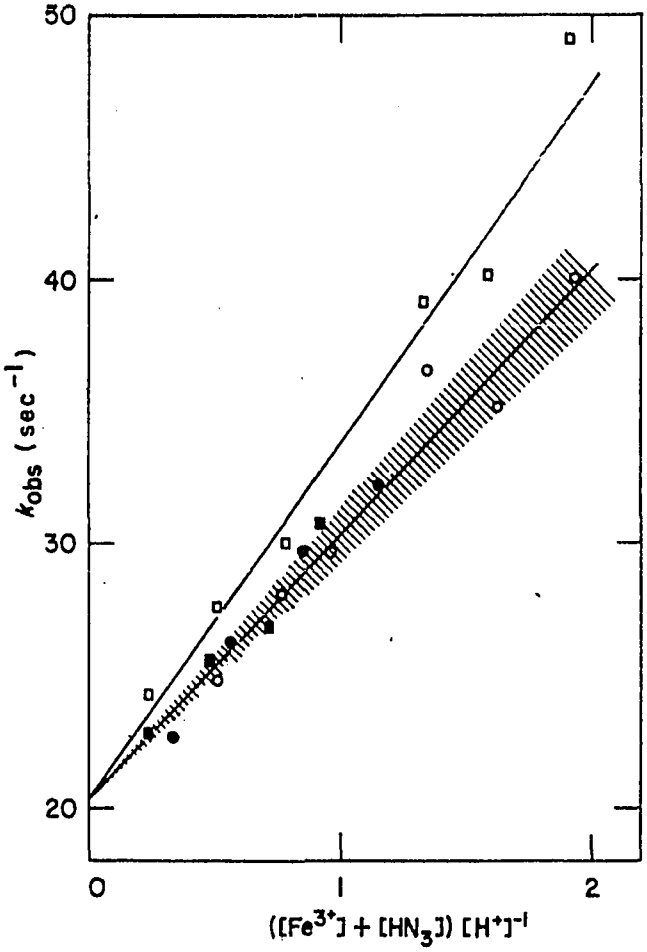

Figure 5. Evaluation of the formation rate constant k_f' in the plot suggested by Eq 12. The points refer to the following series of rate experiments all at 25.0° and 1.00M ionic strength; □ high HN_3 aquation; O high HN_3 formation; ● high Fe^{3+} formation; ■ high Fe^{3+} aquation. The latter 3 series are represented by a single line; the shading represents two standard deviations on either side of the line of best fit

$k_f'[H^+]$ lead to calculated equilibrium quotients for Eq 5 of $Q_{N_3} = 0.67 \pm 0.05$ or $Q_{N_3} = 0.498 \pm 0.035$, respectively. Although these values lie near the published value (32,33), $Q_{N_3} = 0.591$, the differences are larger than acceptable for experiments of this precision and especially the systematic direction of the deviations requires further explanation.

Equilibrium measurements

Because the kinetic procedures resulted in conflicting values for Q_{N_3}, a series of spectrophotometric measurements at 4600Å, where the only absorbing species is the azido complex, was carried out at unit ionic strength, 25.0°, and $[H^+]$ = .0500M. These studies were similar to the earlier work (32, 33) and covered the concentrations of 10^{-4} to 5×10^{-3}M iron(III) and 10^{-3} to 0.35 F hydrazoic acid, with 0.950M lithium perchlorate also present.

In addition to checking earlier work, two series of measurements were made in which iron(III) rather than hydrazoic acid was in excess. Iron(III) was extended to 0.07M in each set, with very low $[HN_3]$. One set of experiments was done at 0.051 - 0.056M H^+, and the other at 0.100 - 0.103M H^+, at 25.0° with ionic strength 1.00M, maintained with lithium perchlorate.

In all equilibrium studies the quantity $\bar{\epsilon}$ is defined as D/C_{lim} where D represents the absorbance enhancement due to complex formation and C_{lim} represents the formal concentration

of the reactant at low concentrations. On this basis Eq 13 is derived in the form suggested by Newton and Arcand (46),

$$\bar{\epsilon} = \epsilon_1 - \bar{\epsilon}[H^+]/Q_{N_3}[R]_{xs} \qquad (13)$$

where $[R]_{xs}$ represents the concentration of the reactant at high concentrations, and ϵ_1 is the molar absorptivity of azidoiron(III). Relation 13 allowed evaluation both of ϵ_1 and of Q_{N_3}. An iterative process was employed using the previous Q_{N_3} to calculate $[HN_3]$ and $[Fe^{3+}]$ and then using these concentrations to reevaluate ϵ_1 and Q_{N_3}. The results are shown numerically in Table 5 and graphically in Figure 6 in the plot suggested by Eq 13.

The results of the experiments lead to $Q_{N_3} = 0.596 \pm 0.015$ and $\epsilon_1 = 3570 \pm 60$ $M^{-1}cm^{-1}$ at high $[HN_3]$, in excellent agreement with the published values (32,33) derived from measurements under similar concentration conditions. The values in the high iron series, again using $Q_d = 2.4 \times 10^{-3}M$ in treating these data, are $Q_{N_3} = 0.512 \pm 0.015$ and $\epsilon_1 = 4400 \pm 160$ $M^{-1}cm^{-1}$ at 0.05 and 0.10M H^+.

Europium(II)-Iron(III) Reaction in Perchlorate Solution

Rate law

Aquoiron(III) was reduced by europium(II) in perchlorate solution according to the stoichiometry given in Eq 14.

$$Fe^{3+} + Eu^{2+} = Fe^{2+} + Eu^{3+} \qquad (14)$$

The rate law at constant hydrogen ion concentration is given by Eq 15. The second order rate constant k' was occasionally

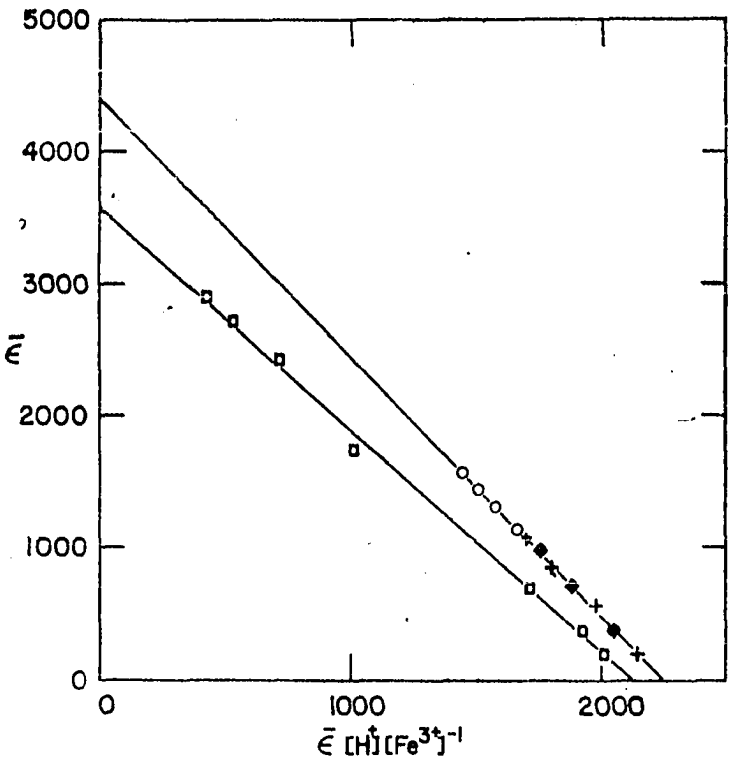

Figure 6. Evaluation of Q_{N_3} and $^{e}_{FeN_3}$ at 4600Å in plots suggested by Eq 13. The lower line refers to data at high HN_3, and the upper to data at high Fe^{3+} at 0.05 F (0) and 0.1F (+) perchloric acid. The abscissa at high HN_3 is $\bar{\epsilon}[H^+][HN_3]^{-1}$

Table 5. Spectrophotometric data for evaluation of Q_{N_3} at 25.0°, 1.0M ionic strength

Expt No.	$[H^+]$ M	$10^3 C_{Fe}$ M	$10^3 C_{HN_3}$ M	$\bar{\epsilon}^a$ M-1cm-1	$10^3[R]_{xs}$ M	$\bar{\epsilon}[H^+]/[R]_{xs}$ M-1cm-1
1	0.0503	5.00	5.00	190	4.74	2010
2	0.0504	5.00	10.00	368	9.56	1940
3	0.0501	1.00	20.0	684	19.9	1730
4	0.0500	0.100	86.0	1740	86.0	1010
5	0.0500	0.100	172	2426	172	705
6	0.0500	0.100	258	2710	258	525
7	0.0500	0.100	344	2890	344	420
8	0.0505	10.0	0.242	385	9.48	2050
9	0.0513	20.0	0.242	688	18.7	1890
10	0.0524	30.0	0.242	930	27.7	1760
11	0.0535	40.0	0.242	1136	36.5	1670
12	0.0548	50.0	0.242	1300	45.2	1580
13	0.0562	60.0	0.242	1442	53.8	1506
14	0.0577	70.0	0.242	1556	62.3	1440
15	0.1002	10.0	0.242	210	9.77	2150
16	0.1006	20.0	0.242	398	19.5	2060
17	0.1010	30.0	0.242	570	29.1	1980
18	0.1014	40.0	0.242	717	38.6	1880
19	0.1020	50.0	0.242	852	48.0	1810
20	0.1026	60.0	0.242	984	57.4	1760
21	0.1032	70.0	0.242	1099	66.8	1700

[a]This quantity is defined in the text.

$$\frac{-d[Eu(II)]}{dt} = \frac{-d[Fe(III)]}{dt} = k'[Fe(III)][Eu(II)] \qquad (15)$$

evaluated as the quotient of the observed pseudo-first-order rate constant and the concentration of the reagent in excess. The constant k' was more often derived from a plot of log(B/A) vs time, as suggested by the integrated rate law given in Eq 16, where [A] and [B] are reactant concentrations. The

$$\ln \frac{[B]}{[A]} = \ln \frac{[B]_0}{[A]_0} + ([B_0]-[A]_0)k't \qquad (16)$$

concentration of the limiting reagent (A) was calculated as a function of time from the fractional change of deflection D (Eq 17);

$$[A] = [A]_0 \frac{D_0 - D}{D_0 - D_\infty} \quad . \qquad (17)$$

Values of D_0, D, and D_∞ were read from the oscilloscope trace. The concentration of the ion in excess was then obtained from the stoichiometry by Eq 18, to make available

$$[B] = [B]_0 - [A]_0 + [A] \qquad (18)$$

all the quantities needed to evaluate k' according to Eq 16.

Evaluation of k' according to Eq 16 was complicated in the faster experiments by the time lag between mixing and first observation. The point of observation was removed from the mixing chamber by a distance corresponding to a time of 3-4 msec.

The time delay was obtained from a pseudo-first-order reaction with initial concentrations $[Fe(III)] = 39.0 \times 10^{-4}$, $[Eu(II)] = 2.60 \times 10^{-4}$, and $[H^+] = 0.300$. Linear plots of $D-D_\infty$ vs time were constructed from the observed data. The true (as opposed to the observed) D_0-D_∞ value was obtained by measuring the oscilloscope deflections caused by each of the individual reactant solutions and by the equilibrium mixture; D_0 was taken as midway between the reactant deflections and D_∞ as the equilibrium deflection. The $D-D_\infty$ plots were

extrapolated to the true D_0-D_∞ ; the time delays between true D_0-D_∞ and the first observed $D-D_\infty$ were read from the plot. The time delay measured for the high syringe speed setting used for the fast reactions was 3.5 ± 0.9 msec. In those fast second order experiments where appreciable reaction had occurred during the first 3.5 msec, values for [A] and [B] at first observation were calculated on the basis of an estimated value for k and the known delay time. These calculated concentrations were called $[A]_0$ and $[B]_0$ for use in Eq 16.

A series of 13 measurements of k' were made at 15.8°, in solutions containing 0.876M H^+ and 1.00M ionic strength. The reactant concentrations were varied over the ranges $2\times10^{-5} < [Fe(III)]_0 < 1.5\times10^{-2}$M and $8\times10^{-5} < [Eu(II)]_0 < 3\times10^{-3}$M. These measurements included experiments with excess Fe(III) and with excess Eu(II); the results are summarized in Table 6. For each experiment about 4 concentration-time plots were obtained from the given pair of solutions; the numbers in Table 6 are the averages of the individual values for k'. Figure 7 is a copy of one of the oscilloscope traces used to evaluate k' for experiment 5 in Table 6. The observed and calculated numbers obtained from the trace, used to make the plot in Figure 8 as suggested by Eq 16, are shown in Table 7. The plot in Figure 8 describes the reaction to 96% of completion. The slope of the line in Figure 8 is 2.875 sec^{-1};

Table 6. Rate measurements for the reaction of Fe^{3+} and Eu^{2+} at 15.8°, 0.876M H^+, and 1.00M ionic strength in perchlorate solution

Expt No.	10^4[Fe(III)] M	10^4[Eu(II)] M	λ Å	$10^{-4}k'$ $M^{-1}sec^{-1}$
1	0.200	0.744	2400	1.54 ± .04[a]
2	2.50	10.3	3300	1.34 ± .29
3[b]	3.43	3.355	3300	1.64 ± .14
4[c]	5.00	10.6	3500	1.57 ± .09
5	6.00	10.3	3500	1.52 ± .05
6	9.00	32.3	4000	1.48 ± .03
7(1)	11.0	5.89	3300	1.60 ± .07
7(2)	11.0	5.89	3800	1.51 ± .14
8[d]	12.25	8.75	3400	1.62 ± .06
9	50.0	4.42	3400	1.41 ± .05
10	50.0	4.8	3400	1.53 ± .02
11	50.0	5.30	3400	1.36 ± .07
12	75.0	4.8	3400	1.47 ± .04
13	150	4.8	3300	1.62 ± .12

[a]The indicated uncertainty is the average deviation from the mean of successive measurements of the same reaction.

[b]Eq 16 does not apply in this run since $[B]_0-[A]_0$ was quite small. The integrated second order rate law assuming $[B]_0 = [A]_0 = 3.392\times10^{-4}$ was used.

[c]Added Eu^{3+}, 1×10^{-3}M.

[d]Added Fe^{2+} and Eu^{3+}, each 8.8×10^{-4}M.

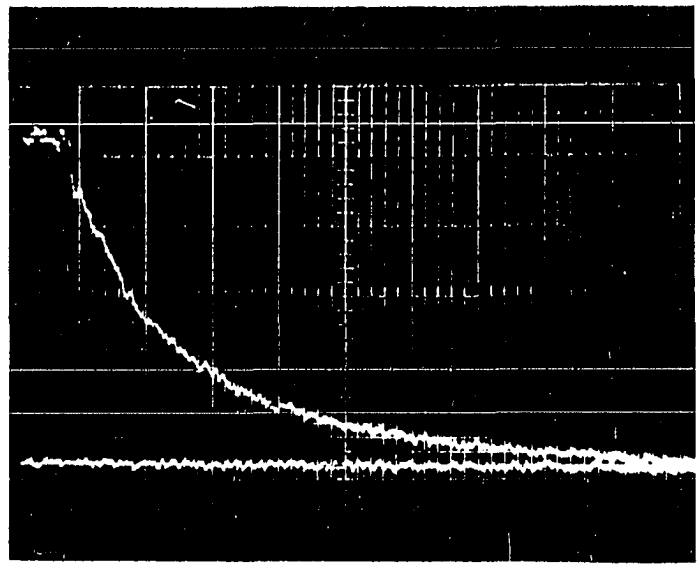

Figure 7. An oscilloscope trace for the reaction between Eu(II) and Fe(III) in perchlorate solution. This trace is from Experiment 5, Table 8, and is the basis for the calculations shown in Table 7

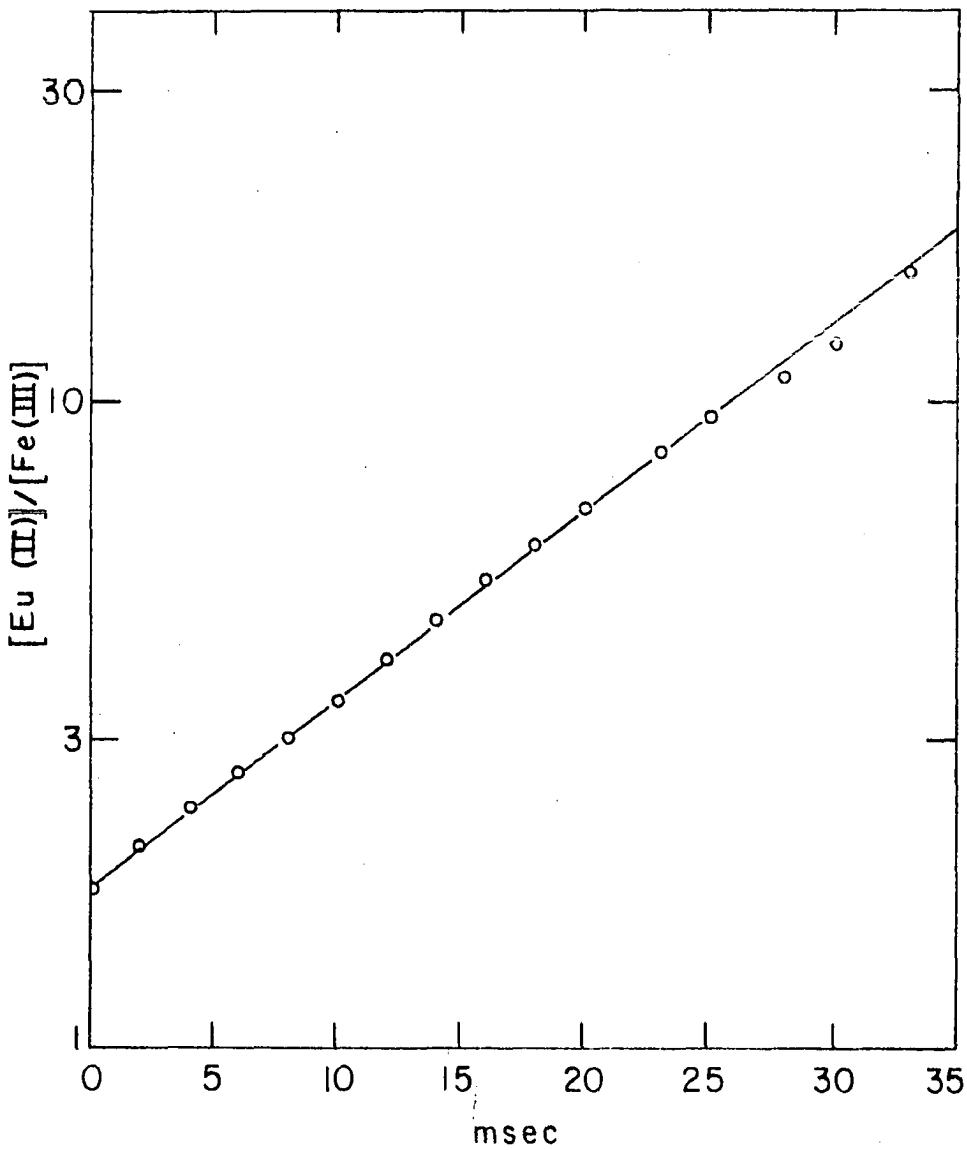

Figure 8. A semi-logarithmic plot of [Eu(II)]/[Fe(III)] vs time, based on the oscilloscope trace shown in Figure 7

Table 7. Calculations derived from the concentration-time plot shown in Figure 7 , and used to construct the ln(B/A) vs time plot shown in Figure 8

Time (sec)	D[a]	10^{-4}[Fe(III)][b] M	10^{-4}[Eu(II)][c] M	[Eu(II)]/ [Fe(III)]
0.00	26.3	5.65[d]	9.95[d]	1.76
0.02	19.9	4.10	8.40	2.05
0.04	16.0	3.15	7.45	2.37
0.06	13.5	2.545	6.85	2.69
0.08	11.7	2.11	6.41	3.04
0.10	10.2	1.745	6.05	3.47
0.12	8.9	1.43	5.73	4.00
0.14	7.9	1.19	5.49	4.61
0.16	7.1	0.994	5.29	5.32
0.18	6.55	0.860	5.16	6.00
0.20	6.05	0.740	5.04	6.81
0.23	5.4	0.582	4.88	8.39
0.25	5.1	0.509	4.81	9.45
0.28	4.8	0.436	4.74	10.9
0.30	4.6	0.388	4.69	12.1
0.33	4.2	0.291	4.59	15.8
0.35	4.0	0.242	4.54	18.8
	3.0			

[a]Arbitrary deflection units.

[b]Calculated according to Eq 17.

[c]Calculated according to Eq 18.

[d]Estimated concentrations at the time of the first observation; the concentrations at the instant of mixing are listed in Table 6 , for experiment 5.

thus according to Eq 16, the value of k' is (2.875 sec^{-1}) (2.303)/$4.3x10^{-4}M$ = $1.54x10^{4}M^{-1}sec^{-1}$, where $4.3x10^{-4}M$ = $[Eu(II)]_0-[Fe(III)]_0$.

The adequacy of Eq 16 (and thus the rate law in Eq 15 and the stoichiometry in Eq 14) is strongly supported by the absence of trends in k' over the wide ranges of $[Fe(III)]_0$ and $[Eu(II)]_0$. In addition, the absence of wavelength dependences and product concentration dependences (expts 4 and 8) are evidence for the absence of more complicated rate behavior than asserted by Eq 15. The mean value for k' listed in Table 6 is $1.51x10^{4}M^{-1}sec^{-1}$.

Hydrogen ion and temperature variations

Experiments at 15.8° demonstrated that k' was a function of $[H^+]$; k' was measured at various acidities and temperatures in the ranges $0.015 < [H^+] < 1.00M$ and $1.4° < T < 25.0°$. The results of these experiments are given in Table 8 and Figure 9, and show a linear relationship between k_{obsd} and $[H^+]^{-1}$.

The acid dissociation of iron(III) (Eq 10) was sufficiently important at low hydrogen ion concentrations that it was taken into account in deriving a rate law in terms of species. The data of Milburn (45) were used for the correction shown in Eq 19. Milburn (45) reported $\Delta H_a = 10.2 \pm 0.3$

$$[Fe^{3+}] = Fe(III)\ \frac{[H^+]}{[H^+] + Q_a} \qquad (19)$$

Table 8. Observed and calculated rate constants for the reaction of Eu(II) and Fe(III) as a function of temperature and $[H^+]$ in perchlorate solution

Expt No.	Temp °C	$[H^+]$ M	$10^4[Fe(III)]_0$ M	$10^4[Eu(II)]_0$ M	Å	$10^{-4}k'_{obsd}$ $M^{-1}sec^{-1}$	$10^{-4}k'_{calcd}$[a] $M^{-1}sec^{-1}$
1	1.6	0.0150	2.00	0.326	2700	18.0	15.2
2	1.6	0.0200	2.00	0.299	2700	14.4	11.5
3	1.4	0.0310	20.0	3.84	3300	8.14	7.49
4	1.4	0.0360	20.0	3.8	3300	5.95	6.51
5	1.6	0.0400	2.00	0.345	2700	6.92	5.99
6	1.4	0.0500	30.0	4.08	3300	4.92	4.79
7	1.4	0.100	40.0	3.8	3300	2.70	2.57
8	1.4	0.200	80.0	4	3300	1.33	1.46
9	1.4	0.500	100.0	4	3300	0.729	0.788
10	1.4	0.879	200.0	4	3300	0.616	0.595
11	1.4	0.939	100.0	4	3300	0.613	0.579
12	15.8	0.015	0.200	0.871	2400	53.2	45.5
13	15.8	0.0167	0.800	0.290	2700	46.7	41.2
14	15.8	0.020	0.800	0.331	2700	36.1	34.7
15	15.8	0.031[b]	8.55	2.375	3500	22.4	23.0
16	15.8	0.031	7.50	3.14	3300	23.4	23.0
17	15.8	0.036	7.50	3.50	3300	17.9	19.9
18	15.8	0.050[b]	4.00	6.20	3300	10.4	14.6
19	15.8	0.050	2.00	0.318	2700	16.4	14.6
20	15.8	0.0700	3.00	7.175	3500	8.54	10.61
21	15.8	0.100[b]	6.00	2.35	3500	6.67	7.60
22	15.8	0.100	3.00	6.70	3500	7.25	7.60

[a]See text for a discussion of the calculation procedure.

[b]Only one value for k'_{obsd} (the average) at a given temperature and acidity was used in the computer calculation.

Table 8. (Continued

Expt No.	Temp °C	$[H^+]$ M	$10^4[Fe(III)]_0$ M	$10^4[Eu(II)]_0$ M	Å	$10^{-4}k'_{obsd}$ $M^{-1}sec^{-1}$	$10^{-4}k'_{calcd}$[a] $M^{-1}sec^{-1}$
23	15.8	0.130[b]	3.00	6.84	3500	5.59[c]	5.97
24	15.8	0.130	3.00	7.18	3500	6.15	5.97
25	15.8	0.20	4.00	7.44	3500	3.30	4.07
--[d]	15.8	0.876				1.51	1.31
26	15.8	1.00	7.50	3.85	3500	1.25	1.21
27	25.0	0.0286	0.200	0.735	2400	54.9	47.7
28	25.0	0.0300	0.200	0.844	2400	51.7	45.6
29	25.0	0.040	0.200	0.805	2400	38.9	34.8
30	25.0	0.050	1.80	0.296	2700	28.8	28.2
31	25.0	0.0571	0.200	0.826	2400	27.7	24.9
32	25.0	0.0667	0.200	1.61	2700	24.6	21.5
33	25.0	0.0800	1.50	2.80	2700	18.1	18.1
34	25.0	0.100	7.00	3.30	3200	13.6	14.6
35	25.0	0.111	6.00	2.25	3200	13.3	13.2
36	25.0	0.133	0.200	0.774	2400	13.0	11.2
37	25.0	0.167	6.00	2.35	3200	9.14	9.08
38	25.0	0.20[b]	8.00	2.97	3200	7.81	7.68
39	25.0	0.20	9.00	2.89	3200	7.45	7.68
40	25.0	0.40[b]	11.0	2.74	3200	4.18	4.16
41	25.0	0.40	12.0	3.76	3200	3.98	4.16
42	25.0	0.953[b]	12.0	4.43	3200	2.09	2.11
43	25.0	0.953	20.0	4.32	3200	2.13	0.11

[c]The simple average of expts 23 and 24 was not used in the computer calculations; the value for k_{obsd} for expt 24 is the average of a larger number of individual measurements than for expt 23, so 24 was more heavily weighted.

[d]Data obtained at 15.8°, 0.876M H^+ are listed in Table 6.

kcal/mole and $\Delta S_a = 21 \pm 1$ eu for Eq 10. Taking 10.2 kcal/mole as correct, it was necessary to use $\Delta S_a = 21.48$ eu to exactly recalculate Milburn's value $Q_a = 1.65 \times 10^{-3}$M at 25.0°. The values $\Delta H_a = 10.2$ kcal/mole and $\Delta S_a = 21.48$ eu were used to fit the k' data listed in Table 8 to Eq 20 by the computer

$$k' = \left\{ k_1 + \frac{k_2}{[H^+]} \right\} \frac{[H^+]}{[H^+] + k_a} \qquad (20)$$

technique already described (44). The computer-calculated values for k' are listed in Table 8.

The lines drawn in Figure 9 are the computer-calculated lines of best fit, while the points are the observed values. The calculated values of the constants k_1 and k_2 at three temperatures and the associated activation parameters are shown in Table 9. The values listed in Table 9 fit the data

Table 9. Temperature dependences of the rate constants for reaction of Eu(II) and Fe(III) in perchlorate solution, at ionic strength 1.00M, maintained with Li^+

Rate constant	Value of the rate constant 1.6°	15.8°	25.0°	$\Delta S^{\neq}$ [a] eu	$\Delta H^{\neq}$ [a] kcal/mole
k_1	3410	4920	6140	-29.4 ± 9.2	3.5 ± 2.6
k_2	2280	7160	14200	1.3 ± 1.8	12.2 ± 0.5

[a]The indicated uncertainties represent standard deviations.

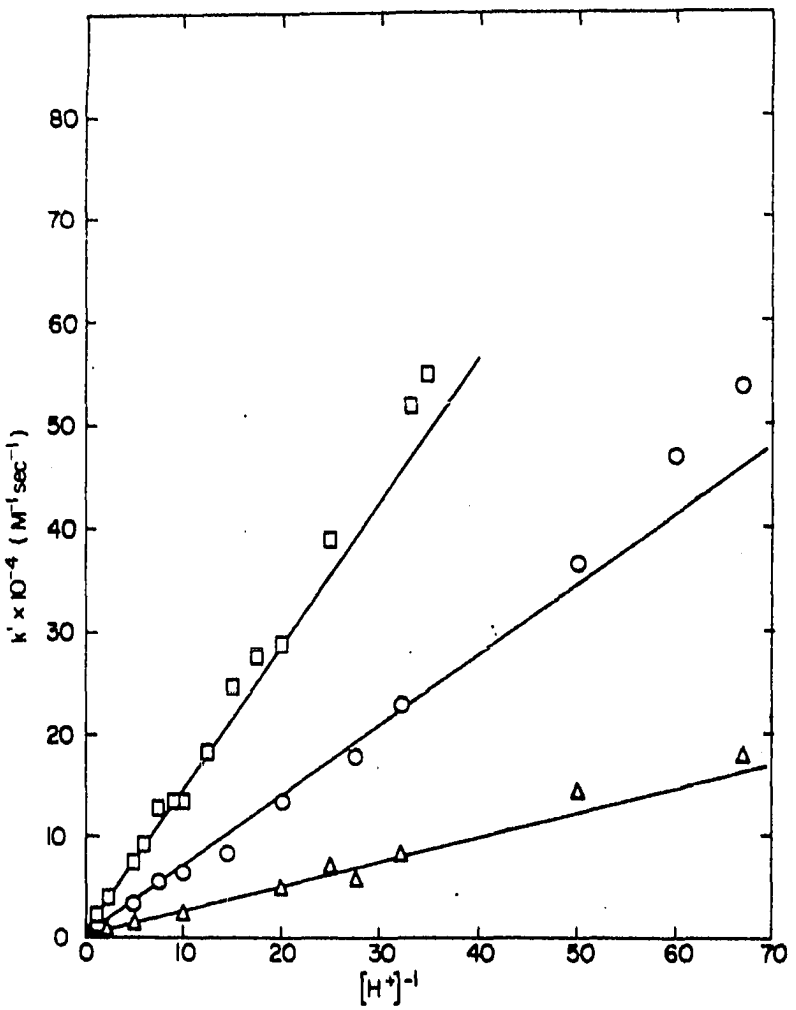

Figure 9. The temperature and hydrogen ion dependence of k' for reduction of Fe(III) by Eu(II) in perchlorate solution. The temperatures 1.4, 15.8, and 25.0° are denoted by △ , 0, and □ , respectively

with an average deviation between k'_{obsd} and k'_{calc} of 8.6%. This fit is deemed adequate; a more complicated rate law is not justified because the apparent systematic deviations between observed and calculated values (e.g. $k'_{obsd} > k'_{calc}$ at low $[H^+]$; see Figure 9) are small relative to the non-systematic scatter. Thus, Eq 21 is a complete rate law that adequately fits the data; an alternate rate law is discussed in a later section.

$$\frac{-d[Fe(III)]}{dt} = -\frac{d[Eu(II)]}{dt} = \left\{k_1 + \frac{k_2}{[H^+]}\right\} \frac{[H^+]}{[H^+] + Q_a} \qquad (21)$$

$$[Fe(III)][Eu^{2+}]$$

Bennett and Sheppard (30) reported a value for $k' > 10^5$ $M^{-1}sec^{-1}$ at 0°, 1.0M $HClO_4$, obtained from a quenched-flow experiment, quenched after 0.06 sec, in which $[Eu^{2+}]_0 = [Fe^{3+}]_0 = 10^{-4}M$. Our results extrapolated to 0°, 1.0M H^+, give $k' = 5.5 \times 10^3 M^{-1}sec^{-1}$, with only about 3% reaction occurring after 0.06 sec. It is believed the Bennett and Sheppard report is wrong, due to poor choice of a quenching solution. The bipyridine-acetate ion quenching solution had stopped the reaction $Fe^{2+} + Co^{3+}$, where presumably it acted by formation of $Fe(bip)_3^{2+}$. Its effect on the $Eu^{2+} + Fe^{3+}$ reaction would probably be an acceleration, however, owing to lowering of $[H^+]$ and probably also owing to strong complexing of the Fe^{2+} product.

Chromium(II)-Iron(III) Reaction in Perchlorate Solution

The reduction of aquoiron(III) by chromium(II) in perchlorate solution has been studied by Dulz and Sutin (16). The stoichiometry and rate law are shown in Eqs 22 and 23, where

$$Fe^{3+} + Cr^{2+} = Fe^{2+} + Cr^{3+} \tag{22}$$

$$\frac{-d[Cr^{2+}]}{dt} = \frac{-d[Fe^{3+}]}{dt} = k'[Fe^{3+}][Cr^{2+}] \tag{23}$$

k' is defined by Eq 24. The Cr^{2+} - Fe^{3+} reaction is thus

$$k' = k_1 + \frac{k_2}{[H^+]} \tag{24}$$

exactly analogous in kinetic form to the Eu^{2+} - Fe^{3+} reaction. The earlier investigation (16) was carried out exclusively at 25°; in this work the rate parameters were restudied as a function of temperature. The data were treated just as described for the Eu^{2+} - Fe^{3+} reaction, including the writing of the rate law according to Eq 25, to account for the acid

$$\frac{-d[Cr(II)]}{dt} = \frac{-d[Fe(III)]}{dt} = \left\{k_1 + \frac{k_2}{(H^+]}\right\}\left\{\frac{[H^+]}{(H^+] + Q_a}\right\} \left\{[Fe(III)][Cr^{2+}]\right\} \tag{25}$$

hydrolysis of Fe^{3+}. The results of experiments at three temperatures and a variety of acid concentrations are shown in Table 10 and in Figure 10. The points in Figure 10 represent observed values, and the lines are the calculated lines of best fit. The calculated values of k_1 and k_2 at three temper-

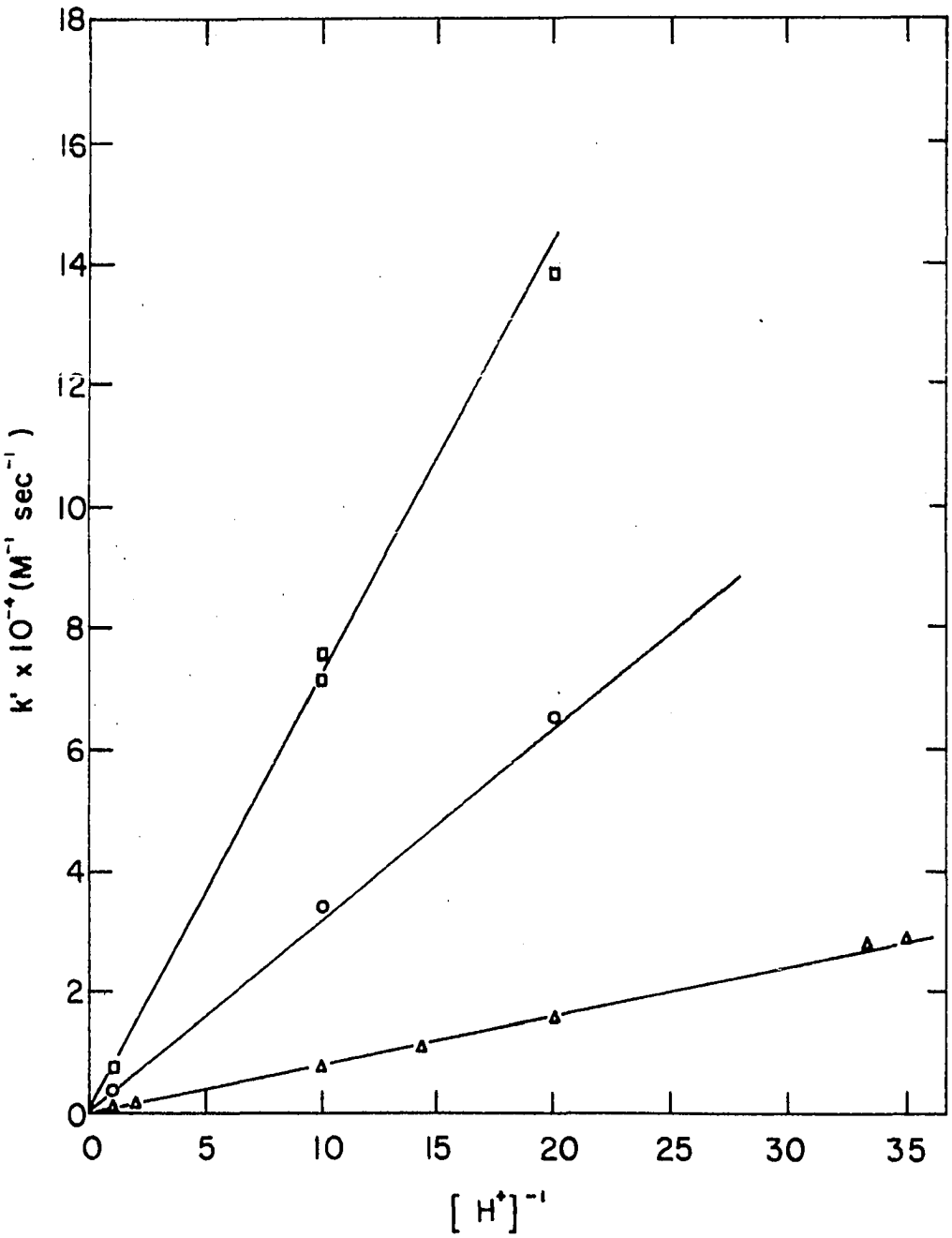

Figure 10. The temperature and hydrogen ion dependence of k' for reduction of Fe(III) by Cr(II) in perchlorate solution. The temperatures 1.6, 15.8, and 25.0° are denoted by △ , 0, and □ , respectively

Table 10. Observed and calculated rate constants for the reaction of Cr(II) and Fe(III) as a function of temperature and $[H^+]$ in perchlorate solution

Expt No.	Temp °C	$[H^+]$ M	$10^4[Fe(III)]_0$ M	$10^4[Cr(II)]_0$ M	λ Å	$10^{-4}k'_{obsd}$ $M^{-1}sec^{-1}$	$10^{-4}k'_{calcd}$ $M^{-1}sec^{-1}$
1	1.6	0.02857	0.300	6.34	2400	2.92	2.81
2	1.6	0.0300	0.200	3.41	2400	2.82	2.68
3	1.6	0.0500	0.300	4.81	2400	1.64	1.63
4	1.6	0.0700	0.200	3.24	2400	1.10	1.17
5	1.6	0.100	0.300	8.23	2400	0.794	0.829
6	1.6	0.500	0.500	15.8	2400	0.179	0.186
7	1.6	1.0	0.500	16.1	2400	0.108	0.105
8	15.8	0.0500	0.240	2.60	2500	6.53	6.36
9	15.8	0.100	0.300	4.55	2400	3.42	3.23
10	15.8	1.00	0.715	15.3	2600	0.381	0.363
11	25.0	0.0500	0.300	1.77	2400	13.80	14.3
12	25.0	0.100	0.240	2.65	2500	7.55	7.30
13	25.0	0.100	0.300	2.48	2400	7.18	7.30
14	25.0	1.00	0.715	14.7	2600	.756	0.792

atures and the associated activation parameters are given in Table 11. Dulz and Sutin (16) reported $k_1 = 2.3 \times 10^3$ and $k_2 = 5.4 \times 10^3$ in 1.00M ionic strength solutions (maintained with $NaClO_4$) at 25°.

Table 11. Temperature dependences of the rate constants for reaction of Cr(II) and Fe(III) in perchlorate solution at ionic strength 1.00M, maintained with Li^+

Rate constant	Value of the rate constant 1.6°	15.8°	25.0°	$\Delta S^{\ddagger}$ [a] eu	$\Delta H^{\ddagger}$ [a] kcal/mole
k_1	250	420	570	-28.4±16.0	5.2±4.4
k_2	800	3210	7330	8.8±0.9	14.8±0.3

[a]The indicated uncertainties represent standard deviations.

Reductions of Iron(III) in the Presence of Complexing Anions

General

Halide and pseudo-halide ions were found to catalyze the reaction between Fe(III) and Eu(II) species. A list of all the pathways that were discovered for reducing Fe(III) species in the presence of anions other than perchlorate is given in Table 12. At least one of the last two paths listed in Table 12 (called catalyzed paths hereafter) was observed and measured kinetically for each anion investigated. The rate of approach to complexation equilibrium, Eq 26, could be made

$$Fe^{3+} + X^- \rightleftharpoons FeX^{2+} \quad k_f', k_{aq}' \qquad (26)$$

Table 12. Pathways for reduction of iron(III) species by Eu^{2+} and Cr^{2+}

Designation of path	Rate expression	Net reaction corresponding to the path
Aquo path	$k_1[Fe^{3+}][M^{2+}]^a$	$Fe^{3+}+Eu^{2+}=Fe^{2+}+Eu^{3+}$
		$Fe^{3+}+Cr^{2+}=Fe^{2+}+Cr^{3+}$
Hydroxo path	$k_2[Fe^{3+}][M^{2+}]/[H^+]$	$Fe^{3+}+Eu^{2+}=Fe^{2+}+Eu^{3+}$
		$Fe^{3+}+Cr^{2+}=Fe^{2+}+Cr^{3+}$
FeX path	$k_{FeX}[FeX^{2+}][M^{2+}]$	$FeX^{2+}+Eu^{2+}=Fe^{2+}+X^-+Eu^{3+}$
		$FeX^{2+}+Cr^{2+}=Fe^{2+}+CrX^{2+}$
Anion path	$k_X[Fe^{3+}][M^{2+}][X^-]$	$Fe^{3+}+Eu^{2+}=Fe^{2+}+Eu^{3+}$
		$Fe^{3+}+Cr^{2+}+X^-=Fe^{2+}+CrX^{2+}$

[a] M represents Eu or Cr.

slow relative to the rate of reduction of iron species for each anion studied. The slowness of complexation was necessary, in order to separate the contribution of similar catalyzed paths. One way to make the complexation equilibrium relatively slow was to use high concentrations of Eu(II), thus accelerating the reduction reactions relative to ligand substitution. Complexation was also made relatively slow by performing most experiments at low temperatures; in each system studied, $\Delta H^{\ddagger}$ values for k_f and k_{aq} were greater than

H^+ values for k_X and k_{FeX}.

Experiments designed to measure k_X were accomplished by mixing iron(III) solution with Eu(II) solution containing X^- ions. The resulting rate of reduction of iron followed a pseudo-second-order equation, and rate constants were evaluated according to Eq 16, just as in solutions containing only perchlorate anions. However, the observed second order rate constants increased linearly with $[X^-]$. These observations suggest the following two-term rate law (Eqs 27 and 28).

$$\frac{-d[Fe(III)]}{dt} = k_{obsd}[Fe(III)][Eu(II)] \qquad (27)$$

$$k_{obsd} = k' + k_X[X^-] \qquad (28)$$

Equations 27 and 28 are only approximately correct however; the reaction sequence consisting of the formation of FeX^{2+} followed by its reduction (the FeX pathway occurred very rapidly under the conditions employed) made a minor contribution to the net oxidation-reduction process. Consideration of this sequence required replacement of Eq 28 by Eq 29, where the k_f' term represents a correction for this effect which was minor

$$k_{obsd} = k' + k_X[X^-] + \frac{k_f'[X^-]}{[M(II)]_{av}} \qquad (29)$$

for all anions, except perhaps Br^-. The quantity $[M(II)]_{av}$ is the average concentration of Eu(II) (or Cr(II)) during an experiment; M(II) was in excess over Fe(III) in these

studies. Values of k_{FeX} reported in a later section confirm that FeX^{2+} formed in these experiments was very rapidly reduced. The quantity k_{corr} was defined, Eq 30. The slope of

$$k_{corr} = k_{obsd} - \frac{k_f'[X^-]}{[M^{2+}]_{av}} = k' + k_X[X^-] \qquad (30)$$

plots of k_{corr} vs $[X^-]$ for experiments at a common acidity was k_X; the value of the intercept, k', represents the rate constant in perchlorate solution whose value is computed from Eq 20. Intercepts of such plots were in good agreement with the known values of k'. Alternatively, the value of k_X could be computed from a single experiment, according to Eq 31.

$$k_X = \frac{k_{corr} - k'}{[X^-]} \qquad (31)$$

Experiments designed to measure k_{FeX} were accomplished by mixing an Eu(II) solution with an iron(III) solution containing X^- in which the complexation equilibrium given in Eq 26 had been established. Following mixing, the depletion of absorbing species (FeX^{2+} and sometimes also Eu^{2+} and Fe^{3+}) was at first very rapid. This rapid change corresponded to the reduction of FeX^{2+} by Eu^{2+}, the rate constant of which could be measured from the oscilloscope trace. Subsequent to that portion there occurred either of two slower processes, as follows. In experiments in which [Fe(III)] > [Eu(II)], the initial rapid absorbance decrease was followed by an absorbance increase. See Figure 11 for a specific demonstra-

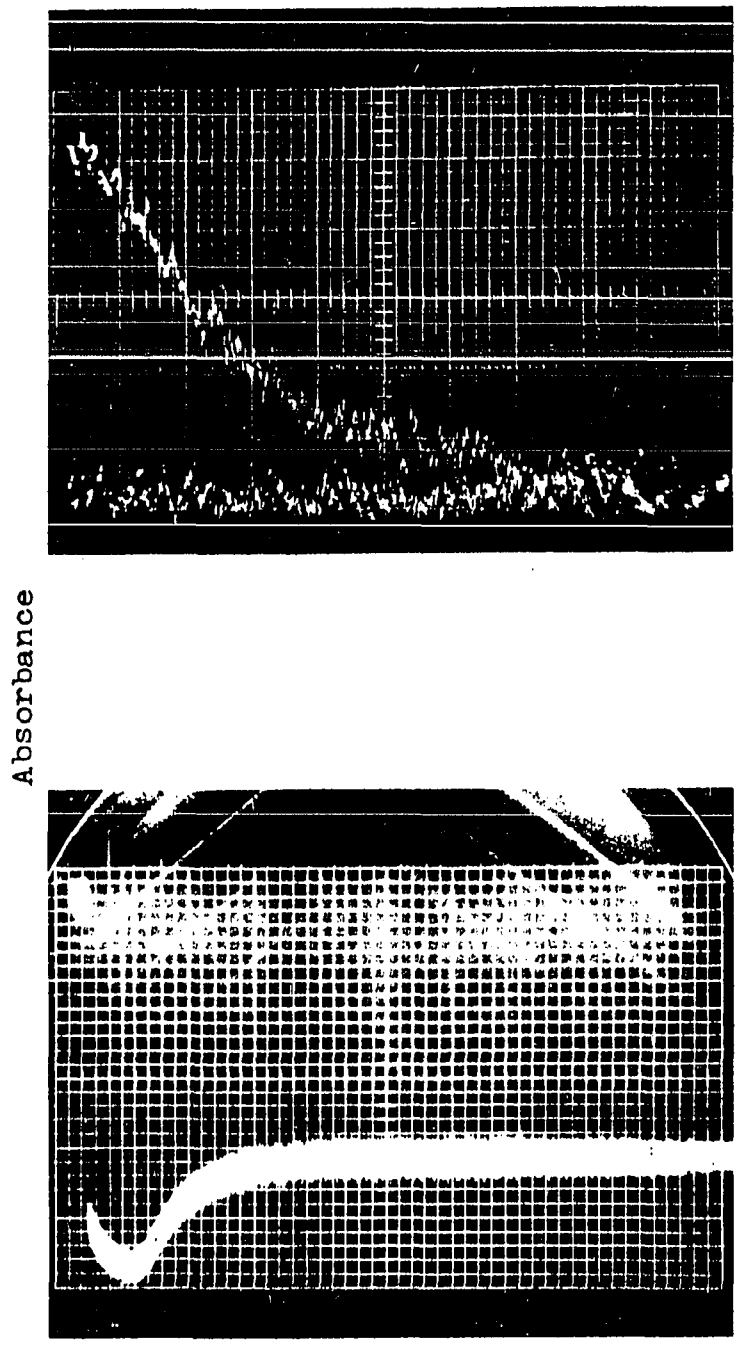

Figure 11. Oscilloscope traces obtained in experiment 5, Table 14. The upper plot spans the first 50 msec after mixing. The lower plot spans the first 20 sec

tion of these changes. In experiments in which [Fe(III)] < [Eu(II)] , and in which FeX^{2+} was the only absorbing species, the absorbance was constant after the rapid decrease; when Eu^{2+} and or Fe^{3+} also absorbed appreciably, the rapid decrease was followed by a slower decrease. These observations are consistent with the following reaction scheme: (1) the FeX path and, to a minor extent, aquation, rapidly consume FeX^{2+}, (2) Eu^{2+} and Fe^{3+} are more slowly consumed via all the pathways (see Table 12) (formation of FeX^{2+} continued to occur, so the FeX path is still significant), and (3) if Eu^{2+} is consumed before Fe^{3+}, FeX^{2+} reforms at its equilibrium concentration according to Eq 26.

The rate laws in Eqs 32 and 33 apply, assuming the

$$\frac{-d[FeX^{2+}]}{dt} = k_{FeX}[FeX^{2+}][Eu^{2+}] + k'_{aq}[FeX^{2+}] - k'_{f}[Fe^{3+}][X^-] \quad (32)$$

$$\frac{-d[Eu^{2+}]}{dt} = k_{FeX}[FeX^{2+}][Eu^{2+}] + \left\{k_1 + \frac{k_2}{[H^+]}\right\}[Fe^{3+}][Eu^{2+}] + k_X[Fe^{3+}][Eu^{2+}][X^-] \quad (33)$$

reaction scheme described above. The data from experiments in which FeX^{2+} solution was mixed with Eu^{2+} solution were treated according to Eq 32; only the k_{FeX} term was important during the initial period of rapidly decreasing absorbance.

Catalysis of the reaction between Fe(III) and Cr(II)

by anions followed the same general patterns described for the Eu(II) reductions (see Table 12). The inertness of the CrX^{2+} product formed in both catalyzed paths permitted its separation and identification, as reported by Dulz and Sutin (16), and in the experimental section of this paper.

Values for the formation rate constant k_f' (Eq 26) were required for every anion studied, in order to calculate the initial concentrations of FeX^{2+} and to make the appropriate rate computations as described in Eq 29.

Chloride

The values of the equilibrium quotient for $FeCl^{2+}$ formation, Eq 34, at 1.6, 15.8, and 25.0°, at 1.00M ionic strength

$$Q_{Cl} = \frac{[FeCl^{2+}]}{[Fe^{3+}][Cl^-]} \qquad (34)$$

are Q_{Cl} = 1.56, 2.25, and 2.90, respectively. These values are based on the data of Woods, Gallagher, and King (47). The values $k_f' = 0.85 + 0.42/[H^+]$ $M^{-1}sec^{-1}$ and $k_{aq}' = 0.54 + 0.27/[H^+]$ sec^{-1} at 1.6° were estimated from Q_{Cl} and the aquation kinetic study by Connick and Coppel(48), where k_f' and k_{aq}' are defined by Eq 35. The Connick and Coppel study (48)

$$\frac{-d[FeCl^{2+}]}{dt} = k_f'[Fe^{3+}][Cl^-] - k_{aq}'[FeCl^{2+}] \qquad (35)$$

was done in solutions at 0.5M ionic strength, maintained with $NaClO_4$, at temperatures higher than 1.6°. The extrapolation from their conditions is undoubtedly quite uncertain.

Experiments to measure k_{Cl} for the Eu(II) reduction were carried out at 1.6°. Concentrations were varied as follows: $2.2\times10^{-4} < [Fe(III)] < 4.0\times10^{-4}M$, $1.8\times10^{-3} < [Eu(II)] < 2.9\times10^{-3}M$, $0.0 < [Cl^-] < 0.90M$, and $0.10 < [H^+] < 1.0M$. The experiments, summarized in Table 13, lead to the average value $k_{Cl} = (6.2\pm1.3)\times10^{3}M^{-2}sec^{-1}$. The results at 0.953M H^+ are shown in Figure 12, according to the plot of k_{corr} vs $[Cl^-]$ suggested by Eq 30. The intercept corresponding to $[Cl^-] = 0$ in Figure 12 is the value of $k_1 + k_2/[H^+]$ at 1.6° and .953M H^+, $5800M^{-1}sec^{-1}$. The scatter of k_{Cl} derived from these experiments is relatively magnified by subtracting the large k' value. The scatter prevents confirmation of a complete lack of variation of k_{Cl} with $[H^+]$. The data are sufficiently precise, however, to demonstrate that the predominant rate term is independent of $[H^+]$ over the range 0.1-1.0M. The size of the k_f' correction in Eq 30 ranged from 2% (experiment 1) to 7% (experiment 4) of k_{obsd}.

When a solution of Eu(II) containing no chloride ion was mixed with an iron(III) solution containing chloride and, therefore, $FeCl^{2+}$, the absorbance decrease at 3350Å (a wavelength of maximum absorbance for $FeCl^{2+}$) was very rapid; initial half-times for the Eu(II) reduction of $FeCl^{2+}$ ranged from 5 to 11 msec at 1.6°, which was near the limit of measurement. Six experiments were done, with a 4.4-fold variation in $[FeCl^{2+}]$ and a 3.9-fold variation in [Eu(II)]. All the

Table 13. Kinetic data on the reaction of Eu(II) with Fe(III) in the presence of Cl^- at 1.6° and 1.00M ionic strength

Expt No.	$[Cl^-]$ M	$[H^+]$ M	10^4]Fe(III)] M	10^4[Eu(II)] M	$10^{-3}k_{obsd}$ $M^{-1}sec^{-1}$	$10^{-3}k_{corr}$[a] $M^{-1}sec^{-1}$	$10^{-3}k_{Cl}$[b] $M^{-1}sec^{-1}$
1	0.25	0.953	4.00	20.1	7.36	7.18	5.5
2	0.474	0.953	4.00	18.0	10.7	10.3	9.5
3	0.474	0.953	4.00	23.4	8.17	7.88	4.4
4	0.60	0.100	2.20	14.4	31.3	29.0	4.9
5	0.70	0.953	4.00	19.4	10.3	9.78	5.7
6	0.80	0.400	2.20	30.0	15.7	15.2	7.6
7	0.90	0.953	4.00	20.1	11.8	11.2	6.0
						Av =	6.2 ± 1.3

[a]Calculated according to Eq 30.

[b]Calculated according to Eq 31.

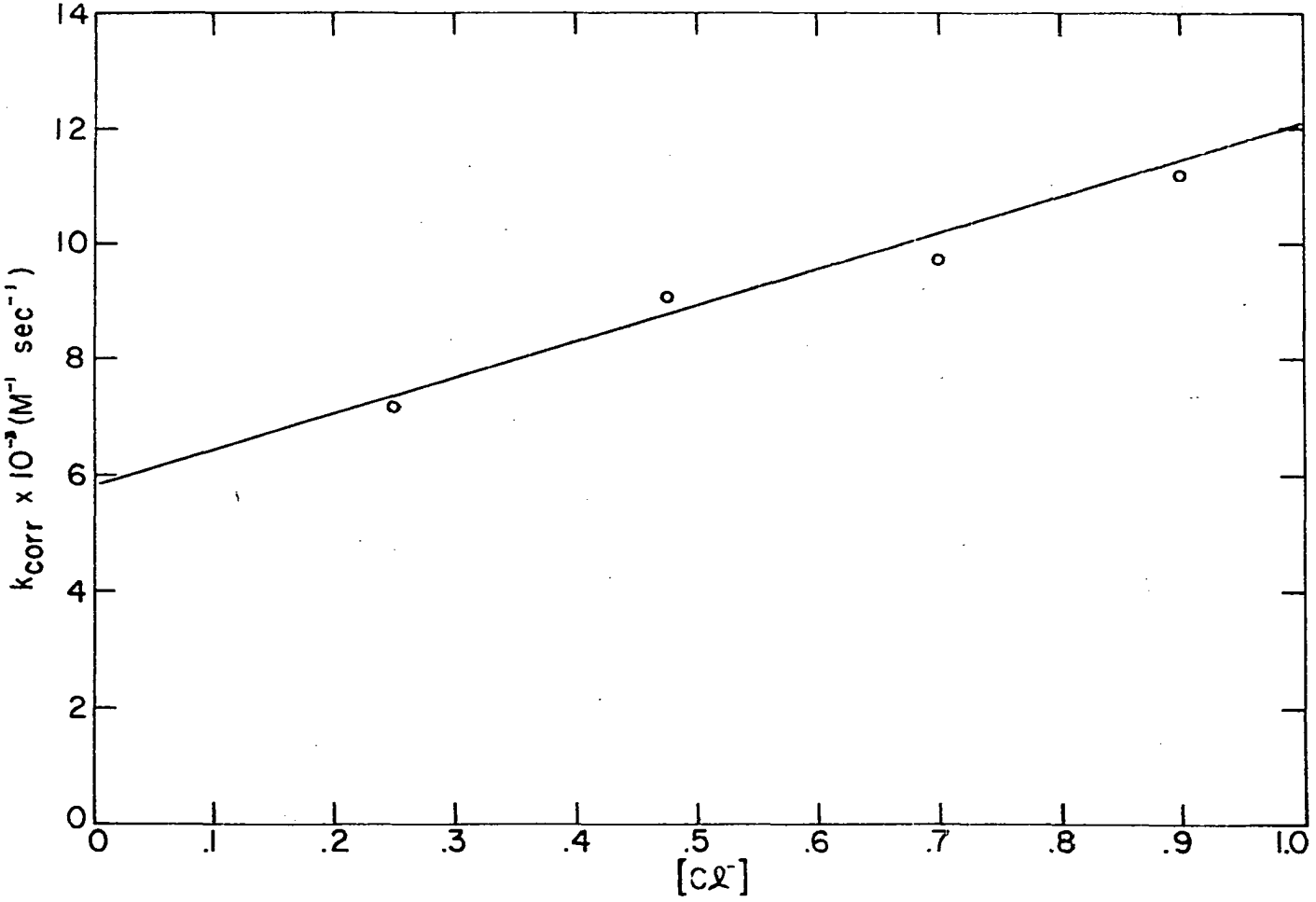

Figure 12. The dependence of the rate of reduction of Fe^{3+} by Eu(II) in chloride solution at 1.6° on $[Cl^-]$

experiments except number 6 (Table 14) were done at 1.00M H^+; experiment 6 at 0.100 M H^+ provided no evidence for an acid dependent path. The data are presented in Table 14; values of k_{FeCl} were calculated from the absorbance changes occurring during the rapid reduction of $FeCl^{2+}$ by Eu(II), using Eq 16. The validity of Eqs 32 and 33, with only the k_{FeCl} path contributing initially was assumed. The value of k_{FeCl}, 2.0×10^6 $M^{-1}sec^{-1}$, proves the k_{FeCl} path is indeed dominant at short times. Based on this value it is computed that even after 90% of the $FeCl^{2+}$ had been depleted, the k_{FeCl} term represented 90 and 97% of Eqs 32 and 33, respectively, in experiment 1, the least favorable case. Absence of a rate trend with the concentration variations described in Table 14 is additional evidence supporting the calculation procedure. Evidence for the correctness of the proposed reaction scheme at long times, when Fe(III) remains after Eu(II) is consumed (point 3 in the preceding section) was provided by experiment 5 (see Figure 11 for the absorbance changes observed in the experiment). The increasing absorbance shown in Figure 11 was assumed to be due to the re-formation of $FeCl^{2+}$ at a rate dictated by the k_f and k_{aq} terms in Eq 32. The observed first-order rate constant was 0.72 sec^{-1}. This rate constant is in fair agreement with 0.9 ± 0.1 sec^{-1} observed at 1.0M H^+ and 1.6°, in an experiment in which 4.86×10^{-5}M Fe(III) was mixed with 1.00M Cl^-, and in poor agreement with the value $k_f'[Cl^-] + k_{aq}' =$

Table 14. Kinetic data on the reaction of Eu(II) with $FeCl^{2+}$ at 1.6° and 1.00M ionic strength

Expt No.	$10^5[Fe(III)]_0$ M	$10^5[FeCl^{2+}]_0$[a] M	$10^5[Eu(II)]_0$ M	$[H^+]$ M	$10^{-6}k_{FeCl}$ $M^{-1}sec^{-1}$
1	2.69	1.66	3.63	1.00	2.4 ± 0.2[b]
2	2.69	1.66	5.20	1.00	1.4 ± 0.2
3	2.69	1.66	7.80	1.00	1.5 ± 0.1
4	5.42	3.30	7.45	1.00	1.7 ± 0.0
5	12.0	7.30	9.55	1.00	2.1 ± 0.2
6	2.69	1.66	2.46	0.100	1.9 ± 0.2
				Av =	2.0 ± 0.4

[a]Calculated using $Q_{Cl} = 1.56$; $[Cl^-] = 0.50M$ (after mixing) in each experiment.

[b]The indicated uncertainty is the average deviation from the mean.

1.45 $M^{-1}sec^{-1}$ extrapolated from the data of Connick and Coppel (48), as described at the beginning of this section.

Dulz and Sutin (16) have reported a study of the chloride-catalyzed paths for reduction of iron(III) by chromium (II). Their observations (at 25.0°, 1.00M H^+) followed the general pattern outlined above for the Eu(II) reductions, with $k_{Cl} = 2x10^4 M^{-2}sec^{-1}$ and $k_{FeCl} = 2x10^7 M^{-1}sec^{-1}$. The inert product of both catalyzed reductions was found (16) to be $CrCl^{2+}$, by an ion exchange procedure.

Attempts to verify the reported (16) value for k_{FeCl} were unsuccessful; the initial rapid absorbance change was apparently nearly complete at the time of the first observation and only crude estimates for k_{FeCl} were possible. Attempts to measure k_{FeCl} at 15.8° were similarly unsuccessful, but the reaction was slower at 1.6° and reasonably reproducible measurements were made. The results of all the experiments are listed in Table 15.

Thiocyanate

Thiocyanate was found to catalyze the reduction of Fe(III) by Eu(II) by the FeX path (Table 12). The anion path, if it exists, is not a major contributor to the reduction.

Approximate values for Q_{NCS} as a function of temperature,

$$Fe^{3+} + NCS^- = FeNCS^{2+} \qquad Q_{NCS}$$

needed for calculating $FeNCS^{2+}$ concentrations, were obtained as follows. Two $FeNCS^{2+}$ solutions were prepared and the

Table 15. Kinetic data on the reaction of Cr(II) with $FeCl^{2+}$ in 1.00 H^+

Expt No.	Temp °C	$10^5[FeCl^{2+}]_0$ M	$10^5[Cr^{2+}]_0$ M	Estimated %[a] of $[FeCl^{2+}]_0$ remaining at first observation	$10^{-6}k_{FeCl^{2+}}$ $M^{-1}sec^{-1}$
1	25.0	0.62[b]	1.40	very small	5
2	25.0	1.02[b]	2.03	very small	10
3	25.0	2.00[b]	4.83	10	6
4	15.8	2.24[c]	2.58	8	40
5	15.8	2.24[c]	3.38	10	30
6	1.6	1.46[d]	5.75	60	1.3 ± .2[e]
7	1.6	1.70[d]	4.74	60	1.3 ± .2
8	1.6	2.01[d]	6.44	60	2.4 ± .4
				Av at 1.6°	1.7 ± .5

[a]The estimates are based on the sizes of the oscilloscope deflections observed.

[b]Calculated on the basis of $Q_{Cl} = 2.90M^{-1}$.

[c]Calculated on the basis of $Q_{Cl} = 2.25M^{-1}$.

[d]Calculated on the basis of $Q_{Cl} = 1.56M^{-1}$.

[e]The indicated uncertainty is the average deviation from the mean.

absorbance of each was measured at 4600Å, at 25.0° and at 4.0°. The results are shown in Table 16, together with values for Q_{NCS} calculated from molar extinction coefficients obtained (by interpolation or extrapolation) from Table 17. The values reported for Q_{NCS} in the two tables are in reasonable agreement at 25°, although the values measured in this study (Table 15) appear slightly high at 4°. The values ΔH°_{NCS}

Table 16. Measured absorbances of $FeNCS^{2+}$ solutions and calculated values for Q_{NCS}

Solution No.	Ionic[a,b] strength	Temp °C	Absorbance in 5 cm_o cell at 4600Å	ϵ_{4600} $M^{-1}cm^{-1}$	Calculated Q_{NCS}
1	1.00	4.0	0.848	4753	209
1	1.00	25.0	0.604	4678	138
2	0.40	4.0	0.930	4742	238
2	0.40	25.0	0.699	4672	166

[a]Maintained with $LiClO_4$.

[b]Concentrations in each solution were: $[H^+] = 0.399$, $[Fe(III)] = 1.524 \times 10^{-4}$, $[NCS^-] = 1.5 \times 10^{-3}M$.

Table 17. Equilibrium data for thiocyanatoiron(III)

Ionic[a] strength	Temp °C	Reported Q_{NCS}, M^{-1}	Reported ϵ_{4600}, $M^{-1}cm^{-1}$	Ref
0.2	25.0	192	4670	49
0.3	25.0	169		49
0.5	25.0	146		49
0.5	2.3	170		50
0.5	14.7	152		50
0.5	25.0	139		50
0.5	35.0	127		50
0.8	25.0	139		49
1.2	5.0	155	4750	49
1.2	25.0	130	4680	49

[a]Maintained with $NaClO_4$.

(Eq 36) = -1.5, -1.6, and -0.8 kcal/mole were reported

$$Fe^{3+} + NCS^{-} = FeNCS^{2+} \qquad (36)$$

respectively, by Laurence (50), Betts and Dainton (51), and by Lister and Rivington (49). The value H^{o}_{NCS} = -3.1 kcal/mole in 1.00M ionic strength solution was calculated from Table 16. These discrepancies are small and could be due to the use of different ionic media. The values in Table 16 were taken as correct and were used to evaluate Q_{NCS} at the desired temperatures, assuming a linear relationship with 1/T. The results are as follows: Q_{NCS} = 216 and 163 M^{-1} at 1.6° and 15.8°, respectively.

Preliminary attempts to measure k_{NCS} indicated the k_f' correction term in Eq 29 was an important correction. For example, in one experiment at 1.6° with initial concentrations as follows, [Fe(III)] = 4.18×10^{-4}, [Eu(II)] = 19.3×10^{-4}, [NCS^-] = 0.25, the observed rate constant was $(1.19 \pm .13)\times10^{4}$ $M^{-1}sec^{-1}$. The contribution of the various terms in Eq 29 to k_{obsd} are as follows; $k_{obsd} = (1.19 \pm .13)\times10^{4} = .796\times10^{4} + .25k_{NCS}) + 23(.25)/17.1\times10^{-4}$, or $(1.19 \pm .13)\times10^{4} = .796\times10^{4} + .34\times10^{4} + .25k_{NCS}$, or $(.06 \pm .13)\times10^{4} = .25\ k_{NCS}$, where 23 $M^{-1}sec^{-1} = k_f'$ at 1.6° and 0.5M H^+, estimated from the data of Below, Connick, and Coppel (40), and $.760\times10^{4}$ $M^{-1}sec^{-1}$ is the non-catalyzed reduction rate constant (see Table 9). Thus, the correction term in Eq 29 amounted to about 80% of the entire catalysis.

Because the k_f' correction term was important in Eq 29, and because the previous study (40) measuring k_f' had been done at 0.4M ionic strength (maintained with $NaClO_4$), at temperatures higher than 1.6°, and at low $[NCS^-]$ ($< 1.96 \times 10^{-3}$M), it was necessary to measure k_f' again, under the conditions used in k_{NCS} measurements.

The results of a series of stopped-flow experiments, in which Fe^{3+} solutions were mixed with NCS^- solutions, are described in Table 18; $[NCS^-]$ did not exceed the still low

Table 18. Results of experiments measuring the rate of approach to equilibrium by iron(III) and NCS^- solutions at 1.6°, 0.5M H^+, 1.00M ionic strength

Expt No.	$10^3(NCS^-]$ M	$10^3[Fe(III)]$ M	k_{obsd} sec^{-1}	k_f'[a] $M^{-1}sec^{-1}$
1	1.01	0.418	0.140	24.8
2	1.01	0.1115	0.138	24.5
3	2.03	0.0698	0.148	22.2
4	3.03	0.0550	0.208	27.1
5	4.03	0.0480	0.186	21.4
6	5.03	0.0441	0.188	19.5
			Av =	23 ± 2

[a]Calculated from Eq 37, with $Q_{NCS} = 216$ M^{-1}.

value of 5×10^{-3}M, in order to minimize the formation of higher complexes. Values for k_f' were calculated from Eq 37, derived

$$k_f' = \frac{k_{obsd}}{[NCS^-] + (Q_{NCS})^{-1}} \qquad (37)$$

from the expressions $k_{obsd} = k_f'[NCS^-] + k_{aq}'$ and $k_{aq}' = k_f'/Q_{NCS}$. The average value for k_f', 23 ± 2 $M^{-1}sec^{-1}$, is in good agreement with the value $k_f' = 23$ calculated from the activation data reported previously (40).

A second series of experiments was done, with the intent of measuring k_f' in solutions containing NCS^- at higher concentrations. The experiments were unsuccessful, but were done as follows: an NCS^- solution containing Cr^{2+}, was mixed with an Fe^{3+} solution and the increase in absorbance at 2950-2750Å due to $CrNCS^{2+}$ and $CrSCN^{2+}$ formation (52) was observed. Owing to the very rapid reduction of $FeNCS^{2+}$ ($k > 2 \times 10^7 M^{-1}sec^{-1}$ at 25°) (13) and the slow reduction of Fe^{3+} ($k' = 1860$ $M^{-1}sec^{-1}$ at 1.6°, 0.5M H^+; see Table 11) by Cr^{2+}, formation of $FeNCS^{2+}$ was expected to be the rate determining step. The results of the experiments are listed in Table 19. The ratio $k_{obsd}/[NCS^-]$, which had been expected to be k_f', increased with increasing $[Cr(II)]_0$, and also with increasing $[NCS^-]$. These trends were not explained, but did leave the existence of a k_{NCS} term in considerable doubt. If thiocyanatoiron(III) complexes form as rapidly as indicated by Table 19, the acceleration noted in experiments such as the one described above can be accounted

Table 19. Results of attempts to measure the rate of formation of $FeNCS^{2+}$ at 1.6°, 0.5M H^+, 1.00M ionic strength

Expt No.	$10^5[Fe(III)]_0$ M	$10^5[Cr(II)]_0$ M	$[NCS^-]$ M	k_{obsd} sec^{-1}	$k_{obsd}/[NCS^-]$ $M^{-1}sec^{-1}$
1	2.00	1.93	0.10	1.93	19.3
2	2.00	3.69	0.25	7.22	28.9
3	3.00	5.29	0.50	18.9	37.8
4	6.00	12.20	0.50	21.6	43.2
5	3.00	50.3	0.50	26.3	52.5
6	4.00	7.60	0.75	39.6	52.7

for without a k_{NCS} path.

The reaction between Eu(II) and $FeNCS^{2+}$ (the k_{FeNCS} path; Table 12) was studied at 1.6°, 1.00M ionic strength. The initial concentrations were varied by factors of 27, 10, and 20 for Eu(II), $FeNCS^{2+}$, and H^+, respectively. One experiment was done with $FeNCS^{2+}$ in excess; the others were done with Eu(II) in excess. The observed second order rate constants were not dependent on $[H^+]$ or either of the reactant concentrations. The rate of the reaction was also measured at 15.8 and 25.0°; the results are listed in Table 20. The data in Table 20 were fitted to the absolute rate theory equation, Eq 9 , as described previously (44). The activation parameters and the values of k_{FeNCS} recalculated from these parameters are shown in Table 21.

Table 20. Kinetic data on the reaction of Eu(II) with $FeNCS^{2+}$ at μ = 1.00M

Expt No.	Temp °C	$10^5[Eu(II)]_0$ M	$10^5[FeNCS^{2+}]_0$ M	$10^5[Fe(III)]_0$ M	$10^3[NCS^-]$ M	$[H^+]$ M	k_{FeNCS}^{10-5} $M^{-1}sec^{-1}$
1	1.6	9.50	1.2	3.05	0.750	0.0500	3.13
2	1.6	5.75	0.75	2.50	1.00	0.100	2.92
3	1.6	0.5	7.5	30.5	0.750	1.00	3.14
4	1.6	4.02	1.2	2.25	3.00	1.00	3.80
5	1.6	4.77	0.95	2.50	1.50	1.00	3.53
6	1.6	5.14	0.60	2.50	0.750	1.00	3.24
7	1.6	8.28	0.47	1.91	0.750	1.00	2.54
8	1.6	13.5	4.7	19.1	0.750	1.00	2.98
	1.6				Av at 1.6°		= 3.2 ± .3
9	15.8	3.28	0.85	4.28	0.750	1.00	5.19
10	15.8	3.28	1.0	5.35	0.750	1.00	4.93
11	15.8	5.55	1.0	5.35	0.750	1.00	5.35
12	15.8	6.10	0.85	4.28	0.750	1.00	4.38
	15.8				Av at 15.8°		= 5.0 ± .3
13	25.0	4.57	0.76	4.40	0.750	1.00	6.53
14	25.0	5.10	1.1	6.30	0.750	1.00	6.45
15	25.0	9.55	1.1	3.18	1.50	1.00	5.62
16	25.0	4.78	1.5	8.80	0.750	1.00	6.46
	25.0				Av at 25.0°		= 6.3 ± .3

Table 21. Observed rate constants, activation parameters, and calculated rate constants for the reaction of Eu(II) with $FeNCS^{2+}$

Quantity	Temperature 1.6°	15.8°	25.0°
$10^{-5}k_{FeNCS}$(obsd, $M^{-1}sec^{-1}$)	3.2±0.3	5.0±0.3	6.3±0.3
$\Delta H^{\ddagger}$ (kcal/mole)		4.37±0.42	
$\Delta S^{\ddagger}$ (eu)		-17.3±1.5	
$10^{-5}k_{FeNCS}$(calc. $M^{-1}sec^{-1}$)	3.1	4.8	6.3

It has been reported that k_{FeNCS} for the reaction between Cr(II) and $FeNCS^{2+}$ is $> 2x10^{7} M^{-1}sec^{-1}$ at 25° (13). In this study, an attempt was made to measure k_{FeNCS} for Cr(II) reduction; it was found to be immeasurably large at 1.6° as well.

Cyanatoiron(III)

An approximate value for Q_{NCO} (Eqs 38,39) was needed for calculation of $FeNCO^{2+}$ concentrations in experiments

$$Fe^{3+} + HNCO = FeNCO^{2+} + H^{+} \qquad (38)$$

$$Q_{NCO} = \frac{[FeNCO^{2+}][H^{+}]}{[Fe^{3+}][HNCO]} \qquad (39)$$

measuring k_{FeNCO} (see Table 12). The reaction described in Eq 38 has been the subject of only one previous study (53), probably because of the instability of HNCO in acid solution with respect to hydrolysis to NH_4^+ and HCO_3^- (39).

The value of Q_{NCO} was obtained from a series of kinetic

experiments, measuring the rate of approach to equilibrium in Eq 38. The experiments were done under conditions of low acidity, to minimize hydrolysis of HNCO, which was significant even during the short time required to reach substitution equilibrium. The experiments were done under conditions of low total cyanate concentration, to prevent a significant effect on $[H^+]$ by the reaction described in Eq 40. The value

$$HNCO = H^+ + NCO^- \qquad K_a \qquad (40)$$

$K_a = 2.9 \times 10^{-4}$ at 18°, ionic strength 0.065 to .20M, has been reported (39). An additional beneficial feature of low [HNCO] experiments is that [HNCO], subject to considerable decrease by hydrolysis, need not be known to interpret the kinetic data. The experiments were done under conditions of high and varying $[Fe^{3+}]$, to obtain both forward and reverse rate constants; k_{obsd} was expected to be of the form shown in Eq 41. The results of the experiments are presented in

$$k_{obsd} = k_f'[Fe^{3+}] + k_{aq}' \qquad (41)$$

Table 22. The observed rate constants did depend on $[Fe^{3+}]$ as expected, and also on $[H^+]$, as expected from the form of Q_{NCO} (Eq 39). A plot of k_{obsd} vs $[Fe^{3+}]/[H^+]$ was linear within the experimental scatter, with slope = .60 sec^{-1} and intercept = .051 sec^{-1}. These facts imply the following equations for k_{obsd} and Q_{NCO}, where $k_f' = k_f/[H^+]$ and $k_{aq}' = k_{aq}$, and the values of k_f and k_{aq} are .60 and .051

$$k_{obsd} = \frac{k_f}{[H^+]}[Fe^{3+}] + k_{aq} \qquad (42)$$

Table 22. The rate of approach to equilibrium by iron(III), cyanate solutions at 2°, ionic strength 1.00M

Expt No.	$[H^+]$ M	$10^3[Fe^{3+}]$[a] M	Type of[b] expt	k_{obsd} sec^{-1}	$[Fe^{3+}]/[H^+]$	k_{calcd} sec^{-1}
1	0.0218	2.11	dilution	0.131	0.0967	0.109
2	0.0261	4.01	formation	0.125	0.154	0.143
3	0.1038	3.96	dilution	0.0735	0.0382	0.0739
4	0.1038	7.18	dilution	0.0861	0.0692	0.0925
5	0.1038	10.8	dilution	0.117	0.104	0.113
6	0.131	2.11	dilution	0.0693	0.0161	0.0607
7	0.133	1.06	dilution	0.0521	0.00796	0.0558
8	0.133	2.12	dilution	0.0568	0.0159	0.0605

[a]The formal concentration of HNCO was about 9×10^{-5}M in each of these experiments.

[b]See experimental section.

$$Q_{NCO} = \frac{k_f}{k_{aq}} = 11.8 \qquad (43)$$

sec^{-1}, respectively, at 2°C and 1.00M ionic strength. The value $Q_{NCO} = 11.8$ is in poor agreement with Lodzinska (53), who reported $[Fe^{3+}][NCO^-]/[FeNCO^{2+}] = 7x10^{-3}$ at ionic strength 0.7M. The value obtained here for the same quotient is $K_a/Q_{NCO} = 2.5x10^{-5}M$. An absorbance measurement of a solution for which $[FeNCO^{2+}]$ was calculated using $Q_{NCO} = 11.8$ led to $\epsilon_{FeNCO} = 2000\ M^{-1}cm^{-1}$.

The anion path (see Table 12) for NCO^- possibly does not contribute appreciably, due to the extremely low concentration of NCO^- in acid solution owing to its protonation. The problems caused by the simultaneous hydrolysis of HNCO in acid solution prevented a study of the path in the Eu(II) or in the Cr(II) reduction.

The value of k_{FeNCO} (see Table 12) was measured at 1.6°, ionic strength 1.00M, in a series of experiments in which $[Eu(II)]_0 > [FeNCO^{2+}]_0$. The observed rate constants were pseudo-first-order; consequently accurate values of $[FeNCO^{2+}]_0$ were not needed. The $FeNCO^{2+}$ solutions were prepared by adding a weighed amount of KNCO to an Fe^{3+} solution in which $[H^+] < 0.02M$. Solutions containing $FeNCO^{2+}$ were mixed with Eu(II) solutions shortly after preparation. The results of the experiments are shown in Table 23, substantiating the rate law in Eq 40. Comparisons of the $[Eu(II)]_0$ and

Table 23. Kinetic data on the reaction of Eu(II) with $FeNCO^{2+}$ at 1.6°, 1.00M ionic strength

Expt No.	$10^5[Eu(II)]_0$ M	$10^5[FeNCO^{2+}]_0$[a] M	10^5C_{Fe} M	10^4C_{NCO} M	$[H^+]$ in the reactant solution, M	$[H^+]$ M	$10^{-6}k_{FeNCO}$[b] $M^{-1}sec^{-1}$
1	4.82	3	10.2	5	0.020	0.051	1.45
2	6.20	3	4.90	10	0.015	0.253	1.60
3	6.70	2	3.70	5	0.010	0.505	1.62
4	8.20	3	4.90	10	0.015	0.507	1.71
5	6.55	3	10.2	5	0.020	0.510	1.57
						Av =	1.59 ± .06

[a]Calculated using Q_{NCO} = 11.8 and not considering the acid hydrolysis of HNCO.

[b]Calculated from the observed pseudo-first-order rate constant as $k_{FeNCO} = k_{obsd}/[Eu(II)]_0$.

$$-d[FeNCO^{2+}]/dt = k_{FeNCO}[Eu^{2+}][FeNCO^{2+}] \quad (44)$$

and $[FeNCO^{2+}]_0$ concentrations listed in Table 23 do not seem to imply that pseudo-first-order behavior should be expected; the observed first order rate behavior is explained by the claim that $[FeNCO^{2+}]_0$ concentrations were much lower than listed in Table 23, owing to the acid hydrolysis of HNCO. The close agreement between the values of k_{FeNCO} calculated for experiments 3 and 5 is cited as evidence that the calculation $k_{FeNCO} = k_{obsd}/[Eu(II)]_0$ is at least approximately correct, although the assumption appears weak in experiment 1. The value for k_{FeNCO} in experiment 1 is not considered significantly low; no acid dependence is claimed for k_{FeNCO}.

Measurement of k_{FeNCO} for the Cr(II) reduction of $FeNCO^{2+}$ was done in the way described above for the Eu(II) reduction. The results, shown in Table 24, support the rate expression shown in Eq 45. The experiments at 1.6° do not

$$-d[FeNCO]/dt = k_{FeNCO}[Cr^{2+}][FeNCO^{2+}] \quad (45)$$

indicate an acid dependence for k_{FeNCO}. Kinetic data were obtained at 15.8, 20.0, and 25.0°. The activation parameters for k_{FeNCO} were calculated by a computer fit (44) of the data to Eq 9 ; the results, with the average observed and the recalculated value for k_{FeNCO} at each temperature, are listed in Table 25.

Table 24. Kinetic data on the reaction of Cr(II) with $FeNCO^{2+}$ at 1.00M ionic strength

Expt No.	Temp °C	$10^5[Cr(II)]_0$ M	$10^5[FeNCO^{2+}]_0$[a] M	10^5C_{Fe} M	10^4C_{NCO} M	$[H^+]$ in Fe reactant solution M	$[H^+]$ M	$10^{-5}k_{FeNCO}$[b] $M^{-1}sec^{-1}$
1	1.6	9.50	3	10.2	5	0.020	0.051	3.38
2	1.6	16.6	3	4.90	10	0.015	0.100	4.69
3	1.6	21.8	3	5.10	5	0.010	0.505	4.35
4	1.6	17.3	3	4.90	10	0.015	0.507	4.40
5	1.6	2.6	3	10.2	5	0.020	0.510	4.99[c]
	1.6						Av =	4.4±.4
6	15.8	7.50	3	3.50	10	0.010	0.505	5.20
7	15.8	7.90	2	5.10	5	0.010	0.505	6.33
8	15.8	10.3	3	6.35	7	0.010	0.505	5.93
	15.8						Av =	5.8±.4
9	20.0	13.6	2	3.50	7	0.010	0.505	5.9
10	25.0	7.45	3	3.50	10	0.010	0.505	6.35
11	25.0	10.1	3	3.50	10	0.010	0.505	8.07
	25.0						Av =	7.2±.9

[a]Calculated using Q_{NCO}=11.8 and not considering the acid hydrolysis of HNCO.

[b]Calculated from the observed pseudo-first-order rate constant as $k_{FeNCO} = k_{obsd}/[Cr(II)]_0$.

[c]The $(D-D_\infty)$ vs time plots in this experiment were curved toward slower reaction at longer times (e.g., second order behavior); k_{obsd} was calculated from the initial slope of the plots.

Table 25. Observed rate constants, activation parameters, and calculated rate constants for the reaction of Cr(II) with $FeNCO^{2+}$

Quantity	Temperature			
	1.6°	15.8°	20.0°	25.0°
$10^{-5}k_{FeNCO}$ (obsd, $M^{-1}sec^{-1}$)	4.4±.4	5.8±.4	5.9	7.2±.9
$\Delta H^{\ddagger}$ (kcal/mole)		2.86±.67		
$\Delta S^{\ddagger}$ (eu)		-22.2±2.4		
$10^{-5}k_{FeNCO}$ (calc, $M^{-1}sec^{-1}$)	4.2	5.7	6.2	6.9

The identity of the Cr(III) product of the Cr(II) reduction of $FeNCO^{2+}$ was investigated. The product was prepared by slow addition of Cr^{2+} to a stirred solution of $FeNCO^{2+}$ with the rigorous exclusion of oxygen. In a typical preparation, 0.075 mmoles Cr^{2+} were added to 17.5 ml of solution containing .91 mmoles Fe(III), 1.5 mmoles $HClO_4$ and 1.0 mmoles KNCO. The product solution was passed through Dowex 50W-X8 cation exchange resin in the Na^+ form; ions presumably with charge 2+ were eluted from the resin by a solution containing 0.98M $LiClO_4$ and 0.02M $HClO_4$. The spectrum of the eluted complex was similar to that for chromium(III) complexes (see Table 26). A total chromium analysis (by the diphenylcarbazide method (54)) on the result of one of the separations allowed evalua-

Table 26. Spectral properties of the product of the reaction of Cr(II) with $FeNCO^{2+}$ and of $Cr(H_2O)_6^{3+}$ and $(H_2O)_5CrNH_3^{3+}$, at room temperature

Quantity	Complex			
	Freshly eluted product	Eluted product after initial first order change[a]	$Cr(H_2O)_6^{3+}$	$(H_2O)_5CrNH_3^{3+}$
λ_{max}, ϵ_{max}	5780, 21.0	5720, 18.7	5750, 13.1	5470, 20.5
λ_{max}, ϵ_{max}	4010, 20.0	4110, 18.3	4080, 15.6	3970, 19.0
$\frac{\epsilon_{max} \text{ at long } \lambda}{\epsilon_{max} \text{ at short } \lambda}$	1.05	1.02	0.845	1.05
2500	110	37[b]	3.8	5.7

[a]See text.

[b]The uv absorbance is temperature dependent in 0.02M $HClO_4$; absorbance increases by about 10% as temperature increases 10°.

tion of extinction coefficients, shown in Table 26. The freshly eluted product was not spectrally stable; the visible and ultraviolet spectra changed with moderate slowness in first order processes catalyzed by Cr^{2+} and H^+ (see Table 27). After the initial first order spectral changes, further small changes occurred and were still occurring after a week at room temperature. The product of the initial first order spectral change was not eluted from Dowex 50W-X8 resin by 1M electrolyte. The approximate spectral properties of the products and, for comparison, those of $Cr(H_2O)_6^{3+}$ and $(H_2O)_5CrNH_3^{3+}$ are shown in Table 26. The ratio of ϵ_{max} at long λ to ϵ_{max} at short λ (see Table 26) was .92 in one solution after 1 week at room temperature. The kinetic behavior of the freshly eluted product is shown in Table 27.

Table 27. Kinetic properties of freshly eluted[a] product of the reaction of Cr(II) and $FeNCO^{2+}$ at room temperature

Expt No.	$[H^+]$	$[Cr^{2+}]$	$10^4 k_{obsd}$[a] sec^{-1}
1	0.020	0.0	6.0
2	0.030	0.0	9.9
3	0.246	0.0	19
4	0.020	0.0078	11
5	0.032	0.046	14

[a]See text.

The observations described above lead to the following conclusions regarding the product of the Cr(II)-$FeNCS^{2+}$ reaction and the changes subsequently occurring in the product. The initial product is a 2+ ion, probably $CrNCO^{2+}$ or $CrOCN^{2+}$, based on ion exchange behavior. No information was obtained relating to the possibility of linkage isomerism occurring rapidly, before or during separation of the +2 product. The freshly eluted product undergoes ligand modification in a first order process, leading to a 3+ ion that is not $Cr(H_2O)_6^{3+}$ or $(H_2O)_5CrNH_3^{2+}$, based on spectra. Again based on spectra, the 3+ ion undergoes further change, probably aquation to $Cr(H_2O)_6^{3+}$.

Azide

The value of the rate constant k_{FeN_3} was found to be very large, near the limit of stopped-flow measurability; experiments to measure it were similar to those already described for other k_{FeX} constants (see Table 12). The results of the measurements are listed in Table 28. The rate constant k_{FeN_3} was assumed to be second order. Initial concentrations were not varied sufficiently to completely verify that point. Table 28 indicates that k_{FeN_3} is independent of $[H^+]$ in the range 0.05 to 0.65M.

Haim and Sutin (13) have reported k_{FeN_3} for the Cr(II) reduction of FeN_3^{2+} to be immeasurably large by stopped-flow methods; $> 2\times10^7 M^{-1}sec^{-1}$ at 25°. The lower limit $2\times10^7 M^{-1}sec^{-1}$

Table 28. Kinetic data on the reaction of Eu(II) with FeN_3^{2+} at 1.6°, 1.00M ionic strength

Expt No.	$10^5[Eu(II)]_0$ M	$10^5[FeN_3^{2+}]_0$[a] M	$10^5[Fe(III)]_0$ M	$[H^+]$ M	$10^{-7}k_{FeN_3}$ M-1sec-1
1	3.17	0.96	11.5	0.050	1.06 ± .07
2	4.52	1.92	25.7	0.613	0.905 ± .036
3	2.60	0.96	5.25	0.650	1.77 ± .28
4	3.10	0.96	16.8	0.650	1.24 ± .24
5	3.67	1.92	12.5	0.650	0.85 ± .15
					Av = 1.2 ± .3

[a]Calculated using Q_{N_3} = .364 at 1.6°; evaluation of this number is described in the fluoride section.

was established for k_{FeN_3} in this study at 1.6° as well, in an experiment with $[Cr(II)]_0 = 2.66 \times 10^{-5}$, $[FeN_3^{2+}]_0 = 1.44 \times 10^{-5}$, and $[H^+] = 1.00M$.

Fluoride

A measurement of Q_F was required for the design of experiments to measure the rate of reduction of FeF^{2+}. Since the spectrum of FeF^{2+} is very similar to that of Fe^{3+}, a procedure was devised to use both HF and HN_3 in solutions of Fe(III). The intense visible absorption band of FeN_3^{2+} ($\lambda = 4600\text{Å}$, $\epsilon = 4400\ M^{-1}cm^{-1}$) provided a convenient analysis for FeN_3^{2+}. The known equilibrium quotient Q_{N_3} provided $[Fe^{3+}]$, whence $[FeF^{2+}]$ was computed from the mass balance. The absorbances of solutions containing iron(III), HF, and HN_3 were measured at 4600Å as described in the experimental section. Complexation of iron(III) by HF caused the measured absorbance to be lower than if HN_3 were the only complexing agent. The concentrations of FeN_3 were computed from measured absorbances, and the concentrations of Fe^{3+} were calculated from the equilibrium quotient Q_{N_3}. The concentration of iron(III) complexed by fluoride was calculated by difference. A small correction for FeF_2^+ was made ($Q_2 = [FeF_2^+][H^+]/[FeF^{2+}][HF] = 12.6$ (55) at 1.6°) and Q_F was calculated, using Eq 47. The

$$Fe^{3+} + HF = FeF^{2+} + H^+ \qquad (46)$$

$$Q_F = \frac{[FeF^{2+}][H^+]}{[Fe^{3+}][HF]} \qquad (47)$$

results are described in Tables 29 and 30. The numbers Q_F = 166 and Q_{N_3} = .364 were taken as valid at 1.3° and 1.00M ionic strength. The value for Q_F compares reasonably well with 202 at 1.6°, 0.50M ionic strength, extrapolated from the data of Connick et al. (55). The value for Q_{N_3} at 1.3°, with the value .51 at 25.0°, leads to ΔH° for Eq 5 = 2.32 kcal/mole, in good agreement with ΔH° = 2.03 kcal/mole, reported by Wallace and Dukes (32) in 1.0M HNO_3.

One experiment was done to test the existence of the anion path (see Table 12) for fluoride. The initial concentrations were $[Eu(II)]_0 = 29.6\times10^{-4}$, $[Fe(III)]_0 = 2.20\times10^{-4}$, C_{HF} = 0.050, and $[H^+]$ = 1.00M. The observed rate constant, 5680 $M^{-1}sec^{-1}$ indicates no catalysis when compared to the uncatalyzed rate constant, also 5680 $M^{-1}sec^{-1}$ (Table 9), and considering the value of the k_f' correction term in Eq 29. The value of the correction is about 50 $M^{-1}sec^{-1}$, using the data of Pouli and Smith (56) to obtain a value for k_f'.

The rate constant k_{FeF} (see Table 12) was too large to measure by the stopped-flow procedures used to measure k_{FeX} for other anions, partly because the absence of an intense absorption band for FeF^{2+} prevented studies at ideal concentration conditions. The competition procedure outlined in the experimental section was used to measure k_{FeF} at 1.6°. The differential equation describing the rate of change of $[FeN_3^{2+}]$ with respect to $[FeF^{2+}]$ in the presence of Eu^{2+},

Table 29. The absorbance of solutions containing Fe(III), HF, and HN_3 at ionic strength 1.00M

Expt No.	Temp °C	C_{HClO_4} M	$10^3 C_{Fe}$ M	$10^3 C_{HF}$ M	$10^2 C_{HN_3}$ M	Absorbance/5 cm	$10^5[FeN_3^{2+}]$ M
1	1.4	0.7904	8.13	0.00	2.083	1.692[a]	8.053
2	1.3	0.7904	8.13	2.068	2.083	1.440	6.838
3	1.4	0.7904	8.13	4.136	2.083	1.218	5.784
4	1.3	0.7904	8.13	6.204	2.083	1.037	4.924
5	1.3	0.893	7.28	6.000	3.300	1.288	6.116
6	1.3	0.893	7.28	8.260	3.300	1.100	5.223
7	1.3	0.893	7.28	12.00	3.300	0.871	4.136

[a]This value leads to $\epsilon_{FeN_3} Q_{N_3} = 1600$; taking $_{FeN_3} = 4400$, as already described, leads to $Q_{N_3} = 0.364$.

Table 30. Calculations leading to Q_F at ionic strength 1.00M

Expt No.	Temp °C	$[H^+]$ M	$10^3[Fe^{3+}]$ M	$10^3[HF]$ M	$10^5[FeF_2^+]$ M	$10^3[FeF^{2+}]$ M	Q_F
2	1.3	0.7916	6.852	0.8424	1.6	1.194	163
3	1.4	0.7927	5.793	1.794	6.3	2.216	169
4	1.3	0.7937	4.932	2.916	14	3.008	166
5	1.3	0.8960	4.375	3.039	12	2.727	184[a]
6	1.3	0.8967	3.737	4.559	21	3.281	173
7	1.3	0.8977	2.959	7.320	40	3.8799	161
							Av = 166 ± 4

[a]This number was not included in the average value for Q_F.

assuming second order rate laws, can be derived from Eqs 48 and 49, by division. The result is shown in Eq 50.

$$\frac{-d[FeN_3^{2+}]}{dt} = k_{FeN_3}\,[FeN_3^{2+}][Eu^{2+}] \tag{48}$$

$$\frac{-d[FeF^{2+}]}{dt} = k_{FeF}\,[FeF^{2+}][Eu^{2+}] \tag{49}$$

$$\frac{d[FeN_3^{2+}]}{d[FeF^{2+}]} = \frac{k_{FeN_3}\,[FeN_3^{2+}]}{k_{FeF}\,[FeF^{2+}]} \tag{50}$$

The depletion of Eu(II) by reaction with Fe^{3+} is negligible during the times required for reaction with FeN_3^{2+} and FeF^{2+}. Integration of Eq 50 yields Eq 51, where the subscripts A

$$\frac{\ln \dfrac{[FeN_3^{2+}]_A}{[FeN_3^{2+}]_0}}{\ln \dfrac{[FeF^{2+}]_A}{[FeF^{2+}]_0}} = \frac{k_{FeN_3}}{k_{FeF}} \tag{51}$$

denote concentrations immediately after all the Eu(II) has been oxidized, but before iron(III) complexes re-form or aquate. The quantities in Eq 51 were evaluated from photographs like the one shown in Figure 13. The lines in Figure 13 , from top to bottom, are the oscilloscope deflections caused respectively by the following solutions: Fe(III) reagent only (containing HN_3 and HF), mixed solutions while the reactant syringes are moving forward (e.g. Eu(II) has been

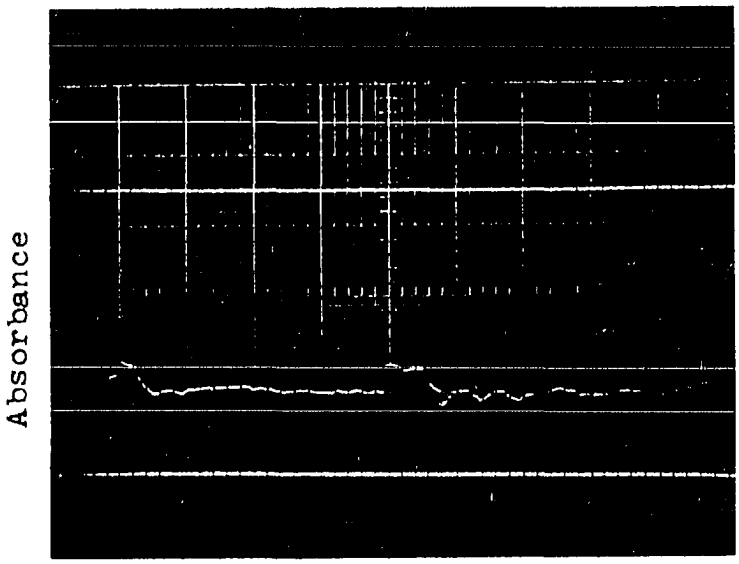

Figure 13. An oscilloscope trace showing the absorbances of FeN_3^{2+}-FeF^{2+} solution at equilibrium, after dilution and reaction with Eu^{2+} (both before and after equilibrium was established), and of Eu^{2+} solution

oxidized, but the complexation equilibria have not been re-established), the mixed solutions at equilibrium, and Eu(II) reagent only. The absorbances attributed to the lines are, from top to bottom, respectively, D, A, D/4, and 0. The equilibrium absorbance D/4 arises from the shift in the equilibria described by Eqs 5 and 46 upon dilution; the total iron(III) concentration was much greater than the Eu(II) concentration, so the effect of mixing on the complexation equilibria was that of dilution only (see Table 31 for initial Fe(III) and Eu(II) concentrations). The quantities needed for evaluation of k_{FeF} from Eq 51 were obtained from oscilloscope deflections like those shown in Figure 13, according to Eqs 52 and 53, where $[FeX^{2+}]_0$ values were

$$[FeN_3^{2+}]_A = 2[FeN_3^{2+}]_0 \ \frac{A}{D} \qquad (52)$$

$$[FeF^{2+}]_A=[FeF^{2+}]_0- [Eu^{2+}]_0-([FeN_3^{2+}]_0-[FeN_3^{2+}]_A) \qquad (53)$$

calculated from Q_X and $[Eu^{2+}]_0$ was obtained by analysis. The results of the experiments are shown in Tables 31 and 32. The values of A/D predicted for experiments 6 and 7 in Table 31 are .50 and 0.0, on the basis of initial concentrations of Eu(II), FeN_3^{2+}, and FeF^{2+}; the observed values, .490 and 0.007, are in fair agreement. The average value for k_{FeF}, from Table 32, is $k_{FeF} = (1.9 \pm 0.3)\times10^7 M^{-1}sec^{-1}$; k_{FeF} appears to be independent of $[H^+]$ in the range $0.15 < [H^+] < 0.50M$.

Table 31. Data on the competitive oxidation of Eu(II) by FeF^{2+} and FeN_3^{2+} at 1.6°, 1.00M ionic strength

Expt No.	$[H^+]$ M	$10^5[Eu(II)]_0$ M	$10^5[FeN_3^{2+}]_0$[a] M	$10^5[FeF^{2+}]_0$[b] M	$10^3[Fe(III)]$ M	A/D obsd
1	0.15	6.05	3.635	7.58	1.12	0.250
2	0.50	2.43	3.635	3.35	1.08	0.375
3	0.50	2.835	3.635	1.69	1.06	0.250
4	0.50	3.351	3.635	3.35	1.08	0.306
5	0.50	6.13	3.635	6.75	1.12	0.250
6	0.50	0.0	3.6	0.0	1.0	0.490
7	0.50	10	3.6	3.4	1.1	0.007

[a]Calculated using $Q_{N_3} = 0.364$.

[b]Calculated using $Q_F = 166$.

Table 32. Calculations for the competitive oxidation of Eu(II) by FeF^{2+} and FeN_3^{2+} at 1.6°, 1.00M ionic strength

Expt No.	$[H^+]$ M	$10^5[FeN_3^{2+}]_A$[a] M	$10^5[FeF^{2+}]_A$[b] M	k_{FeN_3}/k_{FeF}	$10^{-7}k_{FeF}$[c] $M^{-1}sec^{-1}$
1	0.15	1.818	3.347	0.848	1.42
2	0.50	2.726	1.829	0.476	2.52
3	0.50	1.818	0.672	0.751	1.60
4	0.50	2.225	1.409	0.567	2.12
5	0.50	1.818	2.437	0.680	1.76
					Av = 1.9 ± .3

[a]Calculated according to Eq 52.

[b]Calculated according to Eq 53.

[c]Calculated using $k_{FeN_3} = 1.2 \times 10^7$.

The value for k_{FeF} in the Cr(II) reduction of FeF^{2+} was obtained in the conventional stopped-flow manner. The results of the experiments at 1.6° are listed in Table 33.

Table 33. Kinetic data on the reaction of Cr(II) with FeF^{2+} at 1.6°, 1.00M ionic strength

Expt No.	$10^5[Cr(II)]_0$ M	$10^5[FeF^{2+}]_0$ [a] M	$10^5 C_{Fe}$ M	$[H^+]$ M	$10^{-5}k_{FeF}$ $M^{-1}sec^{-1}$
1	6.66	2.55	10.4	0.10	8.7[b]
2	6.40	3.50	10.4	0.985	5.48
3	6.24	2.55	10.4	1.00	7.02
4	5.42	7.00	12.3	1.00	7.42
5	5.20	3.00	5.26	1.00	6.16
6	5.20	2.55	10.4	1.00	9.00
7[c]	3.63	3.50	6.15	1.00	7.68
8	2.12	5.35	13.5	1.00	9.30
					Av = 7.6 ± 1.1

[a] Calculated using $Q_F = 166$.

[b] Estimated from initial slopes of the plot suggested by Eq 16, using an estimate for D_∞. The uncatalyzed aquation (Table 9) at $.10[H^+]$ interfered with evaluation of k_{FeF}.

[c] The rate constant was calculated assuming $[Cr(II)]_0 = [FeF^{2+}]_0 = 3.56 \times 10^{-5}M$.

The calculated values for k_{FeF} are badly scattered, but no trends with concentration changes are noted. The initial concentrations were varied by factors of 3, 3, and 10 for Cr(II), FeF^{2+}, and H^+, respectively. Experiments were done with $[Cr(II)_0 > [FeF^{2+}]_0$ and with $[Cr(II)]_0 < [FeF^{2+}]_0$. The average value for the rate constant is $k_{FeF} = (7.6 \pm 1.1)$

$x10^5 M^{-1}sec^{-1}$.

The chromium product of the reaction between Cr(II) and FeF^{2+} was found to be exclusively CrF^{2+}, by the ion exchange technique described in the experimental section. The product was prepared by mixing 0.004M FeF^{2+} with 0.00296M Cr^{2+} (0.00362M Fe^{3+}, 0.65M H^+, 1.00M ionic strength, after mixing) at 1.6°. From the ion exchange separation, 0.222 mmoles of Cr^{2+} yielded .219 mmoles of CrF^{2+} (identified by the visible spectrum), for a 98.5% yield. The expected yield, assuming quantitative formation of CrF^{2+} by the FeF path is 99.4%. The expected yield was calculated from Eq 54, where

$$\frac{d[FeF^{2+}]}{d[Fe^{3+}]} = \frac{k_{FeF}}{k'} \frac{[FeF^{2+}]}{[Fe^{3+}]}$$

$$\ln \frac{[FeF^{2+}]}{[FeF^{2+}]_0} = \frac{k_{FeF}}{k'} \ln \frac{[Fe^{3+}]}{[Fe^{3+}]_0} \qquad (54)$$

$k' = 1.49x10^3\ M^{-1}sec^{-1}$ = the composite rate constant for the uncatalyzed reduction of Fe^{3+} in .65M H^+. The observed and expected yield are in good agreement.

Bromide

Values for Q^1_{Br} and k'_f (Eqs 55 and 56) were needed for the

$$Fe^{3+} + Br^- = FeBr^{2+} \qquad k'_f,\ k'_{aq} \qquad (55)$$

$$Q^1_{Br} = \frac{[FeBr^{2+}]}{[Fe^{3+}][Br^-]} \qquad (56)$$

study of bromide catalysis of the reduction reaction of iron (III). These quantities are also of considerable interest in their own right. The measurement of these quantities is described below. It is important to state that these numbers are difficult to evaluate since Q^i_{Br} is small. The measurement was further complicated by the existence of significant concentrations of outer-sphere $Fe^{3+}\cdot Br^-$ complex in solutions containing the high bromide concentrations needed to evaluate Q^i_{Br} and k'_f. The formation of the outer-sphere complex was assumed to conform to Eqs 57 and 58.

$$Fe^{3+} + Br^- = Fe^{3+}\cdot Br^- \qquad \text{(very rapid)} \qquad (57)$$

$$Q^o_{Br} = \frac{[Fe^{3+}\cdot Br^-]}{[Fe^{3+}][Br^-]} \qquad (58)$$

Five distinct types of experiments were done to measure different kinetic and equilibrium aspects of the complexation reactions. The studies were as follows: (1) k'_{aq} for the reverse of Eq 55 was evaluated by studying the rate of approach to equilibrium under conditions where very little $FeBr^{2+}$ was formed, (2) k'_f for Eq 55 was evaluated from the very rapid oxidation of Cr^{2+} by $FeBr^{2+}$ under conditions where formation of $FeBr^{2+}$ was the rate limiting step, (3) Q^i_{Br} was evaluated from the yield of $CrBr^{2+}$ when Cr^{2+} was mixed with equilibrium solutions of $FeBr^{2+}$ under conditions where the reaction of Cr^{2+} and the $FeBr^{2+}$ initially present was the major reaction leading to $CrBr^{2+}$, (4) the sum $(Q^i_{Br} + Q^o_{Br})$

was evaluated from spectrophotometric measurements at high and varying concentrations of Br^-, and (5) molar extinction coefficients, ϵ^1_{FeBr} and ϵ^o_{FeBr}, were evaluated from the measured absorbances of 4 solutions: the separate Fe^{3+} and Br^- reactant solutions, the freshly mixed reactants containing ion pairs but not inner-sphere $FeBr^{2+}$, and the mixed solutions after equilibration with respect to Eq 55, containing both inner and outer-sphere complexes.

The rate law for approach to equilibrium by Eq 55 has been reported (37) and is shown in Eq 59. Since the equi-

$$\frac{d[FeBr^{2+}]}{dt} = k_f'[Fe^{3+}][Br^-] - k_{aq}'[FeBr^{2+}] \qquad (59)$$

librium constant Q_{Br} is known to be small (36), kinetic experiments can be devised in which only a small fraction of Br^- or Fe^{3+} is complexed at equilibrium. Such experiments measure k_{aq}' alone, as shown in an earlier section. The results of a series of measurements of k_{aq}' are shown in Table 34.

A series of experiments were done to measure k_f' in 1.00M H^+ at 1.6°. The value of k_{FeBr} (to be discussed later) in the Cr(II) reduction of $FeBr^{2+}$ is greater than 2×10^7 $M^{-1}sec^{-1}$ at 1.6°, and the value of k' for uncatalyzed Cr(II) reduction of Fe(III) is much smaller. Solutions containing Cr(II) and Br^- were mixed with Fe(III) solutions and the rate of disappearance of Fe^{3+} was monitored at 2500-2400Å. The rate

Table 34. Rate of approach to equilibrium by solutions containing iron(III) and bromide ions, in 1.00M H^+

Expt No.	Temp °C	$10^3 C_{Fe}$ M	C_{Br^-} M	Type of expt[a]	k_{obsd} sec^{-1}
1	1.6	14.2	0.0142	dilution	10.4
2	1.6	25.6	0.0256	formation	11.3
3	1.6	3.00	0.133	formation	10.9
4	1.6	2.00	0.200	dilution	10.7
5	1.6	1.00	0.400	formation	11.1
6	1.6	0.800	0.500	formation	10.5
7	15.8	51.2	0.080	formation	55.6

[a]See experimental section.

behavior was described by Eq 29, where the observed rate constant for Fe^{3+} reduction contained a significant contribution from the k_f' term. The results of the experiments were very imprecise due to the electronic instability of the stopped-flow apparatus at the sensitivity required for observation of the changes. The data are shown in Table 35. The values for

Table 35. The rate of formation of $FeBr^{2+}$ from Fe^{3+} and Br^- at 1.6°, 1.00M H^+

Expt No.	$[Br^-]$ M	$10^4[Cr(II)]_0$ M	$10^5[Fe(III)]$ M	k_{obsd} sec^{-1}	$k_f'[Br^-]$[a] sec^{-1}
1	0.15	1.66	2.00	0.307	0.0521
2	0.30	0.925	1.50	0.299	0.111
3	0.35	1.80	2.00	0.515	0.105
4	0.50	1.15	2.00	0.497	0.182

[a]See text.

$k_f'[Br^-]$ were calculated from Eq 29, where values of all the quantities except k_f' were known. The value of k' is 1.05×10^3 $M^{-1}sec^{-1}$ from Table 11, and the value of k_{Br} is 3900 $M^{-2}sec^{-1}$, as will be shown later. A plot of $k_f'[Br^-]$ vs $[Br^-]$ is shown in Figure 14. The solid line in Figure 14 was chosen as the best fit, leading to $k_f' = 0.34 \pm 0.03$ $M^{-1}sec^{-1}$ in 1.00M H^+, at 1.6°. Assuming k_{obsd} in Table 34 is of the form $k_{obsd} = k_f'[Br^-] + k_{aq}'$, and using $k_f' = 0.34$, the average value computed for k_{aq}' from Table 34 is 10.7 sec^{-1}. These values for k_f' and k_{aq}' imply $Q_{Br}^i = (0.34 \pm 0.03)/10.7 = 0.032 \pm 0.003$ M^{-1}.

The value of Q_{Br}^i was determined independently by a product analysis technique. Solutions containing $FeBr^{2+}$ in equilibrium with Fe^{3+} and Br^- were mixed (in the stopped-flow mixer) with solutions containing an excess of Cr^{2+}. The concentration of $CrBr^{2+}$ in the resulting solutions, determined by the ion exchange procedure already described, was not a direct measure of Q_{Br}^i because the reaction of excess Cr^{2+} with Fe^{3+} in the presence of Br^- also formed some $CrBr^{2+}$ by the anion path (Table 12). The reaction of Cr^{2+} with O_2 dissolved in water in the presence of Br^- ions was also shown to produce some $CrBr^{2+}$.

The relative concentrations in the product analysis experiments measuring Q_{Br}^i were as follows: $[FeBr^{2+}]_0 < [Cr^{2+}]_0 < [Fe(III)]_0$. The total $[CrBr^{2+}]$ in the product solution was assumed to form in the following ways: (1) The

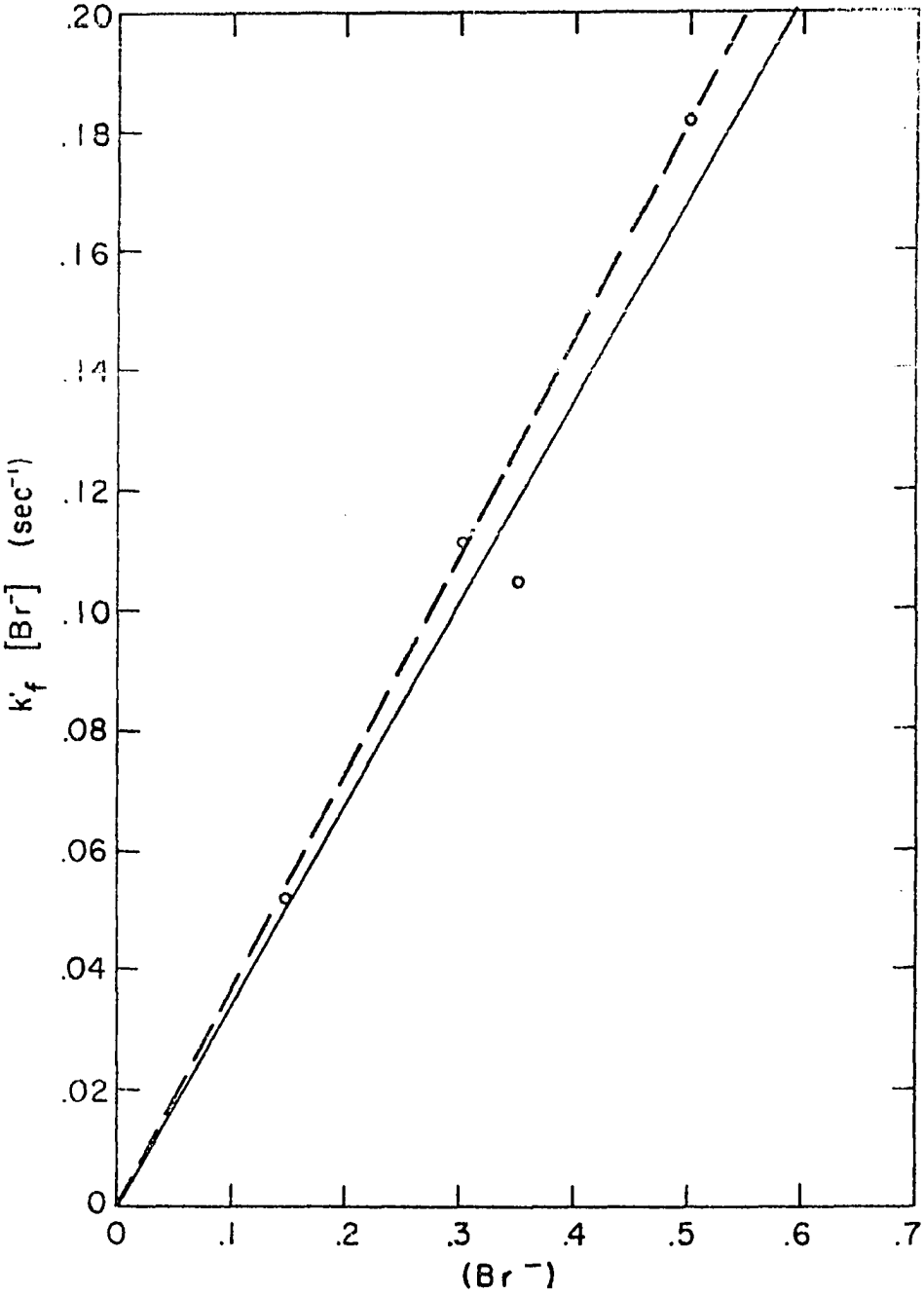

Figure 14. The relation between the formation rate of $FeBr^{2+}$ from Fe^{3+} and Br^-, and $[Br^-]$. The lower line is the line of best fit. The upper line was chosen as more correct on the basis of product analysis experiments

very rapid oxidation of Cr^{2+} by the $FeBr^{2+}$ in the Fe(III) solution at the instant of mixing, (2) oxidation of excess Cr(II) by the anion path, and (3) oxidation of excess Cr(II) by $FeBr^{2+}$ formed after the initial $FeBr^{2+}$ was reduced. The last two pathways were minimized by using solutions with high [Fe(III)], low [Br^-], and low excess [Cr(II)], but were not eliminated entirely. The $CrBr^{2+}$ found in the direct reaction of $FeBr^{2+}$ and Cr^{2+} was computed by an iterative procedure: a value for Q^1_{Br} was assumed, permitting calculation of the concentrations of all reactants in the mixed solutions immediately after the reduction of the $FeBr^{2+}$ initially present. These concentrations, together with previously measured rate constants for k', k_{Br} and the value for k'_f consistent with $k'_{aq} = 10.7\ sec^{-1}$ and the assumed value for Q^1_{Br}, were used to calculate the concentration of each species as a function of time, until the Cr^{2+} was consumed. A Runge-Kutta numerical method (see Appendix A) was used to do the calculation. The total [$CrBr^{2+}$] calculated was compared to the observed quantity and a new value for Q^1_{Br} was selected for the next calculation. The process was continued until the calculated and observed $CrBr^{2+}$ concentrations were the same. The convergent results are shown in Table 36. Also shown in Table 36 are the results of two divergent calculations, to demonstrate the sensitivity of the calculation. The average value for Q^1_{Br} from Table 36 is $0.039\ M^{-1}$; from the kinetic measurements,

Table 36. Results of Q^1_{Br} measurements at 1.6°, 1.00M H^+, by product analysis

Expt No.	C_{Fe}[a] M	C_{HBr} M	$10^4[Cr(II)]_0$ M	$10^4[CrBr^{2+}]_{obsd}$ M
1[c]	0.0300	0.111	5.75	3.60
1[c]	0.0300	0.111	5.75	3.60
1	0.0300	0.111	5.75	3.60
2	0.0250	0.133	3.85	3.59
3	0.0300	0.111	3.89	3.18

Expt	Assumed Q^1_{Br}, M^{-1}	$10^4[CrBr^{2+}]_{calcd}$ M	$10^4[CrBr^{2+}]_{cor}$[b] M	Calc Q^1_{Br}, M^{-1}
1[c]	0.04	4.016	2.21	0.0334
1[c]	0.02	2.935	1.99	0.0301
1	0.0319	3.602	2.103	0.0319
2	0.0473	3.591	3.099	0.0473
3	0.0373	3.187	2.444	0.0373

[a]All concentrations listed are those in the mixed solutions.

[b]The value of $[CrBr^{2+}]_{cor} = [CrBr^{2+}]_{calcd} - [FeBr^{2+}]_0$, where $[FeBr^{2+}]_0$ is the calculated value, based on the assumed Q^1_{Br}.

[c]Results of non-convergent calculations.

it is 0.032 ± 0.003 M^{-1}. The average value, $Q^i_{Br} = 0.034$, was chosen for use in further calculations. The dotted line in Figure 14 corresponds to this number. The value to be used for k_f' in further calculations is $k_f' = (0.034\ M^{-1})(10.7\ sec^{-1}) = 0.364\ M^{-1}sec^{-1}$.

A series of absorbance measurements at 4050Å, the wavelength of maximum absorbance for $FeBr^{2+}$ (36), were made at the temperatures 1.6°, 15.8°, and 25.0°, in solutions of 1.00M ionic strength. The results are shown in Table 37. A plot of $\bar{\epsilon}$ vs $\bar{\epsilon}/[R]_{XS}$ (see Eq 13) was expected to give values for ϵ_{FeBr} and Q_{Br}, as in the azidoiron system. The plot, shown in Figure 15 gives much larger values of Q_{Br} than determined by the kinetic or product analysis method, although smaller than determined by Lister and Rivington (36), who found $Q_{Br} = .61$ at 25°, ionic strength 1.2M. The presence of an outer sphere complex, $Fe^{3+}\cdot Br^-$, was proposed in an effort to account for

$$Fe^{3+} + Br^- \rightleftharpoons Fe^{3+}\cdot Br^-$$

$$Q^o_{Br} = \frac{[Fe^{3+}\cdot Br^-]}{[Fe^{3+}][Br^-]}$$

the apparent value of Q_{Br} derived from the spectrophotometric data. Evidence for an absorbing species formed immediately upon mixing Fe^{3+} and Br^- was obtained by stopped-flow measurements. The oscilloscope trace deflections caused by the following solutions were observed: (1) Fe^{3+} reagent only, (2) Br^- reagent only, (3) freshly mixed Fe^{3+} and Br^- reagents,

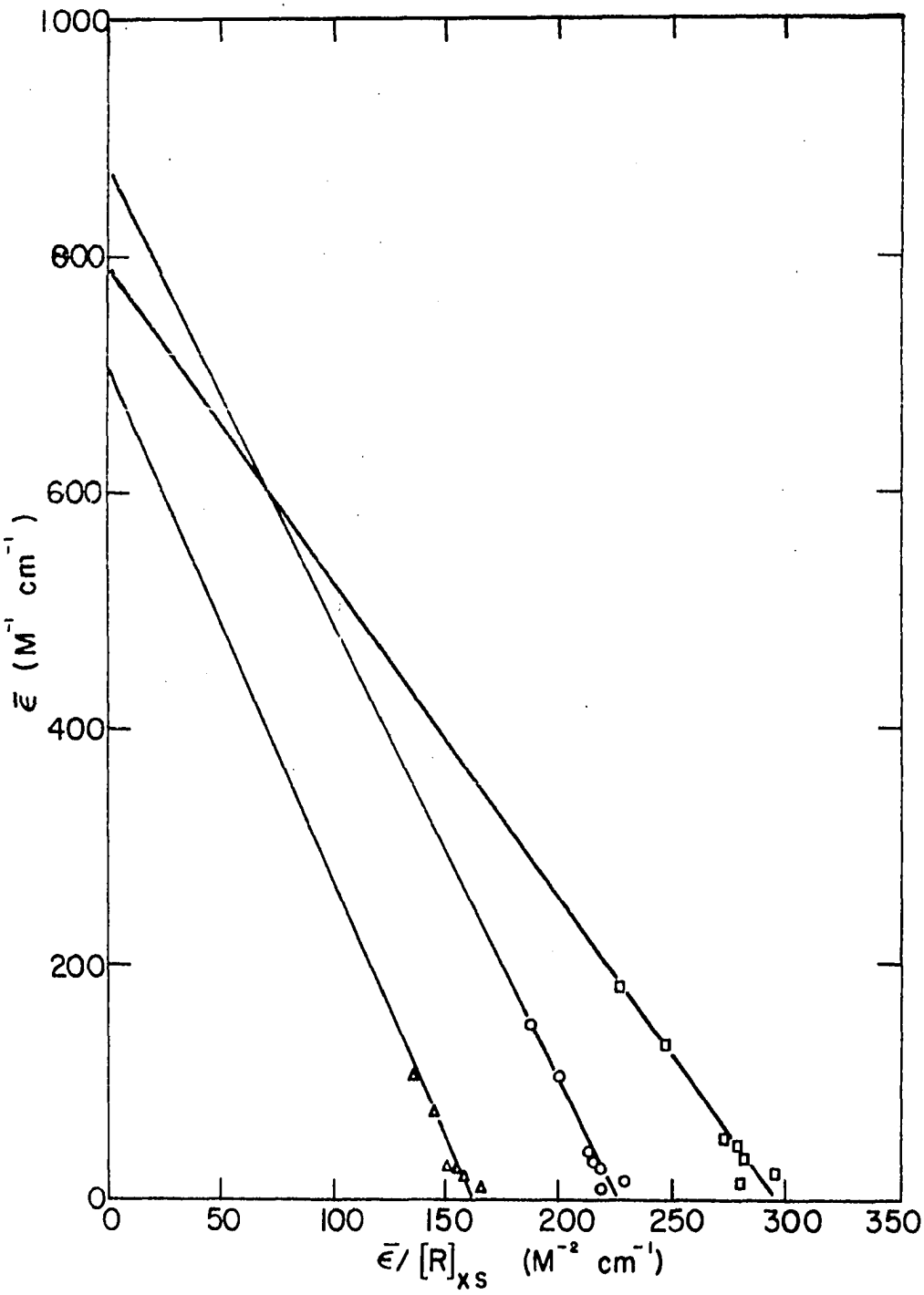

Figure 15. Spectrophotometric data leading to evaluation of ϵ^1_{FeBr} at 4050Å and the sum $Q^1_{Br} + Q^2_{Br}$ at the temperatures 1.6, 15.8, and 25.0°, denoted by Δ, 0, and □, respectively

Table 37. Results of absorbance measurements on $FeBr^{2+}$ solutions at ionic strength 1.00M, at 4050Å

Expt	$10^3 C_{Fe}$	C_{Br}	1.6°		15.8°		25.0°	
			$\bar{\epsilon}$[a]	$\bar{\epsilon}/[R]_{xs}$[a]	$\bar{\epsilon}$	$\bar{\epsilon}/[R]_{xs}$	$\bar{\epsilon}$	$\bar{\epsilon}/[R]_{xs}$
1	7.28	0.0799	13.2	165	18.2	228	23.6	295
2	7.28	0.1332	21.1	158	29.1	218	37.6	282
3	7.28	0.173	26.9	155	37.4	216	48.2	279
4	7.28	0.200	30.4	152	42.6	213	54.6	273
5	3.64	0.533	77.7	146	107	201	131	246
6	3.64	0.800	109	136	150	188	181	226
7[b]	50.0	0.0200	7.52	150	10.88	218	14.0	280

[a]See text.

[b]Total absorbance at each temperature was corrected by subtracting the absorbance of an identical iron solution with $HClO_4$ substituted for the HBr.

continuously observed by continuously driving the reactant syringes, and (4) mixed Fe^{3+} and Br^- solutions that had reached equilibrium with respect to Eq 55. In the absence of a quickly formed absorbing species, deflection (3) above would be expected to be midway between deflections (1) and (2). The results of the experiments are described in Table 38. The data in the table show that species form quickly that absorb light at all the wavelengths listed except 4050Å. The absorbance is assumed to be caused by $Fe^{3+}\cdot Br^-$. After obtaining evidence for the existence of the outer sphere complex, the plot shown in Figure 15 was reinterpreted, according to the following equations. Equation 60 applies if $[Fe^{3+}]$

$$\bar{\epsilon} = \frac{\epsilon^i_{FeBr}[FeBr^{2+}] + \epsilon^o_{FeBr}[Fe^{3+}\cdot Br]}{[Fe^{3+}] + [FeBr^{2+}] + [Fe^{3+}\cdot Br^-]}$$

$$\bar{\epsilon} = \frac{\epsilon^i_{FeBr}Q^i_{Br} + \epsilon^o_{FeBr}Q^o_{Br}}{Q^i_{Br} + Q^o_{Br}} - \frac{\bar{\epsilon}}{(Q^i_{Br}+Q^o_{Br})[Br^-]} \qquad (60)$$

is the limiting reagent; Eq 61 is more general. Equation 61

$$\bar{\epsilon} = \frac{\epsilon^i_{FeBr}Q^i_{Br} + \epsilon^o_{FeBr}Q^o_{Br}}{Q^i_{Br} + Q^o_{Br}} - \frac{\bar{\epsilon}}{(Q^i_{Br}+Q^o_{Br})[R]_{xs}} \qquad (61)$$

shows that the slopes in Figure 15 lead to the sum $Q^i_{Br} + Q^o_{Br}$, and (since $\epsilon^o_{FeBr} = 0$ at 4050A) the intercept is $(\epsilon^i_{FeBr})(Q^i_{Br})/(Q^i_{Br}+Q^o_{Br})$. Thus, Eq 61 permits evaluation of Q^o_{Br} at 1.6° and ϵ^i_{FeBr} at 4050Å from Figure 15, assuming the previously estab-

Table 38. Absorbances of Fe^{3+} and Br^- solutions separately, and of mixed Fe^{3+}, Br^- solutions at 1.6°, 1.00M H^+

Expt No.	λ[a] Å	$10^4 C_{Fe}$[b] M	C_{Br}[b] M	Oscilloscope deflections[c]				Absorbance in 2 cm cell[d]		
				Fe^{3+}	Br^-	Fresh mixture	Equil. mixture	Fe^{3+}	Br^-	Equil. mixture
1	4050	100	0.16	1	0	0	17	0[e]		
2	3300	100	0.16	23	0	18.5	25	0.18[e]		
3	2700	1.529	1.00	10.5	0	6.0	6.5	0.559	0.021	0.312
4	2600	1.529	1.00	19.0	0	10.6	12	0.960	0.046	0.529
5	2580	1.529	1.00	19.5	0	10.4	12	1.040	0.054	0.572

[a]Monochromator wavelength setting.

[b]Concentrations before mixing.

[c]Arbitrary units.

[d]Measured by Cary recording spectrophotometer.

[e]Calculated rather than measured.

lished value $Q^i_{Br} = .034\ M^{-1}$ at 1.6°. The slope and intercept of the 1.6° line in Figure 15 are -4.35 and 702; thus, $Q^i_{Br} + Q^o_{Br} = 1/4.35 = .230$, $Q^o_{Br} = .230 - .034 = .196$. The calculated value for ϵ^i_{FeBr} is $(702)(.230)/.034 = 4750\ M^{-1}cm^{-1}$. If ϵ^i_{FeBr} is assumed to be independent of temperature, then Q^i_{Br} and Q^o_{Br} can also be evaluated at the temperatures 15.8 and 25.0° by application of Eq 61. The results are expected to be only approximate, due to the scattered data and long extrapolations necessary for obtaining the intercepts in Figure 15.

Table 39. Values for Q^i_{Br} and Q^o_{Br} determined from Figure 15 and Eq 61, assuming $\epsilon^i_{FeBr} = 4750$ at each temperature, and $Q^i_{Br} = .034$ at 1.6°

Temp °C	Slope of line	Intercept of line	Q^i_{Br} M-1	Q^o_{Br} M-1
1.6	-4.35	702	0.034	0.20
15.8	-3.85	870	0.048	0.21
25.0	-2.68	787	0.062	0.31
25.0[a]	-1.65	495	0.063	0.54

[a]Re-calculated from the data of reference (36), obtained at 1.2M ionic strength, maintained with $NaClO_4$.

The values for Q^i_{Br} and Q^o_{Br} at 1.6° were used to calculate approximate molar extinction coefficients for both $FeBr^{2+}$ and $Fe^{3+} \cdot Br^-$; the calculations are shown in Table 40. The calculation procedure is as follows. Column C was calculated by comparing the number of units of oscilloscope deflection for Fe^{3+} and for the equilibrium mixture, to the absorbances of

Table 40. Calculation of molar extinction coefficients for $Fe^{3+}\cdot Br^{-}$ and $FeBr^{2+}$

A	B	C[a]	D[a]	E[a]
Expt No.	λ_o A	(Abs/cm)/unit	From stopped-flow (Abs/cm) due to both complexes	From stopped-flow (Abs/cm) due to $Fe^{3+}\cdot Br^{-}$
3	2700	0.0250	0.043	0.029
4	2600	0.0220	0.077	0.043
5	2580	0.0235	0.082	0.0405

A	F	G[a]	H[a]	I[a]	J[a]
Expt No.	From Cary (Abs/cm) due to both complexes	Corrected value (Abs/cm) due to $Fe^{3+}\cdot Br^{-}$	(Abs/cm) due to $FeBr^{2+}$	ε^{o}_{FeBr} $M^{-1}cm^{-1}$	ε^{i}_{FeBr} $M^{-1}cm^{-1}$
3	0.025	0.017	0.008	2500	6800
4	0.037	0.021	0.016	3000	14000
5	0.0385	0.019	0.02	2800	16000

[a]See text for the method of calculation.

the same solutions measured with the Cary spectrophotometer. The numbers shown in Column D were calculated by Eq 62 where

$$D = C(e) - C(i)\ \frac{6.845\text{x}10^{-5}}{7.645\text{x}10^{-5}}\left\{\frac{1}{2}\right\} \qquad (62)$$

C is the number in column C of Table 40, e and i are the deflections reported in Table 38 for the equilibrium mixture and the iron reactant respectively, $7.645\text{x}10^{-5} = C_{Fe}$ in the mixed solution, and $6.845\text{x}10^{-5} = [Fe^{3+}]$, calculated using $Q^{o}_{Br} + Q^{1}_{Br} = 0.23M^{-1}$. Column E was obtained by using Eq 63,

$$E = C(f) - C(i)\ \frac{6.965\text{x}10^{-5}}{7.645\text{x}10^{-5}}\left\{\frac{1}{2}\right\} \qquad (63)$$

where f is the deflection reported in Table 38 for the freshly mixed reactants and $6.965\text{x}10^{-5} = [Fe^{3+}]$, calculated using $Q^{o}_{Br} = 0.20\ M^{-1}$. The numbers listed in column F were calculated by Eq 64, where X, Y, and Z are the absorbances/2 cm reported

$$F = (X-Y) - (Z-Y)\ \frac{6.845\text{x}10^{-5}}{7.645\text{x}10^{-5}}\left\{\frac{1}{2}\right\}\left\{\frac{1}{2}\right\} \qquad (64)$$

in Table 38 for the equilibrium mixture, Br^- reactant, and Fe^{3+} reactant, respectively. The absorbances in column F, measured with the spectrophotometer, were considered more accurate than those in column D, and were taken to be correct. The values in column E were assumed to be in error by the same factors as those in D; corrected absorbances for $Fe^{3+}\cdot Br^-$, shown in column G, were calculated by Eq 65. The numbers in

$$G = (E)(F/D) \qquad (65)$$

column H were calculated by Eq 66. The molar extinction

$$H = F - G \qquad (66)$$

coefficients in columns I and J were calculated on the basis of Q^{i}_{Br} and Q^{o}_{Br} = .034 and .20 M^{-1}, leading to $[Fe^{3+}\cdot Br^{-}]$ = 6.8×10^{-6}M and $[FeBr^{2+}]$ = 1.2×10^{-6}M in the equilibrium solution.

The bromide calalysis of the iron(III), europium(II) reaction by the anion path (see Table 12) was measured at 1.6, 15.8, and 25.0° in solutions containing 1.0 M H^{+}. The values for k_{Br} were calculated according to Eq 31 and are shown in Table 41. The two experiments at 25° lead to an imprecise estimate for k_{Br}, but the average values at 1.6 and 15.8°, $(5.5 \pm 0.8)\times10^{3}$ and $(2.1 \pm 0.7)\times10^{4}$ $M^{-2}sec^{-1}$, respectively, allow the value $k_{Br} = 4.6\times10^{4}$ $M^{-2}sec^{-1}$ at 25° to be calculated, assuming $\ln(k_{Br})$ decreases linearly with T^{-1}. The value $k_{Br} = 4.6\times10^{4}$ $M^{-2}sec^{-1}$ is not inconsistent with the experiments done at 25°. The dependence of k_{Br} on $[H^{+}]$ was not investigated, because values for k'_{f} were known only in 1M H^{+}. Because none of the other k_{X} rate constants measured in this study were dependent on $[H^{+}]$, k_{Br} was assumed to be similarly independent. The activation parameters $\Delta H^{\ddagger}$ = 14 kcal/mole and $\Delta S^{\ddagger}$ = 10 eu were calculated for k_{Br}, using Eq 9 .

The general approach for measuring k_{FeX} (see Table 12) was to mix an equilibrium solution of FeX^{2+} with Eu^{2+} and assume the only significant path for FeX^{2+} concentration

Table 41. Results of experiments measuring k_{Br} for the reaction between Eu(II) and Fe(III) in 1.0M H^+

Expt No.	Temp °C	$[Br^-]$ M	$10^3[Eu(II)]_0$ M	$10^3[Fe(III)]_0$ M	$10^{-4}k_{obsd}$ $M^{-1}sec^{-1}$	$10^{-4}k_{corr}$[a] $M^{-1}sec^{-1}$	$10^{-4}k_{Br}$[b] $M^{-2}sec^{-1}$
1	1.6	0.200	4.18	1.00	0.699	0.697	0.64
2	1.6	0.291	5.15	1.00	0.761	0.759	0.66
3	1.6	0.400	4.35	1.00	0.737	0.733	0.41
4	1.6	0.500	2.35	0.200	0.851	0.846	0.55
5	1.6	0.640	4.25	1.00	0.904	0.898	0.52
	1.6						Av= 0.55±0.08
6	15.8	0.0500	2.89	0.400	1.31	1.30	1.8
7	15.8	0.0750	3.77	0.400	1.38	1.37	2.1
8	15.8	0.100	3.17	0.400	1.54	1.53	3.2[c]
9	15.8	0.100	2.21	0.200	1.49	1.48	2.7
10	15.8	0.200	1.93	0.200	1.43	1.40	1.1
11	15.8	0.300	1.97	0.200	1.71	1.67	1.5
12	15.8	0.400	1.70	0.200	1.63	1.56	0.88[c]
13	15.8	0.500	1.39	0.200	1.86	1.76	1.1
	15.8						Av= 2.1±0.7
14	25.0	0.500	0.211	0.0300	5.71	4.41	4.7
15	25.0	0.500	1.85	0.200	3.34	3.19	2.3

[a]Calculated according to Eq 30, with k_f' values taken from Table

[b]Calculated according to Eq 31, with k' values taken from Table 9.

[c]Not included in the average value.

changes was the Eu^{2+} reduction path. However, the Eu^{2+} reduction of $FeBr^{2+}$ was not fast enough to justify that assumption (see Eqs 32 and 33). Three different methods used to estimate k_{FeBr} without the assumption were: (1) some of the data at 1.6° were treated according to a more complete integrated rate law, (2) all the data were fitted to Eqs 32 and 33 using a trial and error Runge-Kutta numerical method (see Appendix B), and (3) the data at 25° were treated according to an integrated rate law based on the assumption that $[FeBr^{2+}]$ was constant during each experiment.

Application of method 1: two types of experiments were done at 1.6°. In some experiments an $FeBr^{2+}$ solution was mixed with an Eu(II) solution and the decrease in $[FeBr^{2+}]$ was observed at its absorption maximum (4050Å) just as in experiments to measure other k_{FeX} values. The concentration conditions $[Fe(III)]_0 > [Eu(II)]_0 > [FeBr^{2+}]_0$ were used; the more desirable condition, $[Eu(II)]_0 > [Fe(III)]_0$, was not practical because it would cause the absorbance change to be too small or the reaction time to be too short. The concentrations of Fe^{3+}, Eu^{2+}, and Br^- were assumed to be nearly constant during the depletion of the $FeBr^{2+}$ present at the instant of mixing, and Eq 68 was derived, following the method of Guggenheim (42).

$$\frac{-d[FeBr^{2+}]}{dt} = (k_{FeBr}[Eu^{2+}]+k'_{aq})[FeBr^{2+}] - k'_f[Fe^{3+}][Br^-]$$

$$k_{FeBr}[Eu^{2+}] + k'_{aq} = \beta = \text{constant} \qquad (67)$$

$$k'_f[Fe^{3+}][Br^-] = \alpha = \text{constant}$$

$$(\beta\ [FeBr^{2+}]_t - \alpha) = (\beta\ [FeBr^{2+}]_0 - \alpha)e^{-\beta t}$$

$$(\beta\ [FeBr^{2+}]_{t+\tau} - \alpha) = (\beta\ [FeBr^{2+}]_0 - \alpha)e^{-\beta(t+\tau)}$$

τ = a constant time increment

$$[FeBr^{2+}]_t - [FeBr^{2+}]_{t+\tau} = \frac{1}{\beta}\ (\beta\ [FeBr^{2+}]_0 - \alpha)e^{-\beta t}(1-e^{-\beta\tau})$$

$$\ln([FeBr^{2+}]_t - [FeBr^{2+}]_{t+\tau}) = A' - \beta t$$

A' = a constant

$$\ln([FeBr^{2+}]_t - [FeBr^{2+}]_{t+\tau}) = \ln \frac{D_t - D_{t+\tau}}{D_0 - D_\infty}$$

D_t = oscilloscope deflection at a time t.

$A = A' + \ln(D_0 - D_\infty)$ = a constant

$$\ln(D_t - D_{t+\tau}) = A - \beta t \qquad (68)$$

According to Eq 68, the slope of a plot of $\ln(D_t - D_{t+\tau})$ vs time is β; k_{FeBr} was evaluated from β, $[Eu^{2+}]$, and k'_{aq}, according to Eq 67. The results of the two experiments treated according to Eq 68 are given in Table 42. The value for k_{FeBr} at 1.6° was taken as 1.4×10^6 $M^{-1}sec^{-1}$; k_{FeBr} was assumed to be independent of $[H^+]$.

Application of method 2: experiments were done at 1.6, 15.8, and 25.0°, using a different procedure than was used

Table 42. Results of experiments measuring k_{FeBr} for the reaction between $FeBr^{2+}$ and Eu(II) in 1.00M H^+ at 1.6°, calculated according to Eqs 67 and 68

Expt No.	$[Br^-]$ M	$10^4[Eu(II)]_0$ M	$10^4[FeBr^{2+}]_0$ M	$10^4[Fe(III)]_0$ M	β sec^{-1}	$10^{-6}k_{FeBr}$ $M^{-1}sec^{-1}$
1	0.500	0.285	0.070	2.13	43.2±6.5[a]	1.3
2	0.500	0.522	0.070	2.13	81±13	1.4

[a]The indicated uncertainty is the average deviation from the mean in repeat experiments using the same set of reactant solutions.

for the experiments described in Table 42. A solution containing an equilibrium mixture of Fe^{3+}, $FeBr^{2+}$, and Br^- was mixed with a solution containing Eu(II) and Br^-; the concentration of Br^- was the same in each solution so $FeBr^{2+}$ was at its equilibrium concentration at the instant of mixing. The progress of the reaction was monitored at 2700-2580Å, where the species Eu^{2+}, Fe^{3+}, $FeBr^{2+}$, and $Fe^{3+}\cdot Br^-$ absorb. A Runge-Kutta numerical procedure (see Appendix B) was used to compare the observed absorbance changes with those predicted by the measured rate constants k_{Br}, k'_{aq}, and k'_f, the measured extinction coefficients, and an assumed value for k_{FeBr}. The value $k_{FeBr} = 1.4 \times 10^6$ $M^{-1}sec^{-1}$ was taken as correct at 1.6°. The results of the final calculations, using the values for k_{FeBr} at 15.8 and 25.0° that lead to the best agreement between observed and calculated absorbances are shown in Table 43. The sensitivity of the agreement to the choice of k_{FeBr} was poor; the sensitivity is demonstrated by calculations shown in the table using poor choices for k_{FeBr}, for the thirteenth experiment.

Application of method 3: The Runge-Kutta treatment indicated that the $FeBr^{2+}$ concentration in the experiments at 25° was relatively constant, never falling below 85% of the initial concentration. Equation 69 was derived, assuming $[Fe^{3+}]$ and $[FeBr^{2+}]$ were constant during an experiment.

Table 43. Observed and calculated absorbances (arbitrary scale) in experiments measuring the rate of the bromide catalyzed reduction of Fe(III) by Eu(II), in 1.00 M H^+

Expt No.	Temp °C	$[Br^-]$ M	10^{-6} k_{FeBr} M^{-1} sec^{-1}	Time after mixing, msec	10^5 [Eu(II)] M	10^4 [Fe(III)] M	10^6 $[FeBr^{2+}]$ M	Abs calcd	Abs obsd
1	1.6	0.500	1.4	0	2.85	2.06	7.00	3.08	3.08
				5	2.71	2.06	5.63	2.38	2.38
				10	2.59	2.06	4.60	1.86	2.02
				80	0.97	2.02	1.15	0.06	0.03
2	1.6	0.500	1.4	0	5.22	2.06	7.00	3.40	3.40
				5	4.97	2.06	4.80	2.27	2.04
				10	4.79	2.05	3.39	1.55	1.38
				80	3.83	1.98	0.57	0.40	0.00
3	1.6	0.0488	1.4	0	3.00	5.00	0.820	6.82	6.82
				50	2.51	4.96	0.239	5.34	5.17
				100	2.14	4.92	0.211	4.33	4.21
				200	1.55	4.86	0.252	3.05	2.84
4	1.6	0.0810	1.4	0	3.00	5.00	1.35	7.00	7.00
				50	2.46	4.95	0.402	5.17	5.20
				100	2.06	4.91	0.358	4.20	4.16
				200	1.44	4.85	0.433	2.79	2.69

[a]The value used in the Runge-Kutta calculation.

[b]The values resulting from the Runge-Kutta calculation.

[c]The quantity called [Fe(III)] includes $[Fe^{3+}\cdot Br^-]$, but not $[FeBr^{2+}]$.

[d]The observed and calculated absorbances were normalized to a common scale; the reported values have arbitrary units.

Table 43. (Continued)

Expt	Temp	$[Br^-]$	10^{-6}[a] k_{FeBr} M^{-1} sec^{-1}	Time after mixing, msec	10^5[b] [Eu(II)] M	10^4[b,c] [Fe(III)] M	10^6[b] $[FeBr^{2+}]$ M	Abs[d] calcd	Abs[d] obsd
5	1.6	0.110	1.4	0	3.00	5.00	1.83	7.15	7.15
				50	2.40	4.95	0.553	5.02	5.30
				100	1.99	4.91	0.496	4.00	4.09
				200	1.35	4.85	0.608	2.55	2.40
6	1.6	0.140	1.4	0	3.00	5.00	2.32	7.20	7.20
				50	2.35	4.95	0.712	4.76	5.05
				100	1.92	4.91	0.645	3.69	3.79
				200	1.27	4.84	0.801	2.23	2.04
7	15.8	0.05	2.3	0	5.70	3.50	0.830	1.23	1.23
				50	4.38	3.37	0.283	0.887	0.878
				100	3.40	3.27	0.321	0.658	0.608
				200	2.06	3.14	0.399	0.344	0.292
8	15.8	0.075	2.3	0	3.20	3.50	1.24	6.62	6.62
				50	2.34	3.42	0.614	4.22	4.27
				100	1.72	3.36	0.690	2.80	2.74
				200	0.92	3.27	0.837	0.98	0.90
9	15.8	0.100	2.3	0	3.23	3.50	1.64	6.94	6.94
				50	2.28	3.41	0.825	4.23	4.28
				100	1.62	3.35	0.938	2.74	2.68
				200	0.80	3.26	1.15	0.91	0.77
10	15.8	0.120	2.3	0	3.20	3.50	1.95	7.05	7.05
				50	2.19	3.41	1.01	4.14	4.56
				100	1.51	3.34	1.15	2.61	2.72
				200	6.95	3.25	1.42	0.82	0.74
11	15.8	0.170	2.3	0	3.91	3.50	2.73	9.42	9.42
				50	2.54	3.38	1.31	5.36	5.38
				100	1.66	3.29	1.54	3.43	3.03
				200	0.67	3.18	1.98	1.33	0.96

Table 43. (Continued

Expt	Temp	[Br⁻]	10^{-6} k_{FeBr} M^{-1} sec^{-1} [a]	Time after mixing, msec	10^{5} [Eu(II)] M [b]	10^{4} [Fe(III)] M [b,c]	10^{6} [$FeBr^{2+}$] M [b]	Abs calcd [d]	Abs obsd [d]
12	25.0	0.03	3.3	0	1.20	1.20	0.220	5.05	5.05
				100	0.880	1.17	0.161	3.45	3.41
				200	0.648	1.15	0.169	2.37	2.34
				420	0.332	1.11	0.183	0.89	0.87
13	25.0	0.065	3.3	0	1.20	1.20	0.470	4.87	4.87
				100	0.811	1.16	0.353	3.02	3.08
				200	0.550	1.14	0.375	1.88	1.92
				420	0.233	1.10	0.409	0.51	0.55
13	25.0	0.065	6.0	0	1.20	1.20	0.470	4.87	4.87
				100	0.765	1.16	0.298	2.84	3.08
				200	0.484	1.13	0.335	1.69	1.92
				420	1.168	1.10	0.395	0.40	0.55
14	25.0	0.100	3.3	0	1.20	1.20	0.717	5.44	5.44
				100	0.747	1.16	0.551	3.08	3.23
				200	0.466	1.13	0.590	1.80	1.88
				350	0.227	1.10	0.629	0.72	0.78

$$\frac{-d[Eu^{2+}]}{dt} = \frac{-d[Fe^{3+}]}{dt}$$

$$= (k' + k_{Br}[Br^-])[Fe^{3+}][Eu^{2+}] + k_{FeBr}[FeBr^{2+}][Eu^{2+}]$$

$$k_{obsd} = (k' + k_{Br}[Br^-])[Fe^{3+}]_{Av} + k_{FeBr}[FeBr^{2+}]_{Av}$$

$$k_{FeBr} = \frac{k_{obsd} - (k' + k_{Br}[Br^-])[Fe^{3+}]_{Av}}{[FeBr^{2+}]_{Av}} \qquad (69)$$

The values computed for k_{FeBr} computed for experiments 12, 13, and 14 in Table 43, using Eq 69, were 4.2, 3.5, and 3.5×10^6 $M^{-1}sec^{-1}$ respectively; the values used for $[FeBr^{2+}]_{Av}$ were those calculated by the Runge-Kutta method, using $k_{FeBr} = 3.3 \times 10^6$ $M^{-1}sec^{-1}$. The values calculated by Eq 69 are in fair agreement with that chosen by the Runge-Kutta method. The values of k_{FeBr} at each temperature and the activation parameters for k_{FeBr} are listed in Table 44.

Table 44. Temperature dependence of k_{FeBr} in the reduction of $FeBr^{2+}$ by Eu(II) in 1.00M H^+

Quantity	Temperature		
	1.6	15.8	25.0
k_{FeBr}, $M^{-1}sec^{-1}$	1.4×10^6	2.3×10^6	3.3×10^6
$\Delta h^{\ddagger}$, kcal/mole[a]		5.3	
$\Delta S^{\ddagger}$, eu[a]		-11	

[a]Calculated from Eq 9.

The rate constant k_{Br} for the Cr(II) reduction of Fe(III) was measured in a series of experiments in 1.00M H^+ and at 1.6°. The results are shown in Table 45, and Figure 16. The values for k_{Br}, calculated according to Eq 31, are shown for each experiment in the table. The slope of the line in Figure 16, 3900 $M^{-2}sec^{-1}$, was accepted as the value for k_{Br} at 1.6°.

An attempt to measure k_{FeBr} for the Cr(II) reduction of $FeBr^{2+}$ established the lower limit $k_{FeBr} > 2x10^7$ $M^{-1}sec^{-1}$ at 1.6° in 1.00M H^+. The initial concentrations in the experiments were $[Cr(II)]_0 = 1.75x10^{-6}$, and $[FeBr^{2+}]_0 = 3.5x10^{-6}M$; the reaction was complete before the mixed solutions reached the observation point in the stopped-flow apparatus.

The formation of $CrBr^{2+}$ as the Cr(II) product of both bromide paths in the reduction of Fe(III) by Cr(II) was verified in the following way. Three experiments were done in which Cr^{2+} solution was mixed with an equilibrium solution of Fe(III) and Br^- at 1.6°, and 1.00M ionic strength. The $FeBr^{2+}$ present at the instant of mixing was assumed to form $CrBr^{2+}$ instantly; the remaining Cr(II) and Fe(III) species were assumed to react according to Eq 29, with the k_{Br} path and the k_f' path giving $CrBr^{2+}$ as the only Cr(III) product. The previously described Runge-Kutta procedure (see Appendix A) was used to calculate the $CrBr^{2+}$ concentration that would result after all the Cr(II) had been oxidized; the calcula-

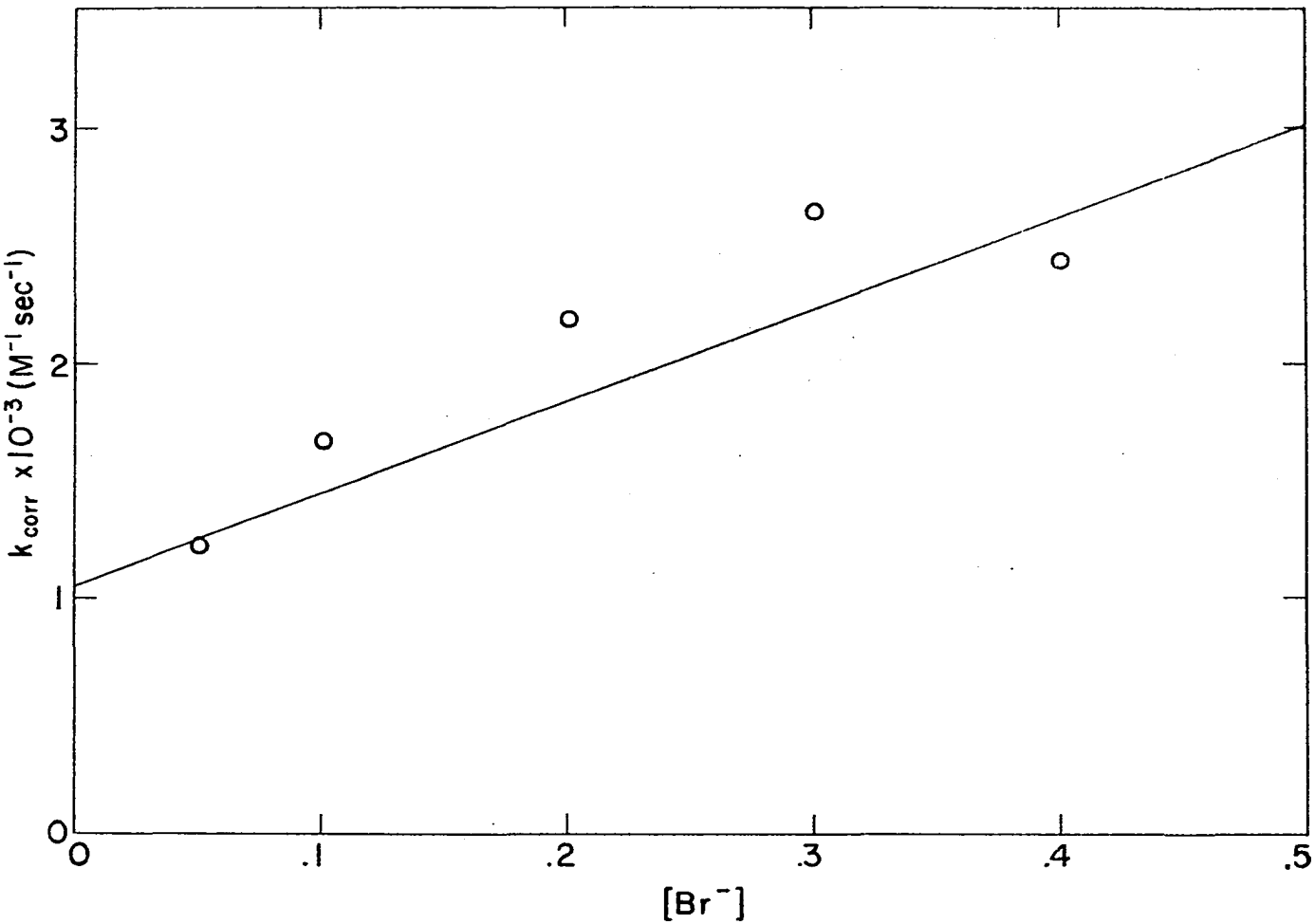

Figure 16. The dependence of the rate of reduction of Fe^{3+} by Cr(II) in chloride solution at 1.6° on [Br^-]

Table 45. Results of experiments measuring k_{Br} for the reaction between Cr(II) and Fe(III) in 1.00M H^+

Expt No.	$[Br^-]$ M	$10^3[Cr(II)]_0$ M	$10^3[Fe(III)]_0$ M	$10^{-3}k_{obsd}$ $M^{-1}sec^{-1}$	$10^{-3}k_{corr}$[a] $M^{-1}sec^{-1}$	$10^{-3}k_{Br}$[a] $M^{-2}sec^{-1}$
1	0.050	4.42	0.131	1.20	1.20	2980
2	0.100	5.00	0.144	1.67	1.66	6090
3	0.200	4.92	0.144	2.19	2.18	5640
4	0.300	4.99	0.144	2.66	2.64	5300
5	0.400	4.87	0.131	2.47	2.44	3470

[a]Calculated according to Eq 31.

tion was compared to the observed $CrBr^{2+}$ concentration, measured by the ion exchange procedure already described. The results are shown in Table 46. The observed values were consistently higher than the calculated values, indicating a probable error in the rate constants chosen for the calculation. The error could be the use of low values for one of the rate constants k_{Br} or k_f'; k_f' does have an inverse acid dependence (37) that was not considered in making the calculation. The observed and calculated values agree reasonably well; the agreement verifies the assumption that both bromide catalyzed paths for oxidation of Cr(II) do yield $CrBr^{2+}$.

Table 46. Observed and calculated concentrations of $CrBr^{2+}$, assuming the k_{Br} and k_{FeBr} paths for oxidation of Cr(II) lead exclusively to $CrBr^{2+}$, at 1.6° and 1.0M ionic strength

Expt No.	$[H^+]$ M	$[Br^-]$ M	$10^3 [FeBr^{2+}]_0$[a] M	$10^3 [Fe(III)]_0$ M	$10^3 [Cr(II)]_0$ M	$10^3 [CrBr^{2+}]_0$[b] calcd, M	$10^3 [CrBr^{2+}]$ obsd, M
1	0.975	0.490	0.1165	4.380	1.395	1.05	1.07
2	0.950	0.460	0.1965	7.645	1.310	0.961	1.14
3	0.962	0.288	0.0840	4.850	1.223	0.818	0.911

[a]Calculated using $Q_{Br} = 0.034\ M^{-1}$, and $Q^o_{Br} = 0.20\ M^{-1}$.

[b]See text for the calculation procedure. The values $k_f' = 0.364\ M^{-1}sec^{-1}$, $k_{Br} = 3900\ M^{-2}sec^{-1}$, and $k' = 1051\ M^{-1}sec^{-1}$ were used in the calculation.

INTERPRETATION AND DISCUSSION

Iron(III) Substitution and Equilibrium Properties

Azidoiron(III) equilibrium and rate discrepancies

The derivation of Eq 13 relating the absorbance of iron (III)-hydrazoic acid solutions to the properties of FeN_3^{2+} required the assumption that only a single monoazidoiron(III) complex existed in such solutions. Significant amounts of a diazido complex would, however, not necessarily cause observable deviations from Eq 13. Kruh (57) and Baes (58) have considered similar complexation equilibria and have shown that conditions of stability and molar absorptivities exist for the second complex that allow it to remain undetected in limited spectral experiments. Linearity of the data in the plot suggested by Eq 13 is a necessary result when a single species forms, but such linearity is not a sufficient condition for concluding that only one complex occurs. Evidence was obtained in this study that implicated higher complexes at high HN_3 concentrations.

The following conclusions have been formed with respect to the discrepant equilibrium and formation rate measurements, invoking both mono and diazido species: (1) Only the equilibrium studies at high iron(III) and low hydrazoic acid correctly evaluated the properties of the monoazidoiron(III) complex: $Q_{N_3} = 0.512 \pm 0.015$ and $\epsilon_1 = 4400 \pm 160$ $M^{-1}cm^{-1}$, (2) the formation rate constant k_f' was correctly evaluated in

both formation and dilution experiments with excess iron(III); the value at 0.0500M H^+ is $k_f' = 200 \pm 9$ $M^{-1}sec^{-1}$ and leads to $Q_{N_3} = 0.498 \pm 0.035$, in agreement with the value determined in the equilibrium measurements as well as with the value obtained from formation experiments with high HN_3 (see Figure 5), (3) the formation experiments with high HN_3 gave the correct value for k_f' because the first reaction is formation of monoazido complex; diazido forms more slowly and in a stepwise manner from monoazido, (4) interference of appreciable diazidoiron(III) ion in the equilibrium studies with high HN_3 and in the kinetic dilution studies with high HN_3 led to wrong values for k_f' and Q_{N_3}, and (5) the two incorrect values for Q_{N_3} at high HN_3 (equilibrium, 0.60; kinetic dilution, 0.67) are not equal; the kinetic value contains a larger contribution from the diazido complex since the diazido complex, which probably aquates faster than the monoazido, has a concentration relative to monoazido that is greater at the start of a dilution experiment than it is at equilibrium.

Azidoiron(III) formation kinetics

The form of the rate constant for aquation Eq 8 and the equilibrium quotient for the net reaction lead to the formation rate law given by Eq 70. Experiments were done that

$$\frac{d[FeN_3^{2+}]}{dt} = \left(k_{1f} + \frac{k_{2f}}{[H^+]}\right)[Fe^{3+}][HN_3] \qquad (70)$$

evaluated the quantity $k_{1f} + k_{2f}/[H^+]$ at $[H^+] = 0.05M$ and 25°,

as described above; the value is 200 ± 9 $M^{-1}sec^{-1}$. The value 10.1 sec^{-1} can be shown to be essentially k_{2f}, as follows. The aquation data demonstrated that the k_{1aq} term accounts for less than 2% of the aquation rate at 0.05M H^+. The principle of microscopic reversibility dictates that the opposing k_{1f} term must similarly account for less than 2% of the formation rate at 0.05M H^+. The small value for k_{1f} 2.6 $M^{-1}sec^{-1}$, can be calculated from the value k_{2f} = 10.1 sec^{-1} at 0.05M H^+, and from Eq 71, relating the various equilibrium and kinetic parameters. Table 47 presents a summary

$$Q_{N_3} = \frac{k_{1f}}{k_{1aq}} = \frac{k_{2f}}{k_{2aq}} = \frac{k_f'[H^+]}{k_{aq}'} \qquad (71)$$

of these parameters.

Table 47. Kinetic and equilibrium properties of FeN_3^{2+} in Fe^{3+}-HN_3 solution at 25°, 1.00M ionic strength

Parameter	Value
k_{2aq}, sec^{-1}	20.0 ± 0.9
k_{2f}, sec^{-1}	10.0 ± 0.2
k_{1aq}, $M^{-1}sec^{-1}$	5.1 ± 1.3
k_{1f}, $M^{-1}sec^{-1}$	2.6 ± 0.8
Q_{N_3}	0.51 ± 0.01
ϵ_1(4600Å), $M^{-1}cm^{-1}$	4400 ± 160

Reaction mechanisms

The rate equation for formation of FeN_3^{2+} indicates parallel activation processes as shown by Eqs 72 and 73.

$$Fe^{3+} + HN_3 = [FeHN_3^{3+}]^{\ddagger} = FeN_3^{2+} + H^+ \quad (72)$$

$$Fe^{3+} + HN_3 = [FeN_3^{2+}]^{\ddagger} + H^+ \quad (73)$$

(An activation process is defined(59) as the formation of an activated complex from the predominant species present, and includes any steps such as gain or less of protons that occur prior to formation of the activated complex.) The transition state for the first reaction probably needs no explanation beyond noting the stabilizing role of hydrogen ion commonly found in the substitution reactions of basic ligands (1,56, 60-64). The transition state for the second process could reasonably form by either of the elementary steps, Eq 74 or 75. If Eq 74 pertains, the measured rate constant is k_{2f} =

$$(H_2O)_6Fe^{3+} + N_3^- = (H_2O)_5FeN_3^{2+} + H_2O \quad (74)$$

$$(H_2O)_5FeOH^{2+} + HN_3 = (H_2O)_5FeN_3^{2+} + H_2O \quad (75)$$

$k_{74}Q_a'$, where Q_a' is the acid dissociation constant for HN_3. If Eq 75 is correct, then the measured rate constant is $k_{2f} = k_{75}Q_a$. For hydrazoic acid, Q_a' is 7×10^{-5}M (31) and for aquoiron(III), Q_a is 1.65×10^{-3}M (45). The rate constant calculated for the reaction of Fe^{3+} and N_3^- (k_{74}) is 1.4×10^5 $M^{-1}sec^{-1}$, and that calculated for the reaction $FeOH^{2+} + HN_3$ (k_{75}) is 6.1×10^3 $M^{-1}sec^{-1}$. These formulations are not

kinetically distinguishable, since the acid dissociation reactions of iron(III) and hydrazoic acid are quite fast.

Seewald and Sutin (31) noted the similarity of rate constants for reactions analogous to Eq 75 for a series of iron (III) complexes where the ambiguity connected with the role of hydrogen does not exist (i.e., the reactions of Fe^{3+} with Cl^-, Br^-, NCS^-, HF, and HN_3); values of k all lie in the range 2.0 (for Br^-) to 127 $M^{-1}sec^{-1}$ (for NCS^-). Moreover, these rate constants are substantially lower than those found for processes analogous to reaction 74, again considering unambiguous reactions (i.e., the reactions of $FeOH^{2+}$ with Cl^-, Br^-, NCS^-, and SO_4^{2-}). The second-order rate constants for the latter reactions lie in the range 10^4-$3x10^5$ $M^{-1}sec^{-1}$. These two groups of rate constants presumably represent substitution on $Fe(H_2O)^{3+}$ and on $(H_2O)_5FeOH^{2+}$, respectively (31). The calculated value for $Fe^{3+} + N_3^-$ lies outside the range of values for other substitution reactions of Fe^{3+} by a factor of $> 10^3$, whereas the value for $FeOH^{2+} + HN_3$ gives a value close to the range observed for substitution on $FeOH^{2+}$. Seewald and Sutin (31) concluded then, that Eq 75 is probably the correct formulation. On the basis of this reasonable conclusion, the rate determining feature of Eq 73 can be viewed as elimination of water in the outer-sphere complex $(H_2O)_5FeOH \cdot HN_3^{2+}$.

The data on iron(III) substitution rates obtained in this work provide better values for the ligands N_3^- and Br^-

than were used by Seewald and Sutin (31), and also provide previously unreported rate data for the ligand NCO^-. These data can be used to extend the reactivity comparisons presented by Seewald and Sutin (31). The measured equilibrium and rate data for formation of $FeNCO^{2+}$ were obtained at 1.6°. The calculated value of the second-order formation rate constant assuming the mechanism involves reaction of Fe^{3+} and NCO^- is 2.1×10^3 $M^{-1}sec^{-1}$ at 1.6°. The value is estimated to be 4×10^4 $M^{-1}sec^{-1}$ at 25°, using the activation enthalpy for $Fe^{3+} + NCS^-$, 20.2 kcal/mole (40). This value lies considerably outside the range of rate constants, 2-127 $M^{-1}sec^{-1}$, noted for other substitutions on Fe^{3+}. Using the alternate formulation, the second-order rate constant for $FeOH^{2+}$ + HNCO is 1.6×10^3 at 1.6°. The value is estimated to be 1.9×10^4 $M^{-1}sec^{-1}$ at 25°, using the activation enthalpy for $FeOH^{2+}$ + HNNN, 16.7 kcal/mole. (The value 16.7 is the sum ΔH_{2aq} + ΔH°, obtained from Table 3 and the report of Wallace and Dukes (32) respectively.) The value 1.9×10^4 lies within the range of rate constants 2×10^3 - 3×10^5 noted for substitution on $FeOH^{2+}$.

The revised and extended series of calculations are shown in Table 48. The results support the previous conclusions (31). It is concluded that all the basic anions, SO_4^{2-}, HSO_4^-, F^-, N_3^-, and NCO^-, probably substitute on iron(III) in the acid independent step by the method sug-

Table 48. Rate constants for formation of FeL^{2+} complexes at 25°

L	k, $M^{-1}sec^{-1}$ Fe^{3+} + L	k, $M^{-1}sec^{-1}$ $FeOH^{2+}$ + L	Ref
Cl^-	9.4	$1.1x10^4$	31,48
Br^-	2.0	$1.9x10^3$	This work
NCS^-	127	$1.0x10^4$	31,40
SO_4^{2-}	$(6.4x10^3)^a$	$3x10^5$	31,65
HSO_4^-		$(1.4x10^5)^a$	31,65
F^-	$(5.0x10^3)^a$		31,56
HF	11.4	$(3.1x10^3)^a$	31,56
N_3^-	$(1.4x10^5)^a$		This work
HN_3	2.6	$(6.1x10^3)^a$	This work
NCO^-	$(4x10^4)^{a,b}$		This work
HNCO		$(1.9x10^4)^{a,b}$	This work

[a]Calculated values, using measured rate constants and acid dissociation constants.

[b]Corrected to 25°; the correction is described in the text.

gested by Seewald and Sutin (31). This method involves reaction of the protonated anion, HX, with hydroxoiron(III).

Bromoiron(III)

The equilibrium and rate parameters found in this study for substitution of Br^- on Fe(III) are markedly different from those reported previously (36,37). The equilibrium data

of Lister and Rivington (36) agree with data obtained under similar conditions in this study, but the earlier data (36) were treated in terms of a single complex. The earlier value (36), $Q_{Br} = 0.61\ M^{-1}$ at 25°, 1.2M ionic strength was actually the sum $Q^i_{Br} + Q^o_{Br}$ and can be compared with the sum $Q^i_{Br} + Q^o_{Br} = 0.37\ M^{-1}$ measured in this study at 25°.

The kinetic parameters for Eq 55 actually measured by Matthies and Wendt (37) at 22 ± 2°, 1.7M ionic strength, were aquation rate constants, since the concentration of $FeBr^{2+}$ formed was quite small relative to the reactant concentrations. However, these workers presented their results in terms of formation rate constants ($k_f = Q^i_{Br} k_{aq}$). Since they (37) used the value $Q^i_{Br} = 0.625\ M^{-1}$, (from the reports of Lister and Rivington (36) and Rabinowitch and Stockmayer (35)) their results are necessarily incorrect. The values $k'_f = (20 + 31/[H^+])\ M^{-1}sec^{-1}$ reported by Matthies and Wendt (37), together with the value of Q^i_{Br} used in their computations permits calculation of their observed aquation rate, $k'_{aq} = (32 + 50/[H^+])\ sec^{-1}$. This expression leads to $k'_{aq} = 82\ sec^{-1}$ in 1.0 M H^+ at 22 ± 2°, 1.7M ionic strength, which is not inconsistent with the values 55.6 and 10.7 sec^{-1} in 1.0 MH^+, 1.0M ionic strength, measured in this study at 15.8 and 1.6°, respectively. Thus, consideration of the outer sphere complex of ion pair $Fe^{3+}\cdot Br^-$ apparently removes the discrepancies between this work and the earlier reports (36,37).

Iron(III) Reduction

Discussion of iron(III) reductions will be concerned with several questions. The question of what reaction pathways are followed, both in the absence and in the presence of complexing anions, will be considered. The form of the rate laws describing the several paths will be considered, in order to learn the compositions of the activated complexes. Questions concerning the structures of the activated complex will be discussed, first in terms of the direct evidence available from identification of the products of Cr^{2+} reductions, and then in terms of indirect evidence available for the Eu^{2+} reductions. The Marcus relation (1,23) will be used to estimate the rate constant for electron exchange between Eu(II) and Eu(III). Finally, the rate patterns for a series of oxidation-reduction reactions will be considered in an attempt to understand the influence of ligands X^- on the rates of reduction of the metal complexes MX^{2+}.

Iron(III) Reductions in Perchlorate Solution

Mechanism of aquoiron(III) reduction by europium(II)

The rate equation found for the reaction of Fe^{3+} and Eu^{2+} in acidic aqueous solution consists of two terms (see Eq 21) suggesting a mechanism involving two parallel reaction paths. However, the question of whether the k_1 term is an actual reaction pathway should be considered. It has been

noted several times (9,66-71) that medium effects can introduce rate law terms that do not correspond to reaction pathways, even at constant ionic strength. In the Eu(II)-Fe(III) reaction, the rate term $k_2[Fe^{3+}][Eu^{2+}][H^+]^{-1}$ carries most of the reaction, although at $[H^+] = 1.00M$ at 1.6^o, the term $k_1[Fe^{3+}][Eu^{2+}]$ accounts for 60% of the observed rate. If the k_1 term represents an activity effect only, then the effect can be accounted for empirically by a Harned-type correction factor (72). The observed rate constant k' can be represented as the product of an intrinsic rate constant k_2^0 and a correction factor, according to Eq 76. For small values of $[H^+]$,

$$k' = k_2^0[H^+]^{-1} \exp(\beta[H^+]) \qquad (76)$$

Eq 76 becomes Eq 77. According to this model the rate term k_1

$$k' = k_2^0[H^+]^{-1} (1+\beta[H^+] + \cdots\cdot) = k_2^0[H^+]^{-1} + k_2^0 \qquad (77)$$

in Eq 21 is solely a medium effect. The data given in Table 8 were fitted to this functional relationship, assuming k_2^0 obeyed the Eyring relation (Eq 9) and that $\beta = \beta^0 (1+aT)$ where a is a temperature coefficient and T is the temperature in ^oC. Values of the constants which best reproduce the data are $k_2^0 = (RT/Nh)\exp[(0.7\pm1.4)/R - (12000\pm400)/RT]$ and $\beta = (0.96 \pm 0.10)[1-(0.027\pm0.005)T]$. The data in Table 8 were reproduced with a mean deviation of 8.0%, compared to 8.6% based on the two-term model of Eq 21. The two models fit the data about equally well and predict the same functional dependence of

rate on $[H^+]$. The value of the Harned factor β is, however, abnormally large (66,70,71). (A reasonable value of β would be 0.1, not 1 (66)). It is concluded that medium effects are not the sole contributors to the rate effect, and that the k_1 term in Eq 21 almost certainly represents a genuine pathway. The k_1 term may include a contribution from medium effects, but this contribution cannot be resolved at present.

Since the rate terms in Eq 21 are believed to represent independent reaction paths, parallel activation processes are postulated. Net activation processes consistent with the kinetics are described in Eqs 78 and 79. The first of these

$$Fe(H_2O)_6^{3+} + Eu_{aq}^{2+} = [FeEu(H_2O)_m^{5+}] \qquad (78)$$

$$Fe(H_2O)_6^{3+} + Eu_{aq}^{2+} = [FeEu(H_2O)_nOH^{4+}] \quad +H^+ \qquad (79)$$

reactions is most simply accounted for by the elementary step involving direct reaction between Fe^{3+} and Eu^{2+}. Several possible sequences of elementary reactions could account for the second of these reactions. The sequence considered most plausible involves formation of hydroxoiron(III) ion in a labile equilibrium, with reaction between Eu^{2+} and $FeOH^{2+}$, according to Eqs 80 and 81. The empirical rate constant k_2

$$Fe(H_2O)_6^{3+} \rightleftharpoons (H_2O)_5FeOH^{2+} + H^+ \text{ (rapid, } Q_a) \qquad (80)$$

$$(H_2O)_5FeOH^{2+} + Eu_{aq}^{2+} \rightarrow \text{(rate determining, } k_{FeOH}) \qquad (81)$$

was defined in terms of concentrations of species predominant under the conditions of the experiments. In terms of the sequence Eqs 80 and 81, k_{FeOH} can be calculated from the relation $k_{FeOH} = k_2/Q_a$. Milburn (45) gives values for Q_a as a function of temperature at 1.00M ionic strength. Activation parameters for k_{FeOH} can be calculated from the relations $\Delta H_{FeOH} = \Delta H_2 - \Delta H_a^o$, and $\Delta S_{FeOH} = \Delta S_2 - \Delta S_a^o$, where the subscript 2 refers to the empirically measured rate constant k_2 and the subscript a refers to the acid dissociation described in Eq 80. Values and activation parameters for k_{FeOH} are given in Table 49.

Table 49. Calculated values and activation parameters for k_{FeOH} for the reduction of $FeOH^{2+}$ by Eu^{2+} at 1.00M ionic strength

Quantity	Temperature			$\Delta H^{\ddagger}$ or ΔH^o	$\Delta S^{\ddagger}$ or ΔS^o
	1.6°	15.8°	25.0°	kcal/mole	eu
$10^{-3}k_2$, sec^{-1}	2.28	7.16	14.2	12.2±0.5	1.3±1.8
10^3Q_a, M	0.381	0.954	1.65	10.2±0.3	21.5±1
$10^{-6}k_{FeOH}$, $M^{-1}sec^{-1}$	6.0	7.5	8.6	2.0±0.8	-20±3

Mechanism of the reduction of aquoiron(III) by chromium(II)

The reaction between Fe^{3+} and Cr^{2+} was studied in detail by Dulz and Sutin (16), at 25° and 1.00M ionic strength, maintained with $NaClO_4$. These workers reported a two term rate law (Eq 25) exactly analogous to that found in this study for

the reaction between Fe^{3+} and Eu^{2+}. The work of Dulz and Sutin (16) was extended in this study to include the temperatures 1.6 and 15.8° as well as 25°. Lithium perchlorate was used to maintain ionic strength in this study; the results were interpreted in terms of the rate law reported by Dulz and Sutin (16). The evidence that the k_1 term in Eq 25 corresponds to a true reaction pathway is weaker than it was for the Fe^{3+}-Eu^{2+} reaction. The k_1 term represents 23% of the observed rate at 1.6°, 1.00M H^+ for the Cr^{2+} reaction, as compared to 60% for the Eu^{2+} reaction; the k_1 term represents 29% of the observed rate at 25°, 1.00M H^+ from the work of Dulz and Sutin (16) using Na^+ media, but only 7% under the same conditions in this study, using Li^+ media. Nevertheless, by analogy with the Eu^{2+} reaction, at least part of the k_1 term in Eq 25 is assumed to arise from a reaction pathway, leading to a mechanistic interpretation identical in form to that for the Fe^{3+}-Eu^{2+} reaction (and also identical to that proposed by Dulz and Sutin (16)). Values for k_{FeOH} and the associated activation parameters are presented in Table 50.

Table 50. Calculated values and activation parameters for k_{FeOH} for the reduction of $FeOH^{2+}$ by Cr^{2+} at 1.00M ionic strength

Quantity	Temperature			$\Delta H^{\ddagger}$ or ΔH°	$\Delta S^{\ddagger}$ or ΔS°
	1.6°	15.8°	25.0°	kcal/mole	eu
$10^{-3}k_2$, sec^{-1}	0.804	3.21	7.33	14.8 ± 0.3	8.8 ± 0.9
$10^{3}Qa$, M	0.381	0.954	1.65	10.2 ± 0.3	21.5 ± 1
$10^{-6}k_{FeOH}$, $M^{-1}sec^{-1}$	2.1	3.4	4.4	4.6 ± 0.6	-13 ± 2

Reduction of Iron(III) in the Presence of Complexing Anions

Mechanisms of chromium(II) reductions

The formation of CrX^{2+} as the chromium product in Cr^{2+} reductions of FeX^{2+}, and the form of the rate expression, $-d[FeX^{2+}]/dt = k_{FeX}[FeX^{2+}][Cr^{2+}]$, prove the net activation process is that described in Eq 82, where X occupies the

$$(H_2O)_5FeX^{2+} + Cr(H_2O)_6^{2+} = [(H_2O)_5CrXFe(H_2O)_5^{4+}] + H_2O \quad (82)$$

inner coordination sphere of both metal ions. The formation of CrX^{2+} was verified in this study for the anions F^- and Br^-. The formation of CrX^{2+} has previously been verified (16) for Cl^-; formation of $CrSCN^{2+}$ (or possibly a mixture of $CrSCN^{2+}$ and $CrNCS^{2+}$) has been reported (52)[1].

The interpretation of the reactions involving cyanate, iron(III), and chromium(II) requires qualification; the product of the reaction between iron(III) and HNCO was not clearly identified, and neither was the product of the reaction between Cr(II) and the iron(III) complex. The evidence relating to the iron(III)-cyanate reaction will be discussed, followed by speculation concerning the possible products of the Cr(II)-iron(III) complex reaction.

The evidence relating to the cyanate reactions consists of some cobalt(III)-cyanate measurements by Sargeson and Taube (73), and rate and spectral data obtained in this study.

---

[1]N. Sutin, Upton, New York. Isomeric thiocyanatochromium(III) species. Private communication. 1967.

The iron(III)-cyanate reaction is postulated to be a substitution reaction, as shown in Eq 38, but Sargeson and Taube (73) found the cobalt(III) reactions described by Eqs 83 and 84, where en represents ethylenediamine and where Ø represents

$$(NH_3)_5Co\text{Ø}H_2^{3+} + NCO^- = (NH_3)_5Co\text{Ø}\overset{O}{\overset{\|}{C}}\text{-}NH_2^{2+} \qquad (83)$$

$$\underline{cis}\text{-}(en)_2Co(\text{Ø}H_2)_2^{3+} + NCO^- = (en)_2Co\left\langle{}^{O}_{\text{Ø}}\right\rangle CNH_2^{2+} + H_2O \qquad (84)$$

water labeled with O^{18}. Reactions 83 and 84 occurred in basic solution; net reaction 84 occurred in a stepwise manner, with addition to one water molecule, followed by displacement of the other in a chelation step. Both reactions were followed by hydrolysis, in solutions that were neutral before addition of NCO^-, to form carbonatocobalt(III) species. The half-time for water exchange with cis-$(en)_2Co(OH_2)_2^{3+}$ was 25 minutes, while the half-time for formation of the carbonato complex, after addition of NCO^- was only 14 minutes (73). The substitution inertness of Co(III) is probably the cause for reaction 83 and the first step of reaction 84 being preferred over an actual substitution. Substitution on iron occurs much more rapidly however; the value of the rate constant calculated for substitution of HNCO on $FeOH^{2+}$, shown in Table 48, is consistent with the iron(III)-cyanate reaction being an actual substitution reaction. Even if HNCO does form a complex directly with Fe(III), it could be proposed that carbamate

is formed nevertheless, after the substitution. That proposal does not seem likely in view of the high rate of aquation of iron(III) complexes relative to the rate of carbamate formation noted by Sargeson and Taube (73). The visible absorption peak for the product of the iron(III)-cyanate reaction, at about 3400Å, with ϵ about 2000 $M^{-1}cm^{-1}$ is consistent with a pseudohaloiron(III) complex.

The following paragraph is presented as a possible explanation for the behavior of the chromium(III) product of the reaction between $FeNCO^{2+}$ and Cr(II).

The initial product is probably $CrOCN^{2+}$ and possibly also contains $CrNCO^{2+}$, by analogy with the similar $FeNCS^{2+}$ reduction (13) and from the observation that the product has a 2+ charge. This study did not definitely establish however, that the Cr(III) product even contains the cyanate ion. The spectral changes that the freshly separated (from 3+ ions) chromium(III) product exhibited could be due to carbamate formation by O-bonded cyanate to give a chelate like the product of Eq 84. The chelate would have to be protonated to account for the 3+ charge observed for the complex. Finally, the very slow spectral changes that the Cr(III) product was still exhibiting after a week could be caused by aquation or hydrolysis of the chelate; Sargeson and Taube (73) noted that aquation of the monodentate cobalt(III) product of Eq 83 was only half complete in about 10 hours in 1.0 MH^{+} at 25°. The entire

reaction scheme that has been described is presented in the following diagram, where no evidence was obtained for the two isomeric cyanatochromium(III) species or for their interconversion by Cr^{2+}.

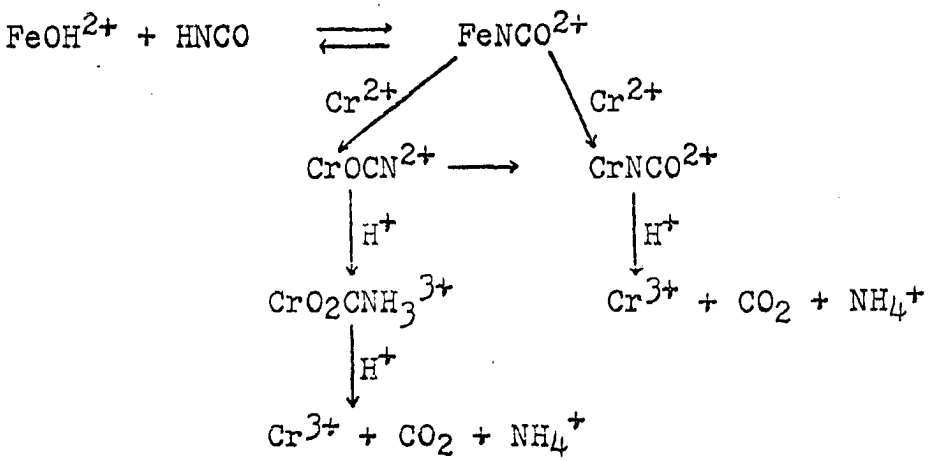

The formation of CrX^{2+} in reductions of Fe(III) by the anion path (see Table 12) and the form of the rate expression, $d[CrX^{2+}]/dt = k_X[Fe^{3+}][Cr^{2+}][X^-]$ do not constitute sufficient evidence to establish all the details of the atomic configurations during the reactions. These facts do establish the composition (exclusive of solvent molecules) and charge of the activated complex ($FeCrX^{4+}$), and that X^- is coordinated to Cr(II) in the activated complex. The additional fact that Fe(III) is not sufficiently labile for X^- to enter its inner coordination sphere during the time of the oxidation-reduction reaction establishes that X^- is not coordinated to Fe(III) in the activated complex. Several activation reactions are consistent with the above observations, and are listed in Eqs 85 through 89. None of these reactions are

$$CrX(H_2O)_5^{+} + Fe(H_2O)_6^{3+} = [(H_2O)_4XCr(H_2O)Fe(H_2O)_5^{4+}] + H_2O \quad (85)$$

$$Cr(H_2O)_6^{2+} + Fe(H_2O)_6^{3+}\cdot X^{-} = [(H_2O)_4XCr(H_2O)Fe(H_2O)_5^{4+}] + 2H_2O \quad (86)$$

$$Cr(H_2O)_6^{2+} + Fe(H_2O)_6^{3+}\cdot X^{-} = [CrX(H_2O)_5\cdot Fe(H_2O)_6^{4+}] + H_2O \quad (87)$$

$$Cr(H_2O)_6^{2+}\cdot X^{-} + Fe(H_2O)_6^{3+} = [(H_2O)_4XCr(H_2O)Fe(H_2O)_5^{4+}] + 2H_2O \quad (88)$$

$$Cr(H_2O)_6^{2+}\cdot X^{-} + Fe(H_2O)_6^{3+} = [CrX(H_2O)_5\cdot Fe(H_2O)_6^{4+}] + H_2O \quad (89)$$

distinguishable from the others; Eq 90 states all the known information unambiguously.

$$Cr(H_2O)_6^{2+} + X^{-}_{aq} + Fe(H_2O)_6^{3+} = [FeCrX(H_2O)_n^{4+}] + mH_2O \quad (90)$$

The transition states for the two anion catalyzed paths (see Table 12) have different structures, but the same charge and the same composition (disregarding the unknown number of solvent molecules); they are isomeric. The anion path was not of measurable importance for fluoride ion; in acidic solution the concentration of F^- is negligibly small. Experiments were not performed to search for the anion path involving N_3^- or NCO^-. The nearly complete protonation of F^-, N_3^- and NCO^- in acid solution probably prevents their

participation in a measurable anion reaction, even though the specific k_X rate constants could be large. The possibility of catalysis by the protonated anion, to give a rate constant k_{HX} probably has no precedent; rate terms for similar reactions containing the factor $k_{HX}/[H^+]$ have been found (9), but the empirically identical factor $k_F[F^-]$ is preferred (9).

Mechanisms of europium(II) reductions

The immediate Eu(III) product of the anion catalyzed Eu(II) reduction of Fe(III) is not identifiable, owing to the lability of Eu(III). The rate of reduction of FeX^{2+} by Eu^{2+} is of the form $k_{FeX}[FeX^{2+}][Eu^{2+}]$ (the same form observed for the Cr^{2+} reductions). The Eu^{2+} reductions appear to be inner sphere and X-bridged, on the basis of the rate patterns shown in Table 51. The general observation has been made that inner sphere, bridged electron transfer reactions proceed at rates very dependent on the identity of the bridge (1). Particularly, azide-bridged reactions normally proceed much faster than thiocyanate-bridged reactions; an exception is the inner sphere, anion-bridged oxidation of $Co(CN)_5^{3-}$ by $Co(NH_3)_5N_3^{2+}$ and $Co(NH_3)_5NCS^{2+}$, in which the N_3^- bridged reaction is faster by a factor of less than 2 (15). These reactions have an unusual feature however, in that the sulfur-bonded form is the stable isomer for $Co(CN)_5SCN^{3-}$ (74) while the nitrogen-bonded form is the stable isomer for $Co(NH_3)_5NCS^{2+}$ (74), permitting stable configurations for thiocyanate

Table 51. A summary of rate parameters for reduction of Fe(III) by Eu(II) and Cr(II) in the presence of various anions at 1.6°, 1.00M ionic strength

Identity of X	Eu^{2+} k_X $M^{-1}sec^{-1}$	$10^5 k_{FeX}$ $M^{-1}sec^{-1}$	$\Delta H^{\ddagger}$ kcal/mole	$\Delta S^{\ddagger}$ eu	Cr^{2+} k_X $M^{-2}sec^{-1}$	$10^5 k_{FeX}$ $M^{-1}sec^{-1}$	$\Delta H^{\ddagger}$ kcal/mole	$\Delta S^{\ddagger}$ eu
H_2O		0.034	3.5	-29		0.0025	5	-30
OH^-		60	2.0	-20		21	4.6	-13
Br^-	5400	14	5.3	-11	3900	>200		
Cl^-	6200	20			2400[a]	17		
F^-	$<3\times10^6$	190				8		
NCS^-		3.1	4.4	-18		200		
NCO^-		16				4.2	2.9	-22
N_3^-		120				200		

[a]Estimated from the data of Dulz and Sutin (16), using $\Delta H^{\ddagger}_{Cl} = 14$ kcal/mole $= \Delta H^{\ddagger}_{Br}$ for the Eu(II)-Fe(III) reaction.

at both ends of the $[(CN)_5Co\text{-}SCN\text{-}Co(NH_3)_5^-]^{\ddagger}$ activated complex for electron transfer. The reactions observed in this study probably cannot attain the stability described above for thiocyanate bridging because the nitrogen-bonded form is stable both for Fe(III) (13,75) and Cr(III) (74) complexes, and probably also for Eu(III) complexes.

In contrast to the rate dependence on the identity of bridging ligands shown by inner sphere reactions, a smaller rate dependence on the identity of non-bridging ligands is shown by outer sphere reactions (1). Particularly, the effect of azide as a ligand is normally not much different than the effect of thiocyanate on similar reactions that occur by outer sphere mechanisms.

Rate comparisons among aquo, hydroxo, and chlorometal ions may also be diagnostic of mechanism (6,16,21,75); large rate enhancement over water-bridging is often caused by hydroxide and chloride-bridging. The specific rate patterns noted for H_2O, OH^-, Cl^-, N_3^-, and NCS^- ligands are presented in Table 52. The similarities noted between the Eu^{2+} rate pattern and that for the inner sphere reducing agents Cr^{2+} and Fe^{2+} are taken as evidence that the Eu^{2+} reactions also occur by inner sphere mechanisms. Specifically, Eu^{2+} and the other inner sphere reducing agents show large rate enhancements due to OH^- and Cl^- in contrast to the outer sphere reducing agent

V^{2+} reactions, where N_3^- has a smaller effect (or about the same effect) than NCS^- does.

Table 52. Relative reactivities[a] of dipositive metal ion reducing agents toward iron(III) complexes

Iron(III) complex	$k_{Fe(III)}/k_{Fe(H_2O)_6^{3+}}$ — Reducing agent, mechanism			
	Cr^{2+}, inner	V^{2+}, outer	Fe^{2+}, inner	Eu^{2+}
$Fe(H_2O)_6^{3+}$	1.0	1.0	1.0	1.0
$(H_2O)_5FeOH^{2+}$	7.8×10^3	<22	8.2×10^2	1.8×10^3
$(H_2O)_5FeCl^{2+}$	1×10^3	26	<3.8	5.1×10^2
$(H_2O)_5FeNCS^{2+}$	$>8\times10^4$	37[b]	13	9.1×10^2
$(H_2O)_5FeN_3^{2+}$	$>8\times10^4$	29[c]	3.1×10^3	3.5×10^3
References	16, This work	6	19,26,33, 75,76,77	This work

[a]Relative rates at 1.00M ionic strength and 25° for all the reducing agents except Eu^{2+} at 1.6°, and Fe^{2+} at 20°.

[b]Ionic strength 0.5M.

[c]Ionic strength 0.55M.

Less direct evidence is available concerning the structure of the activated complex for the anion catalyzed reduction of Fe^{3+} by Eu(II) than for the similar Cr(II) reduction; the Eu(III) product is labile, so that identification of the immediate Eu(III) product is not possible. Equation 91, where

$$Eu_{aq}^{2+} + X^- + Fe(H_2O)_6^{3+} \rightarrow [FeEuX(H_2O)_n^{4+}] + m(H_2O) \quad (91)$$

X^- is not coordinated to Fe(III) and might or might not be coordinated to Eu(II), describes formation of the activated complex.

Electron exchange between Eu(II) and Eu(III)

Only an upper limit has been established for the Eu(II)-Eu(III) electron exchange reaction in perchlorate media. The value $k_{Eu} < 3x10^{-5}$ at 25° can be calculated from the work of Meier and Garner (18), in mixed Cl^--ClO_4^- media. A value that is possibly better can now be calculated, using the theory of Marcus (29). This theory was derived for outer sphere electron transfer reactions, but Sutin and co-workers (1,17) have demonstrated that many inner sphere rate constants are also predicted with moderate accuracy. Equation 92 would normally be used for calculating k_{12}, the rate constant for electron

$$k_{12} = (k_{11}k_{22}K_{12}f)^{\frac{1}{2}} \qquad (92)$$

transfer between two metal ions, where k_{11} and k_{22} are the rate constants for electron exchange for the two metals, K_{12} is the equilibrium constant for the electron transfer reaction; f is defined by Eq 93, where Z is the collision frequency of

$$\log f = \frac{(\log K_{12})^2}{4 \log(k_{11}k_{22}/Z^2)} \qquad (93)$$

two uncharged molecules in solution, and is taken as 10^{11} M^{-1} sec^{-1} (17). The electron exchange and electron transfer reactions are of the form shown in Eqs 94 through 96.

$$M_1^{3+} + M_1^{2+} = M_1^{2+} + M_1^{3+} \quad (k_{11}) \qquad (94)$$

$$M_2^{3+} + M_2^{2+} = M_2^{2+} + M_2^{3+} \quad (k_{22}) \qquad (95)$$

$$M_1^{3+} + M_2^{2+} = M_1^{2+} + M_2^{3+} \quad (k_{12}) \qquad (96)$$

Though a rate constant for electron transfer between two different metals has traditionally been calculated from Eq 92, for comparison to the observed rate constant, such a calculation is made impossible for the Eu(II)-Fe(III) reaction by the lack of Eu(II)-Eu(III) exchange data. The electron exchange rate constant for the Eu(II)-Eu(III) system can be calculated from the same equation however using the k_{12} values for the Eu^{2+} reductions of Cr^{3+} and V^{3+} as well as Fe^{3+}. The calculations are presented in Table 53. Values for k_{12} were calculated from the E^0 data presented by Latimer (79). The k_{22}

Table 53. Calculation of the electron exchange rate constant for the Eu(II)-Eu(III) system in perchlorate media at 25°

M_1	M_2	k_{22} $M^{-1}sec^{-1}$	k_{12} $M^{-1}sec^{-1}$	k_{11} $M^{-1}sec^{-1}$
Eu	Fe	4.2[a]	6140[b]	$9x10^{-11}$
Eu	Cr	$<2x10^{-5}$[c]	$<1.7x10^{-5}$[d]	$<7x10^{-6}$
Eu	V	$1.0x10^{-2}$[e]	$9.0x10^{-3}$[d]	$1x10^{-5}$

[a]Reference 19.

[b]Measured in this work.

[c]Reference 78.

[d]Reference 10.

[e]Reference 30.

values reported for Fe and V are those for the acid independent path only; the value for Cr is probably a composite, measured in 0.5M H^+. The calculated k_{11} values, at least those derived from the Fe and V systems, are for direct reaction between Eu^{2+} and Eu^{3+}, rather than between hydrolyzed species. Meier and Garner (18) found no evidence for hydrolyzed species in the chloride catalyzed Eu(II)-Eu(III) exchange. The calculated exchange rates listed in Table 53 vary widely; the calculations probably do not add materially to knowledge of the Eu(II)-Eu(III) exchange, except to confirm that the exchange is very slow.

Rate trends

The rate constants for reduction of pentaamminehalocobalt complexes by Cr^{2+} have been shown (80) to follow the normal order (1,80) (fluoride-bridged reactions are the slowest of the halide complexes) while the corresponding Eu^{2+} reductions follow the inverted order (14). Similar trends have been observed in this study for reduction of pentaaquohaloiron(III) complexes, but different trends have been observed in other systems, as shown by the data in Table 54. The trends described in Table 54 doubtlessly result from a host of influences, most of them probably related to the reorganization of ligands and solvent molecules that is required for formation of the activated complex. Some factors in the reorganization are as follows: (1) F^- complexes are expected to be smaller

Table 54. Rate trends for the reduction of halometal(III) complexes. The order is denoted N for normal (fluoride slowest) or I for inverted

Reducing agent	Mechanism	Oxidizing agent, reference			
		CrX^{2+}	$(NH_3)_5CrX^{2+}$	$(NH_3)_5CoX^{2+}$	FeX^{2+}
V^{2+}	outer	N[a]		N (14)	
Cr^{2+}	inner	N (81)	N (82)	N (80)	N, this work
Eu^{2+}	inner(?)	N (4)		I (14)	I, this work
Cu^{+}	unknown			N[b]	
Fe^{2+}	inner			I (12)	I (19,83)
$Co(CN)_5^{3-}$	inner			N (15)	
$Ru(NH_3)_6^{2+}$	outer			N (21)	

[a] O. J. Parker, G. Antos, and J. H. Espenson, Ames, Iowa. Reduction of halochromium(III) by vanadium(II). Private communication. 1968.

[b] O. J. Parker and J. H. Espenson, Ames, Iowa. Reduction of cobalt(III) complexes by copper(I). Private communication. 1968.

and more rigid and thus more difficult to perturb, (2) reactions with small negative free energy change require more reorganization energy than those with a large negative change, (3) lengthening of the M(III)-X bond probably requires significant energy, and (4) shortening of the X-M(II) bond is probably also significant. These (and possibly other) conflicting influences seem to be delicately balanced, as indicated by the non-systematic reversals in the trends listed in Table 54. However, comparison of the reducing agents Cr^{2+} and Eu^{2+} does seem to indicate that factor (3) above is more important for Cr^{2+} than for Eu^{2+}. This difference could be due to the differences in lability; the very labile Eu(III) product could be detached from X before significant lengthening of the M(II)-X bond in the product occurs.

REFERENCES

1. N. Sutin, Ann. Rev. Phys. Chem., 17, 119 (1966).
2. J. Halpern, Quart. Rev. (London), 15, 207 (1961).
3. H. Taube, Advan. Inorg. Chem. Radiochem., 1, 1 (1959).
4. A. Adin and A. G. Sykes, J. Chem. Soc., (A), 354 (1968).
5. J. P. Birk and J. H. Espenson, J. Am. Chem. Soc., 90, 1153 (1968).
6. B. R. Baker, M. Orhanovic, and N. Sutin, J. Am. Chem. Soc., 89, 722 (1967).
7. J. H. Espenson, J. Am. Chem. Soc., 89, 1276 (1967).
8. J. H. Espenson, K. Shaw, and O. J. Parker, J. Am. Chem. Soc., 89, 5730 (1967).
9. D. E. Pennington and A. Haim, Inorg. Chem., 6, 2138 (1967).
10. A. Adin and A. G. Sykes, J. Chem. Soc., (A), 1230 (1966).
11. J. H. Espenson and D. W. Carlyle, Inorg. Chem., 5, 586 (1966).
12. J. H. Espenson, Inorg. Chem., 4, 121 (1965).
13. A. Haim and N. Sutin, J. Am. Chem. Soc., 87, 4210 (1965).
14. J. P. Candlin, J. Halpern, and D. L. Trimm, J. Am. Chem. Soc., 86, 1019 (1964).
15. J. P. Candlin, J. Halpern, and S. Nakamura, J. Am. Chem. Soc., 85, 2517 (1963).
16. G. Dulz and N. Sutin, J. Am. Chem. Soc., 86, 829 (1964).
17. G. Dulz and N. Sutin, Inorg. Chem., 2, 917 (1963).
18. J. Meier and C. S. Garner, J. Phys. Chem., 56, 853 (1952).
19. J. Silverman and R. W. Dodson, J. Phys. Chem., 56, 846 (1952).

20. H. Taube and H. Myers, J. Am. Chem. Soc., 76, 2103 (1953).

21. J. F. Endicott and H. Taube, J. Am. Chem. Soc., 86, 1686 (1964).

22. H. Taube, Advan. Chem. Ser., 49, 107 (1965).

23. R. A. Marcus, Ann. Rev. Phys. Chem., 15, 155 (1964).

24. N. Sutin, Ann. Rev. Nucl. Sci., 12, 285 (1962).

25. J. P. Candlin and J. Halpern, Inorg. Chem., 4, 1086 (1965).

26. N. Sutin, J. K. Rowley, and R. W. Dodson, J. Phys. Chem., 65, 1248 (1961).

27. A. M. Zwickel and H. Taube, J. Am. Chem. Soc., 81, 1288 (1959).

28. P. Benson and A. Haim, J. Am. Chem. Soc., 87, 3826 (1965).

29. R. A. Marcus, J. Phys. Chem., 67, 853 (1963).

30. L. E. Bennett and J. C. Sheppard, J. Phys. Chem., 66, 1275 (1962).

31. D. Seewald and N. Sutin, Inorg. Chem., 2, 643 (1963).

32. R. M. Wallace and E. K. Dukes, J. Phys. Chem., 65, 2094 (1961).

33. D. Bunn, F. S. Dainton, and S. Duckworth, Trans. Faraday Soc., 57, 1131 (1961).

34. F. Accascina, F. P. Cavasino, and S. D'Alessandro, J. Phys. Chem., 71, 2474 (1967).

35. E. Rabinowitch and W. H. Stockmayer, J. Am. Chem. Soc., 64, 335 (1942).

36. M. W. Lister and D. E. Rivington, Canad. J. Chem., 33, 1603 (1955).

37. P. Matthies and H. Wendt, Z. Physik. Chem. (Frankfurt), 30, 137 (1961).

38. J. H. Espenson, Inorg. Chem., 3, 968 (1964).

39. M. B. Jensen, Acta Chem. Scand., 12, 1657 (1958).

40. J. F. Below, R. E. Connick, and C. P. Coppel, J. Am. Chem. Soc., 80, 2961 (1958).

41. S. Nakamura, "Electron Transfer Reactions of Pentacyanocobaltate(II)," unpublished Ph.D. dissertation. Library, University of Chicago, Chicago, Illinois. 1964.

42. E. A. Guggenheim, Phil. Mag., 2, 538 (1926).

43. G. W. Haupt, J. Res. Natl. Bur. Std., 48, 414 (1952).

44. R. H. Moore, Los Alamos Scientific Laboratory Report, L.A. 2367 + Addenda (1963).

45. R. M. Milburn, J. Am. Chem. Soc., 79, 537 (1957).

46. T. W. Newton and G. M. Arcand, J. Am. Chem. Soc., 75, 2449 (1953).

47. M. J. M. Woods, P. K. Gallagher, and E. L. King, Inorg. Chem., 1, 55 (1962).

48. R. E. Connick and C. P. Coppel, J. Am. Chem. Soc., 81, 6389 (1959).

49. M. W. Lister and D. E. Rivington, Canad. J. Chem., 33, 1572 (1955).

50. G. S. Laurence, Trans. Faraday Soc., 52, 236 (1956).

51. R. H. Betts and F. S. Dainton, J. Am. Chem. Soc., 75, 5721 (1953).

52. A. Haim and N. Sutin, J. Am. Chem. Soc., 88, 434 (1966).

53. A. Lodzinska, Roczniki Chem., 40, 1369 (1966).

54. G. P. Rowland, Ind. Eng. Chem., Anal. Ed., 11, 442 (1939).

55. R. E. Connick, L. G. Hepler, Z. Z. Hugus, J. W. Kury, W. M. Latimer, and Maak-Sang Tsao, J. Am. Chem. Soc., 78, 1827 (1956).

56. D. Pouli and W. Smith, Canad. J. Chem., 38, 567 (1960).

57. R. F. Kruh, J. Am. Chem. Soc., 76, 4865 (1954).

58. C. F. Baes, J. Phys. Chem., 60, 878 (1956).

59. T. W. Newton and S. W. Rabideau, J. Phys. Chem., 63, 365 (1959).

60. T. W. Swaddle and E. L. King, Inorg. Chem., 3, 234 (1964).

61. T. W. Swaddle and E. L. King, Inorg. Chem., 4, 532 (1965).

62. J. H. Espenson and J. P. Birk, J. Am. Chem. Soc., 87, 3280 (1965).

63. G. C. Lalor and E. A. Moelwyn-Hughes, J. Chem. Soc., 1560 (1963).

64. S. C. Chan, J. Chem. Soc., 2375 (1964).

65. G. G. Davis and W. Smith, Canad. J. Chem., 40, 1836 (1962).

66. T. W. Newton and F. B. Baker, J. Phys. Chem., 67, 1425 (1963).

67. T. W. Newton and F. B. Baker, Inorg. Chem., 4, 1166 (1965).

68. D. H. Huchital and H. Taube, J. Am. Chem. Soc., 87, 5371 (1965).

69. G. Gordon and P. H. Tewari, J. Phys. Chem., 70, 200 (1966).

70. J. H. Espenson and D. E. Binau, Inorg. Chem., 5, 1365 (1966).

71. T. W. Newton and N. A. Daugherty, J. Phys. Chem., 71, 3768 (1967).

72. R. A. Robinson and R. H. Stokes, "Electrolyte Solutions," Butterworths Scientific Publications, London, England, 1955.

73. A. M. Sargeson and H. Taube, Inorg. Chem., 5, 1094 (1966).

74. J. L. Burmeister, Inorg. Chem., 3, 919 (1964).

75. S. Fronaeus and R. Larsson, Acta Chem. Scand., 16, 1447 (1962).

76. E. G. Moorhead and N. Sutin, Inorg. Chem., 6, 428 (1967).

77. R. J. Campion, T. J. Conocchioli, and N. Sutin, J. Am. Chem. Soc., 86, 4591 (1964).

78. A. Anderson and N. A. Bonner, J. Am. Chem. Soc., 76, 3826 (1954).

79. W. M. Latimer, "Oxidation Potentials," 2nd Ed., Prentice-Hall, Inc., New York, New York, 1952.

80. J. P. Candlin and J. Halpern, Inorg. Chem., 4, 766 (1965).

81. D. L. Ball and E. L. King, J. Am. Chem. Soc., 80, 1091 (1958).

82. A. E. Ogard and H. Taube, J. Am. Chem. Soc., 80, 1084 (1958).

83. J. Hudis and A. C. Wahl, J. Am. Chem. Soc., 75, 4153 (1953).

84. J. H. Espenson and O. J. Parker, J. Am. Chem. Soc., in press, (1968).

85. S. Kuo, "Numerical Methods and Computations," Addison-Wesley, Reading, Massachusetts, 1965.

86. D. W. Carlyle and J. H. Espenson, Inorg. Chem., 6, 1370 (1967).

APPENDIX A

Computer Program for Calculating Concentrations of Reactants and Products as a Function of Time for the Reduction of Iron(III) by Chromium(II) in the Presence of Bromide

This program is patterned after that described by Espenson and Parker (84). The program solves the differential equations for the following reaction scheme, using the Runge-Kutta iteration procedure. The symbols A, B, C,

$$A + B \underset{k_2}{\overset{k_1}{\rightleftharpoons}} C$$

$$C + F \xrightarrow{k_3} D + H$$

$$B + A + F \xrightarrow{k_4} D + H$$

$$B + F \xrightarrow{k_5} G + H$$

F, G, H, and D denote the species Br^-, Fe^{3+}, $FeBr^{2+}$, Cr^{2+}, Cr^{3+}, Fe^{2+}, and $CrBr^{2+}$, respectively.

The Runge-Kutta method of solving initial-value problems utilizes the differential equations to approximate concentration changes over a small interval of time, Δt (85). If the interval is small enough, then $X_{n+1} = X_n + (RK)\Delta t$, $y_{n+1} = y_n + (RJ)\Delta t$, and $Z_{n+1} = Z_n + (RH)\Delta t$, where X, Y, and Z are the changes in the concentrations of C, D, and G, respectively, and RK, RJ, and RH are the rates of change with respect to time of these concentrations. The subroutine RNKT calculates

four values for each of the variables RK, RJ, and RH; weighted averages of these variables are used to calculate the new concentration increments, X, Y, and Z.

The definitions of quantities that were read into the program as control information, or data, are given in Table 55.

Table 55. Definitions of control symbols and data symbols for the Runge-Kutta calculation

Symbol	Definition
IPROB	No entry for IPROB stops the program.
NINT	Number of equal time intervals (< 81) covered by the program.
ITR	Controls the number of times a time interval can be subdivided to meet RKTEST.
ITP	If ITP = 0, iterations will not be printed. If ITP = 1, iterations will be printed.
TINT	Number of time units in each time interval.
RKTEST[a]	Fraction that concentration of B is permitted to change in an interval without subdivision of the interval and recalculation.
EA, EB,$\cdots$	Molar absorbance for each species times optical path length.
IA, IB,$\cdots$	Initial concentration of each species.
R_1, R_2,$\cdots$	Known values of the five rate constants.

[a]In preliminary calculations for a new system, the value of RKTEST should be progressively decreased until further decreases do not affect the results of the calculation.

The size of the time interval (TINT) is not critical; the value of TINT is automatically divided by 40, and then by 50, 60, 72, ····, if necessary to meet RKTEST. The actual evaluation is done over the smaller intervals, but the printed values correspond to the interval TINT. If the maximum subdivision permitted by ITR does not result in meeting RKTEST, the program will repeat the calculations, with the iterations printed option in effect.

A listing of the computer program is given on the next pages.

Figure 17. Computer listing for Cr (II) + Fe(III) reactions

```
C  RUNGE-KUTTA CALC FOR CR(III) REDUCTION OF FEBR
C     BR-  +   FE3+ =  FEBR2+     R1 SEC ORDER, R2 FIRST ORDER
C     FEBR2+   +  CR2+   =  CRBR2+   +  FE2+       R3
C     FE3+ +BR- + CR2+ =  CRBR2+   +  FE2+       R4
C     FE3+   + CR2+      =  CR3+     +  FE2+       R5
C     A=BR-, B=FE3+, C=FEBR2+, F=CR2+, G=CR3+, H=FE2+,D=CRBR2+
      COMMON R1,R2,R3,R4,R5,TA,TB,TC,TF,TG,TH,TD
    1 FORMAT(4I6,2E12.7)
    2 FORMAT(6F12.7)
 1001 FORMAT(18A4)
      DIMENSION A(80),B(80),C(80),F(80),TITLE(18),DEN(80),G(80),H(80),D(
     180)
   35 READ (1,1001)(TITLE(I),I=1,18)
      READ (1,1)IPROB,NINT,ITR,ITPRNT,IINT,RKTEST
      IF (IPROB)100,100,37
   37 READ (1,2)EA,EB,EC,EF,EG,EH,ED
      READ (1,2)AI,BI,CI,FI,GI,HI,DI
      READ (1,2)R1,R2,R3,R4,R5
      RKTEST=RKTEST*BI
      A(1)=AI
      B(1)=BI
      C(1)=CI
      F(1)=FI
      G(1)=GI
      H(1)=HI
      D(1)=DI
      DEN(1)=A(1)*EA+B(1)*EB+C(1)*EC+F(1)*EF+G(1)*EG+H(1)*EH+D(1)*ED
      ISTCON=BI
      IF (IITPRNT-1)39,38,39
   38 WRITE (3,4)R1,R2,R3,R4,R5,RKTEST
    4 FORMAT(1H1,T6,@FEBR2+ -CR2+ RXN@/,T6,@R1,R2,R3,R4,R5 = @,1P5E12.5/
     1,T6,@RKTEST = @,1PE12.5)
   39 DO 16 L=1,NINT
      DO 7 K=9,ITR
      TA=A(L)
      TB=B(L)
      TC=C(L)
      TF=F(L)
      TG=G(L)
      TH=H(L)
      TD=D(L)
      CALL RNKT(N,K,IINT)
      IF (IITPRNT-1)26,27,28
   27 WRITE (3,25)K,TA,TB,TC,TF,TG,TH,TD,L
   25 FORMAT(1HO,T6,@K= @,I2/,T6,@CONC. ARE @,1P7E12.5/,T6,@AFTER RNKUTA
     1 CALC, INT. = @,I2)
   28 CONDIF=ABS(ISTCON-TB)
      IF (CONDIF-RKTEST)13,13,14
   14 ISTCON=TB
    7 CONTINUE
      ITPRNT=IITPRNT+1
      IF (IITPRNT-1)8,38,8
    8 WRITE (3,1001)(TITLE(I),I=1,18)
      WRITE (3,122)R1,R2,R3,R4,R5
  122 FORMAT(1HO,T6,@FEBR2+ CR2+ RXN@/,T6,@R1= @1PE10.3/,T6,@R2= @1PE10.
     13/,T6,@R3= @1PE10.3/,T6,@R4= @1PE10.3/,T6,@R5= @1PE10.3)
      WRITE (3,15)ITR
   15 FORMAT(1HO,T6,@NO CONVERGENCE IN @I2,@ ITERATIONS@)
      WRITE (3,22)CONDIF,RKTEST
```

Figure 17. (Continued)

```
   22 FORMAT(1HO,T6,@CONDIF AND RKTEST ARE @1PE12.5,@ AND @1PE12.5)
      WRITE (3,101)K,TA,TB,TC,TF,TG,TH,TD
   10 FORMAT(1HO,T6,@K= @I2/,T6,@TA= @1PE12.5/,T6,@TB= @1PE12.5/,T6,@TC
     1= @1PE12.5/,T6,@TF= @1PE12.5/,T6,@TG = @1PE12.5/,T6,@TH = @1PE12.5
     1/,T6,@TD = @1PE12.5)
      GO TO 35
   13 A(L+1)=TA
      B(L+1)=TB
      C(L+1)=TC
      F(L+1)=TF
      G(L+1)=TG
      H(L+1)=TH
      D(L+1)=TD
      DEN(L+1)=A(L+1)*EA + B(L+1)*EB + C(L+1)*EC + F(L+1)*EF + G(L+1)*EG
     1 + H(L+1)*EH + D(L+1)*ED
   16 CONTINUE
   17 WRITE (3,100)(TITLE(I),I=1,18)
      WRITE (3,122)R1,R2,R3,R4,R5
      WRITE (3,1222)EA,EB,EC,EF,EG,EH,ED
 1222 FORMAT(1HO,T6,@EA = @1PE10.3/,T6,@EB = @1PE10.3/,T6,@EC = @1PE10.3
     1/,T6,@EF = @1PE10.3/,T6,@EG = @1PE10.3/,T6,@EH = @1PE10.3/,T6,@ED
     1= @1PE10.3)
      WRITE (3,24)
   24 FORMAT(1HO,T10,@TIME          B             C             F
     1      G             H             D       ABSORBANCE@)
      ZERO=0.0
      WRITE (3,26)ZERO,BI,CI,FI,GI,HI,DI,DEN(1)
   26 FORMAT(1HO,T4,1P8E14.5)
      MINT=NINT+1
      DO 19 L=2,MINT
      TIME=TINT*FLOAT(L-1)
      WRITE (3,26)TIME,B(L),C(L),F(L),G(L),H(L),D(L),DEN(L)
   19 CONTINUE
      GO TO 35
  100 STOP
      END
```

Figure 17. (Continued)

```
      SUBROUTINE RNKT(N,K,TINT)
      DIMENSION A(80),B(80),C(80),F(80),TITLE(18),DEN(80),G(80),H(80),D(
     180)
      COMMON R1,R2,R3,R4,R5,TA,TB,TC,TF,TG,TH,TD
      K=N*N/2
      DELT=TINT/FLOAT(K)
      DO 8 M=1,K
      RK1=RK(0.0,0.0,0.0)*DELT/2.0
      RJ1=RJ(0.0,0.0,0.0)*DELT/2.0
      RH1=RH(0.0,0.0,0.0)*DELT/2.0
      RK2=RK(RK1,RJ1,RH1)*DELT/2.0
      RJ2=RJ(RK1,RJ1,RH1)*DELT/2.0
      RH2=RH(RK1,RJ1,RH1)*DELT/2.0
      RK3=RK(RK2,RJ2,RH2)*DELT
      RJ3=RJ(RK2,RJ2,RH2)*DELT
      RH3=RH(RK2,RJ2,RH2)*DELT
      RK4=RK(RK3,RJ3,RH3)*DELT
      RJ4=RJ(RK3,RJ3,RH3)*DELT
      RH4=RH(RK3,RJ3,RH3)*DELT
      X=(2.0*RK1+4.0*RK2+2.0*RK3+RK4)/6.0
      Y=(2.0*RJ1+4.0*RJ2+2.0*RJ3+RJ4)/6.0
      Z=(2.0*RH1+4.0*RH2+2.0*RH3+RH4)/6.0
      TA=TA-X-Y
      TB=TB-X-Y-Z
      TC=TC+X
      TF=TF-Y-Z
      TG=TG+Z
      TH=TH+Y+Z
      TD=TD+Y
    8 CONTINUE
      RETURN
      END

      FUNCTION RK(X,Y,Z)
      DIMENSION A(80),B(80),C(80),F(80),TITLE(18),DEN(80),G(80),H(80),D(
     180)
      COMMON R1,R2,R3,R4,R5,TA,TB,TC,TF,TG,TH,TD
      RK=R1*(TA-X-Y)*(TB-X-Y-Z)-R2*(TC+X)-R3*(TC+X)*(TF-Y-Z)
      RETURN
      END

      FUNCTION RJ(X,Y,Z)
      DIMENSION A(80),B(80),C(80),F(80),TITLE(18),DEN(80),G(80),H(80),D(
     180)
      COMMON R1,R2,R3,R4,R5,TA,TB,TC,TF,TG,TH,TD
      RJ=R3*(TC+X)*(TF-Y-Z)+R4*(TB-X-Y-Z)*(TA-X-Y)*(TF-Y-Z)
      RETURN
      END

      FUNCTION RH(X,Y,Z)
      DIMENSION A(80),B(80),C(80),F(80),TITLE(18),DEN(80),G(80),H(80),D(
     180)
      COMMON R1,R2,R3,R4,R5,TA,TB,TC,TF,TG,TH,TD
      RH=R5*(TB-X-Y-Z)*(TF-Y-Z)
      RETURN
      END
```

APPENDIX B

Computer Program for Calculating Concentrations of Reactants and Products as a Function of Time for the Reduction of Iron(III) by Europium(II) in the Presence of Bromide

This program is similar to that described in Appendix A. The program solves the differential equations for the following reaction scheme. The symbols A, B, C, F, G, and H

$$A + B \underset{k_2}{\overset{k_1}{\rightleftharpoons}} C$$

$$C + F \xrightarrow{k_3} G + H + A$$

$$B + F \xrightarrow{k_4} G + H$$

represent the species Br^-, Fe^{3+}, $FeBr^{2+}$, Eu^{2+}, Eu^{3+}, and Fe^{2+}, respectively.

Only two differential equations, with the variables X and Y representing the change in concentration of C and G, respectively, were required for the calculations, because the products of both bromide paths (see Table 12) are the same. The rate constant k_4 is the composite $k' + k_{Br}[Br^-]$. A listing of the program is given on the next pages.

Figure 18. Computer listing for Eu(II) + Fe(III) reactions

```
C      RUNGE-KUTTA SOLUTION TO FEBR REDUCTION BY EU,NON-STEADY-STATE FEBR
C      BR-  +  FE3+  =  FEBR2+      R1,SEC ORDER, R2, FIRST ORDER
C      FEBR2+  +  EU2+  =  EU3+   +   BR-  +   FE2+              R3
C      FE3+    +  EU2+  =  EU3+   +   FE2+                       R4
       COMMON R1,R2,R3,R4,TA,TB,TC,TF,TG,TH
C      A=BR-,B=FE3+,C=FEBR2+,F=EU2+,G=EU3+,H=FE2+
     1 FORMAT(4I6,2E12.7)
     2 FORMAT(6E12.7)
  1001 FORMAT(18A4)
       DIMENSION A(80),B(80),C(80),F(80),TITLE(18),DEN(80),G(80),H(80)
    35 READ (1,1001)(TITLE(I),I=1,18)
       READ (1,1)IPROB,NINT,ITR,ITPRNT,TINT,RKTEST
       IF (IPROB)100,100,37
    37 READ (1,2)EA,EB,EC,EF,EG,EH
       READ (1,2)AI,BI,CI,FI,GI,HI
       READ (1,2)R1,R2,R3,R4
       RKTEST=RKTEST*BI
       A(1)=AI
       B(1)=BI
       C(1)=CI
       F(1)=FI
       G(1)=GI
       H(1)=HI
       DEN(1)=B(1)*EB+F(1)*EF+C(1)*EC
       TSTCON=BI
       IF (ITPRNT-1)39,38,39
    38 WRITE (3,4)R1,R2,R3,R4,RKTEST
     4 FORMAT(1H1,T6,@FEBR+2 -EU+2 RXN@/,T6,@R1,R2,R3, AND R4 = @,1P4E12.
      15/,T6,@RKTEST = @,1PE12.5)
    39 DO 16 L=1,NINT
       DO 7 N=9,ITR
C      TA IS THE CURRENT VALUE OF THE CONCENTRATION OF A, TB ETC.
       TA=A(L)
       TB=B(L)
       TC=C(L)
       TF=F(L)
       TG=G(L)
       TH=H(L)
       CALL RNKT(N,K,TINT)
       IF (ITPRNT-1)28,27,28
    27 WRITE (3,25)K,TA,TB,TC,TF,TG,TH,L
    25 FORMAT(1H0,T6,@K= @,I2/,T6,@CONC.ARE @,1P6E12.5/,T6,@AFTER RNKUTA
      1 CALC. INT. = @,I2)
    28 CONDIF=ABS(TSTCON-TB)
       IF (CONDIF-RKTEST)13,13,14
    14 TSTCON=TB
     7 CONTINUE
       ITPRNT=ITPRNT+1
       IF (ITPRNT-1)8,38,8
     8 WRITE (3,1001)(TITLE(I),I=1,18)
       WRITE (3,122)R1,R2,R3,R4
   122 FORMAT(1H0,T6,@FEBR2+ EU2+  RXN@/,T6,@R1= @1PE10.3/,T6,@R2= @1PE10
      1.3/,T6,@R3= @1PE10.3/,T6,@R4= @1PE10.3)
       WRITE (3,15)ITR
    15 FORMAT(1H0,T6,@NO CONVERGENCE IN @I2,@ ITERATIONS@)
       WRITE (3,22)CONDIF,RKTEST
    22 FORMAT(1H0,T6,@CONDIF AND RKTEST ARE @1PE12.5,@ AND @1PE12.5)
       WRITE (3,10)K,TA,TB,TC,TF,TG,TH
    10 FORMAT(1H0,T6,@K = @I2/,T6,@TA = @1PE12.5/,T6,@TB = @1PE12.5/,T6,@
```

Figure 18. (Continued)

```
     1TC = @1PE12.5/,To,@TF = @1PE12.5,/,T6,@TG = @1PE12.5/,T6,@TH = @1P
     1E12.5)
      GO TO 35
   13 A(L+1)=TA
      B(L+1)=TB
      C(L+1)=TC
      F(L+1)=TF
      G(L+1)=TG
      H(L+1)=TH
      DEN(L+1)=B(L+1)*EB+F(L+1)*EF+C(L+1)*EC
C     ONLY B,C,AND F ABSORB
   16 CONTINUE
   17 WRITE (3,1001)(TITLE(I),I=1,18)
      WRITE (3,122)R1,R2,R3,P4
      WRITE (3,1222)EA,EB,EC,EF,EG,EH
 1222 FORMAT(1HO,T6,@EA= @1PE10.3/,T6,@EB = @1PE10.3/,T6,@EC= @1PE10.3/,
     1T6,@EF = @1PE10.3/,T6,@EG = @1PE10.3/,T6,@EH = @1PE10.3)
      WRITE (3,24)
   24 FORMAT(1HO,T10,@TIME          A             B             C
     1      F              G             H         ABSORBANCE@)
      ZERO=0.0
      WRITE (3,26)ZERO,A1,B1,C1,F1,G1,H1,DEN(1)
   26 FORMAT(1HO,T4,1P8E14.5)
      MINT=NINT+1
      DO 19 L=2,MINT
      TIME=TINT*FLOAT(L-1)
      WRITE (3,26)TIME,A(L),B(L),C(L),F(L),G(L),H(L),DEN(L)
   19 CONTINUE
      GO TO 35
  100 STOP
      END

      SUBROUTINE RNKT(N,K,TINT)
C     THIS SUBROUTINE DEFINES INTERVALS AND SLOPES FOR RUNGE-KUTTA
      DIMENSION A(80),B(80),C(80),F(80),TITLE(18),DEN(80),G(80),H(80)
      COMMON R1,R2,R3,R4,TA,TB,TC,TF,TG,TH
      K=N*N/2
      DELT=TINT/FLOAT(K)
C      DX/DT IS RATE OF CHANGE OF FERR2+
C     DY/DT IS RATE OF CHANGE OF EACH PROD
      DO 8 M=1,K
      RK1=RK(0.0,0.0)*DELT/2.0
      RJ1=RJ(0.0,0.0)*DELT/2.0
      RK2=RK(RK1,RJ1)*DELT/2.0
      RJ2=RJ(RK1,RJ1)*DELT/2.0
      RK3=RK(RK2,RJ2)*DELT
      RJ3=RJ(RK2,RJ2)*DELT
      RK4=RK(RK3,RJ3)*DELT
      RJ4=RJ(RK3,RJ3)*DELT
      X=(2.0*RK1+4.0*RK2+2.0*RK3+RK4)/6.0
      Y=(2.0*RJ1+4.0*RJ2+2.0*RJ3+RJ4)/6.0
      TA=TA-X
      TB=TB-X-Y
      TC=TC+X
      TF=TF-Y
      TG=TG+Y
      TH=TH+Y
    8 CONTINUE
      RETURN
      END
```

Figure 18. (Continued)

```
      FUNCTION RJ(X,Y)
      DIMENSION A(80),B(80),C(80),F(80),TITLE(18),DEN(80),G(80),H(80)
      COMMON R1,R2,R3,R4,TA,TB,TC,TF,TG,TH
      RJ=R3*(TC+X)*(TF-Y)+R4*(TB-X-Y)*(TF-Y)
      RETURN
      END


      FUNCTION RK(X,Y)
      DIMENSION A(80),B(80),C(80),F(80),TITLE(18),DEN(80),G(80),H(80)
      COMMON R1,R2,R3,R4,TA,TB,TC,TF,TG,TH
      RK=R1*(TA-X)*(TB-X-Y)-R2*(TC+X)-R3*(TC+X)*(TF-Y)
      RETURN
      END
```

ACKNOWLEDGMENT

The author is grateful to Dr. James H. Espenson for his advice, and to the Atomic Energy Commission and the National Aeronautics and Space Administration for financial assistance. Some portions of this dissertation have been published (86).